

2008

## Finite Element Optimization of Hip Implant Geometrical Parameters to Determine Safe Zones and Resist Dislocation

Himanshu K. Bhatt  
*Wright State University*

Follow this and additional works at: [https://corescholar.libraries.wright.edu/etd\\_all](https://corescholar.libraries.wright.edu/etd_all)



Part of the [Biomedical Engineering and Bioengineering Commons](#)

---

### Repository Citation

Bhatt, Himanshu K., "Finite Element Optimization of Hip Implant Geometrical Parameters to Determine Safe Zones and Resist Dislocation" (2008). *Browse all Theses and Dissertations*. 891.  
[https://corescholar.libraries.wright.edu/etd\\_all/891](https://corescholar.libraries.wright.edu/etd_all/891)

This Thesis is brought to you for free and open access by the Theses and Dissertations at CORE Scholar. It has been accepted for inclusion in Browse all Theses and Dissertations by an authorized administrator of CORE Scholar. For more information, please contact [library-corescholar@wright.edu](mailto:library-corescholar@wright.edu).

**FINITE ELEMENT OPTIMIZATION OF HIP IMPLANT GEOMETRICAL  
PARAMETERS TO DETERMINE SAFE ZONES AND RESIST DISLOCATION**

A thesis submitted in partial fulfillment  
of the requirements for the degree of  
**Master of Science in Engineering**

By

**HIMANSHU K. BHATT**  
B.E., North Gujarat University, 2006

2008  
Wright State University

WRIGHT STATE UNIVERSITY  
SCHOOL OF GRADUATE STUDIES

November 18, 2008

I HEREBY RECOMMEND THAT THE THESIS PREPARED UNDER MY SUPERVISION BY Himanshu Kishorkumar Bhatt ENTITLED Finite Element Optimization of Hip Implant Geometrical Parameters to Determine Safe Zones and Resist Dislocation BE ACCEPTED IN PARTIAL FULFILLMENT OF THE REQUIREMENTS FOR THE DEGREE OF Master of Science in Engineering.

---

Dr. Tarun Goswami, D.Sc.  
Thesis Director

---

Dr. S. Narayanan, Ph.D.  
Department Chair

Committee on  
Final Examination

---

Dr. Tarun Goswami, D.Sc.

---

Dr. David B. Reynolds, Ph.D.

---

Dr. S. Narayanan, Ph.D.

---

Joseph F. Thomas, Jr., Ph.D.  
Dean, School of Graduate Studies

## ABSTRACT

Bhatt, Himanshu K. M.S.Egr., Department of Biomedical, Industrial and Human Factors Engineering, Wright State University, 2008. Finite Element Optimization of Hip Implant Geometrical Parameters to Determine Safe Zones and Resist Dislocation.

A computational study was performed using finite element analysis (FEA) of three dimensional solid hip implant models. Twelve different hip implant models were designed to investigate the performance of geometrical parameters affecting hip stability. The parameters examined were head diameter, neck diameter, head-to-neck ratio, neck angle and acetabular liner thickness. Component orientations included cup anatomical inclination and cup anteversion, which should be accounted for during total hip implant design as well as in the practice of arthroplasties. A static analysis was performed for all 12 hip designs using stainless steel 316L. von Mises stress, contact stress, contact penetration, and sliding displacement were correlated with the geometrical parameters as well as with anatomical orientations of acetabular component.

Analytical results were used to define safe zones for a combination of geometrical parameters that provided maximum hip stability. Head diameters from 26 mm to 32 mm were found within safe ranges. Lower head diameters showed comparatively higher contact penetration increasing risk of dislocation *in vivo*. The preeminent stress results were found with combinations of 26 mm head and 14 mm neck diameters with 35 degrees of neck angle. Lower cup anatomical inclination tends to provide higher contact surface with femoral head during articulations developing lower contact stresses. The safe combination for cup orientation was observed with cup anatomical inclinations ranging from 35 to 50 degrees and cup anteversion below 20 degrees. New generic and specific equations were developed using the data from FE analysis to

predict penetration. Evaluated penetration can then be used to determine the linear wear rate (*in vivo*).

## TABLE OF CONTENTS

|  | Page |
|--|------|
| CHAPTER 1 INTRODUCTION.....  | 1    |
| 1.1 Dislocation Mechanics.....                                     | 2    |
| 1.1.1 Impingement.....   | 2    |
| 1.1.2 Subluxation.....   | 4    |
| 1.1.3 Engineering Aspects.....                                     | 6    |
| 1.2 Motivation For Study.....                                      | 7    |
| CHAPTER 2 REVIEW OF LITERATURE.....                                | 9    |
| 2.1 Preoperative Factors.....                                      | 11   |
| 2.1.1 Clinical Perspectives.....                                   | 11   |
| 2.1.2 Primary Causes of Dislocation.....                           | 12   |
| 2.1.3 Age, Gender, Weight, and Side of Operation.....              | 14   |
| 2.1.4 Surgical Approach.....                                       | 15   |
| 2.2 Intraoperative Factors.....                                    | 17   |
| 2.2.1 Defects in Acetabular Components.....                        | 17   |
| 2.2.2 Defect in Femoral Components.....                            | 19   |
| 2.3 Postoperative Factors.....                                     | 22   |
| 2.3.1 Dislocation Features and Mechanisms.....                     | 22   |
| 2.3.2 Time of Dislocation.....                                     | 24   |
| 2.3.3 Revision Surgery and Recurrent Dislocations.....             | 27   |
| CHAPTER 3 METHODS AND MATERIALS.....                               | 30   |
| 3.1 Development of 3-Dimensional Solid Hip Models.....             | 30   |
| 3.1.1 Designing of a Baseline Hip Model.....                       | 30   |
| 3.1.2 Geometrical Parameters and Classification of Hip Models..... | 32   |
| 3.1.3 Preparation For Further Processing into ANSYS 11.0.....      | 36   |
| 3.2 Development of Finite Element Model and Fea.....               | 36   |
| 3.2.1 Meshing Strategies and Defining Contact pairs.....           | 37   |
| 3.2.2 Loads and Constrains.....                                    | 41   |
| 3.3 Statistical Terms.....   | 43   |
| CHAPTER 4 RESULTS.....   | 44   |
| 4.1 von Mises Stress.....  | 44   |
| 4.2 Contact Stress.....  | 46   |
| 4.3 Contact Penetration.....                                       | 46   |
| 4.4 Sliding Displacement.....                                      | 47   |
| CHAPTER 5 DISCUSSION.....  | 50   |
| 5.1 Effect of Geometrical Parameters on Maximum Stress.....        | 50   |
| 5.2 Effects of Geometrical Parameters on Contact Stress.....       | 57   |
| 5.3 Effects of Geometrical Parameters on Contact Penetration.....  | 61   |

|  |      |
|--|------|
| 5.4 Effects of Geometrical Parameters on Contact Sliding Displacement..... | 64   |
| 5.5 Prediction Equations - Contact Stresses.....                           | 65   |
| 5.5.1 Generic Equation.....  | 66   |
| 5.5.2 Specific Equation.....   | 67   |
| 5.6 A New Wear Prediction Model.....                                       | 69   |
| 5.6.1 Generic Equation.....  | 70   |
| 5.6.2 Specific Equation.....   | 71   |
| 5.7 Safe Zones.....  | 71   |
| CHAPTER 6 CONCLUSION.....  | 78   |
| REFERENCES.....  | 80   |
| APPENDIX A.....  | I    |
| APPENDIX B.....  | XIII |

## LIST OF FIGURES

| Figure  | Page |
|---|------|
| 1.1 Types of Impingement causing Dislocation. Primary impingement can lead to secondary impingement if patient activity exceeds permissible ROM. The risk of dislocation increases after secondary impingement [11].....  | 3    |
| 1.2 Subluxation during dynamic simulation of Hip Implant into ANSYS 11.0. One of the hip implant encountered the subluxation during an attempt of dynamic simulation.....   | 5    |
| 2.1 Acetabular Cup Inclinations in Primary and Revision THRs. Amongst all total hip dislocations, 90% of the cases were evaluated with 50 degrees or more inclination angle with horizontal axis for acetabular component [31].....   | 19   |
| 2.2 Types of Dislocation. Anterior dislocation usually occurs when the leg is externally rotated or abducted too much; whereas, Posterior dislocation, which occurs when leg is forced to flex during internally rotated or too much abducted position [26].....  | 23   |
| 2.3 Early (within 5 weeks) Dislocations Vs Late Dislocations (within 9 years) [15].....   | 26   |
| 2.4 Correlation of time of dislocation and rate of recurrence. Higher correlation of recurrent dislocations was observed with late compared to early dislocations [15]...   | 29   |
| 3.1 Basic components of a Hip Implant in SolidWorks 2008. A complete hip implant assembly was developed using femoral stem, femoral head and acetabular cup.....  | 32   |
| 3.2 Different prosthetic component orientations showed using antero-posterior and medio-lateral views. Femoral component inclinations include stem flexion and stem abduction angles with vertical axis, and neck angle with horizontal axis. Acetabular component orientations include cup anatomical inclination and cup anteversion angle with horizontal plane..... | 34   |
| 3.3 Flowchart describing systematic procedures for static analysis in ANSYS.....  | 39   |
| 3.4 Hip Model 1 inserted into Femur with free volume mesh in ANSYS 11.0. A model of femur was developed; however, the static analysis in the present study was performed on the stem without femoral bone.....  | 41   |
| 4.1 von Mises Stresses plotted for static analysis of Hip Model 1.....  | 45   |
| 5.1 Oneway Analysis of Maximum Stress by Head Diameter and Neck Diameter. The lowest von mises stresses were examined for 26 mm head diameter designed with 14 mm neck diameter.....  | 51   |
| 5.2 Bar chart of Head Diameter vs. Mean of Maximum stresses using Oneway Anova. Mean stress value for 32 mm head diameter was highest of all analyzed hip models; whereas, the mean stress for 26 mm head diameter was found lowest of all series of  |      |



|   |    |
|---|----|
| hip models.....   | 52 |
| 5.3 Oneway Analysis of Maximum Stress by Neck Diameter. Models with 14 mm head diameters were examined with lowest mean stresses compared to 10 mm and 18 mm neck diameters.....  | 53 |
| 5.4 Oneway Analysis of Maximum Stress by Neck Angle. All hip models with 50 degrees of neck angles showed comparatively higher von mises stresses regardless of the head diameter sizes combined in those models. Neck angle of 25 degrees were evaluated with intermediate stress values with lowest stresses when combined with 32 mm head diameter and highest when combined with 20 mm head diameter..... | 56 |
| 5.5 Oneway Analysis of Maximum Stresses by H-N Ratio with comparison of Head Diameter and Neck Diameter. There was no significant correlation observed between H-N ratio and maximum stresses. The lowest peak stress was retrieved for hip model with H-N ratio of 1.86.....   | 57 |
| 5.6 Oneway Analysis of Contact Stresses by Head Diameter. Large head diameters showed significantly less contact stresses compared to smaller head diameters ( $R^2 = 0.96$ ).....  | 58 |
| 5.7 Oneway Analysis of Contact Stresses by Cup Anatomical Angle. Lower peak contact stresses were examined for cup inclination below 50 degrees when combined with 10 degrees and 20 degrees of cup anteversions. Hip models with 10 degrees of cup anteversion showed significantly lower contact stresses compared to 20 degrees when modeled with 35 degrees of cup inclination.....                       | 60 |
| 5.8 Oneway Analysis of Contact Penetration by Head Diameter ( $R^2=0.78$ ). Highest contact penetration was observed in the hip model with 20 mm head diameter which was less significantly compared due to only one successful analyzed hip model with 20 mm head diameter.....  | 61 |
| 5.9 Oneway Analysis of Contact Penetration by Cup Anatomical Angle compared with Cup Anteversion. A less significant ( $R^2 = 0.15$ ) correlation was observed between contact penetration and cup anatomical angle with horizontal axis.....   | 62 |
| 5.10 Oneway Analysis of Contact Sliding Displacement by Head Diameter. There was no significant correlation found between contact sliding displacement and head diameters ( $R^2 = 0.25$ ).....   | 64 |
| 5.11 Safe Zone definition for combinations of different Head Diameters and Neck Diameters. Head diameter below 26 mm and above 32 mm was examined with higher risk of hip instability.....  | 72 |
| 5.12 Safe Zone definition for combinations of different Head Diameters and Neck Angles. The safe zone was considered as head diameters from 26 mm to 32 mm, and neck angles between 25 to 35 degrees.....   | 73 |

|      |  |    |
|------|--|----|
| 5.13 | Safe Zone definition for combinations of different Head Diameters, Neck Diameters, and Neck Angles. Head diameters between 26 mm to 32 mm, neck diameters between closer to 14 mm, and neck angle between 25 degrees to 35 degrees were examined to be safest ranges for individual performances of these parameters.....  | 74 |
| 5.14 | Safe Zone definition for combinations of different Head Diameters and Cup Anatomical Inclinations. The head diameters between 26 mm to 32 mm were defined as secured region for femoral head designs. The risk area was examined for cup inclinations below 35 degrees as well as above 50 degrees; while, safe zone was described as cup inclination between 35 degrees and 50 degrees..... | 75 |
| 5.15 | Safe Zone definition for combinations of different Cup anatomical Inclinations and Cup Anteversions. Cup anteversions above 15 degrees was found highly sensitive to dislocation. The safe range of cup anteversion was examined between 5 degrees and 15 degrees.....   | 75 |
| 5.16 | Safe Zones for combinations of hip design and non-design related parameters. For head diameters from 26 mm to 32 mm, neck diameters closer to 14 mm and below 18 mm, neck angles between 25 degrees to 35 degrees, cup anatomical inclination from 35 degrees to 50 degrees and cup anteversion below 20 degrees were found within safe ranges for a stable hip implant design.....          | 77 |

## LIST OF TABLES

| Table | Page   |    |
|-------|--|----|
| 2.1   | Patient data for dislocation cases. Age, sex, side of operation and primary causes of dislocation are found significant affecting dislocation statistics. Osteoarthritis was a major contributing factor to all the hip dislocation cases. Mean age of patients with dislocation was reported 70 years ranging from 22 to 94 years. Nearly 67% dislocations were recorded in females; whereas, 33% in males. There was no significance found for the side of operation [24]..... | 12 |
| 2.2   | Dislocation statistics for different surgical approaches and their correlation with femoral head diameters. Dislocation rates for posterior were found 3.5% and 2.7% higher than anterior and lateral, respectively. Difference between instabilities in hips using anterior and posterior was found lowest (1.4%) for 32mm head diameters [3].....  | 16 |
| 2.3   | Dislocations with Acetabular Component Orientation. Amongst all hip instability cases, cups were examined with 31% of too vertical and 29.5% of too retroverted placement [15].....  | 18 |
| 2.4   | Dislocations with Femoral Component Orientation. Hip dislocations are found more sensitive to too anteverted or too retroverted stems as compared to stem loosening or femoral shaft fractures [15].....   | 21 |
| 2.5   | Comparison of studies examined for Early Vs Late Dislocations [3,24].....  | 27 |
| 2.6   | Hip Instability with Previous Surgery and Surgical Approach. Previous hip surgeries, when compared with different surgical approaches (see Table 2.6), showed three folds increase in the frequency of instability with anterior and lateral approaches compared to hip implants without previous surgeries [3].....   | 28 |
| 3.1   | Classification of Hip Models based on the selected design related as well as non-design related parameters. The ranges for all geometrical parameters are also included. The shaded areas on models 1, 5 and 9 help differentiate between all twelve models.....   | 35 |
| 4.1   | von Mises Stresses acquired from static analysis all hip models.....   | 45 |
| 4.2   | Contact Stresses achieved from static analysis of all hip models.....  | 46 |
| 4.3   | Contact penetration achieved from static analysis of all hip models.....   | 47 |
| 4.4   | Sliding Displacement achieved from static analysis of all hip models.....  | 48 |

|     |   |    |
|-----|---|----|
| 4.5 | Stem DOFs Recorded from static analysis of all hip models.....  | 48 |
| 5.1 | Comparison of Neck Diameters with Maximum Stresses using Tukey-Kramer HSD method: (a) Neck Diameter comparability of mean of Maximum stresses using Tukey-Kramer HSD method; (b) Neck Diameter comparison using difference in the mean of Maximum stresses.....   | 54 |
| 5.2 | Comparison of Neck Angles with Maximum Stresses using Tukey-Kramer HSD method. Three hip models with 50 degrees were observed with 65.6% higher mean stresses compared to four hip models with 35 degrees of neck angles. Similarly, three hip models with 25 degrees of neck angles showed 52.8% higher mean stresses compared to analyzed four hip models with 35 degrees of neck angles..... | 55 |
| 5.3 | Comparison of Head Diameters with Mean Contact Stresses using Tukey-Kramer HSD method. Peak contact stress recorded for one hip model with 20 mm head diameter was not found within comparable range of peak contact stresses recorded for rest of the eight hip models with larger head diameters (26 mm to 40 mm).....  | 59 |
| 5.4 | Comparison of Cup Anatomical Angle with Mean Contact Stresses using Tukey-Kramer HSD method. Hip models designed with all four cup anatomical inclinations showed comparable mean contact stresses.....   | 61 |
| 5.5 | Comparison of Head Diameter with Mean Contact Penetrations using Tukey-Kramer HSD method. Mean penetrations showed less significant difference when plotted for 26 mm to 40 mm head diameters; however, there was 7.2% increase in mean penetration observed for 32 mm head diameters compared to 26 mm head diameters.....   | 62 |
| 5.6 | Comparison of Cup Anatomical Angle with Mean Contact Penetrations using Tukey-Kramer HSD method. All four selected cup inclination angles were examined within the comparable range for their observed mean penetrations.....   | 63 |
| 5.7 | Comparison of Head Diameter with Mean Sliding Displacement using Tukey-Kramer HSD method. 40 mm head diameters were observed with lowest sliding displacement between the contact surface of femoral head and target surface of acetabular cup. An intermediate behavior without significant difference in displacements was recorded between 20 mm and 26 mm head diameters.....               | 65 |

## LIST OF ACRONYMS

| Acronym          | Definition                                   |
|------------------|--|
| P                | Contact Penetration in millimeter            |
| $\tau$           | Unit Time                                    |
| ANOVA            | Analysis of Variance                         |
| ANSYS            | Analysis System                              |
| CI               | Cup Inclination                              |
| CP               | Contact Penetration                          |
| CS               | Contact Stress                               |
| DOF              | Degree of Freedom                            |
| FEA              | Finite Element Analysis                      |
| FEM              | Finite Element Method                        |
| HD               | Head Diameter                                |
| H-N Ratio        | Head to Neck Ratio                           |
| LWR              | Linear Wear Rate                             |
| ND               | Neck Diameter                                |
| ROM              | Range of Motion                              |
| SD               | Sliding Displacement                         |
| THA              | Total Hip Arthroplasty                       |
| THR              | Total Hip Replacement                        |
| Tukey-Kramer HSD | Tukey-Kramer Honestly Significant Difference |
| UHMWPE           | Ultra-High Molecular Weight Polyethylene     |

## ACKNOWLEDGEMENTS

My supervisor, Dr. Tarun Goswami, has put in his great efforts to accomplish this research. With his enthusiasm, inspiration, and great efforts, he made research pleasurable for me. He always had time to explain things clear and simple for me. Without his contribution to innovative ideas and experience, I would have been lost. I owe my most genuine gratitude to Dr. Tarun Goswami.

I am thankful to my sisters, Hetal Bhatt and Vaishali Bhatt, my brother-in-law, Rupesh Bhatt, and my nephew, Vyom Bhatt, for providing me support at each and every stages during my research which helped me focus. I also thank Vinit Patel, Shirish Ingawale, Liemin Au, and Danielle Miller for providing guidance at difficulties that I encountered and make me think several ideas to solve them properly, my roommates for providing me friendly environment and providing me enough support, and Nileshta Patel and Krishna Desai for helping me work through my thesis during final stages. Last but not least, my parents, Asmitaben Bhatt and Kishorkumar Bhatt, who are always there for me to encourage me, selflessly love me, and inspire me. They are the one who taught me that “Truth and hard work always prevails”. I dedicate this thesis to my parents.

November 18, 2008

# 1

## INTRODUCTION

Over 45 years ago, Charnley revolutionized the field of total joint arthroplasty [1]. Since then, the life expectancy of the individual THR has not increased yet the extension of hip arthroplasty was made in more successful Total Knee Joint replacement and to date to almost all the joints [2]. A significant increase in the THR surgeries has been recorded with approximately 500,000 alone in the United States [1]. After aseptic loosening, hip dislocation is observed as a major complication with increasing Total Hip Arthroplasties (THAs) [3]. The rate of dislocation observed in primary arthroplasties ranges from 2% to 11%, a quarter of which requires a revision surgery [4-5]. Amongst all reported THRs from 1970 to 1975, the observed primary dislocations were 2.4% along with the revision surgeries of 15.2% of all THAs [6]. The expected increase in revision surgeries is reported from 37,544 in 2005 to 56,918 in 2030 with estimated hospital cost of more than 2 billion dollars in 2030 [7].

*Dislocation* is defined as mal-positioning of femoral head completely disengaged from articulating surface of acetabular cup locating the femoral head outside of the surrounding rim of acetabular component. Exceedance in the range of motion, applied to the prosthetic hip after Total Hip Arthroplasties (THA), causes femoral head to dislocate during articulations. Range of motion (ROM) when exceeds the permissible ROM, it produces adequate forces to femoral

head to be placed outside of the acetabular component. Activities causing dislocation are frequently resisted by the contact forces between head and rim of the acetabular component. These resisting forces occasionally lead the femoral head to position back in to articulating surfaces of the acetabular cup.

Total Hip Replacement (THR) is a reliable treatment method for less active elder population. However, its application in demanding younger patients may create problems. In case of active person, the weight bearing surfaces create comparatively higher number of articulations under increased contact stresses. Under these circumstances, more debris particles between the femoral head and the acetabular cup surfaces are released. Augmentation of wear particles causes the prosthetic component loosening, and improper articulations. A worn out liner may also cause dislocation. Less accurate range of motion leads to the disengagement between femoral head and acetabular cup, which eventually results in hip dislocation.

## **1.1 DISLOCATION MECHANISMS**

Mechanisms of dislocation include impingement and subluxation which are considered to be leading causes of total hip dislocation [8-9].

### **1.1.1 Impingement**

*Impingement* is identified by the contact between two non-articulating surfaces, such as femoral stem neck and acetabular component surfaces, developing resistant forces and/or moments to dislocate [8]. Impingement between femoral component and acetabular component leads to frequent subluxations as well as generation of wear debris particles resulting in long-term dislocation [10].



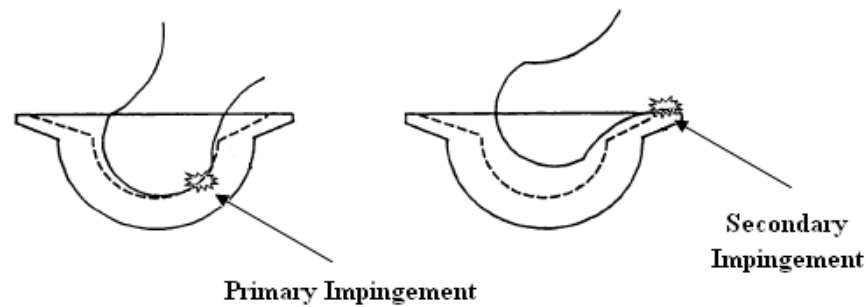


Figure 1.1 Types of Impingement causing Dislocation [11]. Primary impingement can lead to secondary impingement if patient activity exceeds permissible ROM. The risk of dislocation increases after secondary impingement.

Figure 1 [11] explains two different classifications of impingement: Primary and Secondary. Excessive internal or external rotation leads femoral cup to impact on the articulating surfaces of acetabular cup. This mechanism creates primary impingement between contact surfaces of the head and the cup. Primary impingement might not always be followed by secondary forces, if enough resisting forces generate and hold the head into the cup socket. Internally or externally rotated hip implant when forced for flexion or extension, it leads to secondary impingement. Secondary impingement can be metal-on-metal, bone-on-bone or hybrid (metal-on-bone) impingement. After secondary impingement, risk of dislocation increases compared to primary dislocation.

The leading cause of dislocation is the impingement, although impingement might always not be followed by dislocation. After few neck impingement occurrences, the sequence of opposite forces/torques applied to the stem may lead to stem loosening eventually resulting in dislocation [12]. Prior to absolute dislocation, frequent impingements can occur due to restricted ROM that may be followed by

the mal-positioning of prosthetic components [13-14]. Failure to restore the muscular balance during THA can lead to impingement causing dislocation if supplied by sufficient forces for femoral head to dislocate.

### **1.1.2 Subluxation**

*Subluxation* is the supplementary process to the dislocation, usually referred as the partial dislocation [9]. Subluxation occurs when the femoral head makes contact with non-articulating outer rim of acetabular cup but slides back into the acetabular socket before it completely dislocates (see Figure 2). Subsequent to hyper flexing, subluxations are found to be 93% influencing to dislocations after THAs [9].

Sensation of subluxation is often painful and can be notified only after relocation of the femoral head in to the acetabular socket. Observation of subluxations is nearly impossible due to uncertainty of the occurrence. The symptoms of subluxations can be found at the outer surfaces of acetabular component. Major causes of subluxation are thought to be the weakness or muscular imbalance of hip muscle which may be due to neurological disorder [15]. Improper anatomical positioning of acetabular component or femoral components can lead to the subluxation.

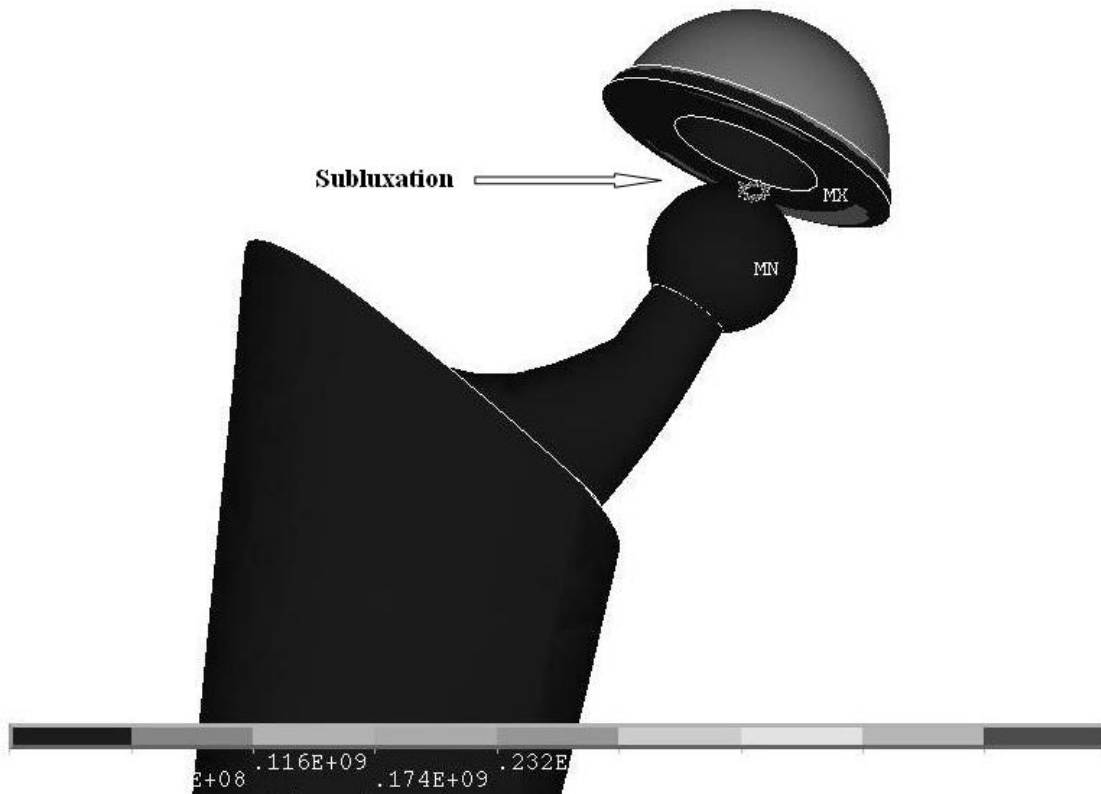


Figure 1.2 Subluxation during dynamic simulation of Hip Implant into ANSYS 11.0. One of the hip implant encountered the subluxation during an attempt of dynamic simulation.

Subluxations are often repeated events and depend on the activity of daily life.

Restoration of muscular tensions can help reduce the occurrence of subluxation

up to some extent. Restrictions of hyperactivities causing subluxations can be

avoided to decrease the rate of dislocation [9]. To reduce the risk of dislocation

after THR, causes of dislocation should be thoroughly evaluated and some safety

mechanisms should be studied and applied during THA [9].

### 1.1.3 Engineering Aspects

Further reported reasons causing dislocation include weakness or loss of contractibility of muscle tension [16], loosening of stem due to fracture in the femoral shaft [15] and soft tissue imbalance caused by loosening of trochanter which increases the possibility of prosthetic components' mal-positioning [17]. During implantation, failure to correct the geometrical orientation of acetabular cup is reported to be one of the major factors leading to dislocation [13].

Acetabular component leads to posterior dislocation if placed too vertical or anterior dislocation if placed too anteverted [13,15]. Improper fixation of the prosthetic components due to previous fractures or defects can result in dislocation of the prosthetic hip during articulations [17].

Geometrical design parameters of hip prosthesis are major factors responsible for dislocation. There are many design parameters affecting dislocation which include femoral head diameter, femoral neck diameter, cup inner diameter, cup liner thickness, head-neck ratio, stem abduction angle, cup anatomical inclination, cup anteversion and other component orientation features. Investigation of ideal combinations of these parameters is essential to help reduce risk of dislocation. Several non-design related parameters are also accounted for in order to reduce dislocation. Non-design related parameters include soft tissue tensions, surgeon experience and surgical techniques used for THA [8]. These variables are considered to be the limitations that affect performance of a hip implant as less significant parameters inducing dislocation.

## 1.2 MOTIVATION FOR STUDY

Despite the rate of dislocation, there are several other additional failure modes that may require a revision THR surgery. Excluding primary hip disease, the incidence of neurological problems was examined up to 22% in primary dislocations with 75% of the recurrent dislocations. Damage to the muscles with primary or revision THR may lead to the loss of contractibility of abductor muscles [16]. In order to reduce the chances of dislocation, muscle tension must be restored back after primary or revision THA.

The chance of dislocation increases after first dislocation, if revised. Recurrent dislocations are observed to be at higher occurrence rate than primary dislocations. The dislocation rate of 5.5% in revision surgeries stayed 3.8% higher than that of 1.8% in primary THRs [6,16]. Besides increasing probability of dislocation, it gives acute pain and abductor muscle damage distressing the confidence of patient as well as surgeon [8,16]. Occurrence of dislocation lengthens hospital stay for patient and often requires revision surgery.

This research emphasizes on optimization of design as well as non-design related parameters of hip prosthesis so that risk of dislocation may be reduced in THR. Twelve different hip implant models were developed with different parameters including head diameter, neck diameter, neck angle, head-to-neck ratio, cup thickness, and cup anatomical orientations. These models were investigated for an individual permissible range of motions (ROMs), contact stresses, and dislocation resisting forces and moments. The results were statistically analyzed to evaluate individual effects of selected parameters on the complete performance of a hip implant. This research also examined

combinations of design related as well as anatomical orientation related factors to reduce the risk of dislocation. Hip models were used to define the dislocation mechanisms including impingement and subluxation along with improved geometrical placement of prosthetic components and calculating permissible ROMs. This study was also performed to determine the safe zones for all design and non-design related parameters based on their individual and collaborative effects on hip dislocation and develop a comparatively stable hip implant.

Since no one will willingly participate in an *in-vitro* study to dislocate his/her hip implant, the computational simulation studies are of significant importance. This investigation was performed using static simulation of fine meshed 3-dimensional total hip implant. Limitations of this study include neglect of soft tissue tension which may improve hip implant stability, if restored back after THR surgery. Finite element model created easily changeable prosthetic component designs, their material specifications, component orientations and applied loading conditions. Such a computational method includes cost savings and before the design is marketed, salient features of designs are determined for a particular design with respect to whether or not it will dislocate.

## 2

# REVIEW OF LITERATURE

Numerous parameters control the long-term performance of an artificial hip implant [18\*]. Factors affecting hip stability need to be examined in order to increase the efficiency of a hip implant. Several factors are being studied to reduce the risk of hip dislocation. Geometrical parameters are found to significantly influence the performance of a hip implant [19]. These geometrical parameters are design as well as non-design related. Design related parameters are femoral head diameter, stem neck diameter, stem length, stem neck angle, and acetabular cup liner thickness. The efficiency of design related parameters may be increased by appropriate manufacturing processes. Non-design related factors include femoral component orientation and acetabular component orientation which needs to be taken care of by physicians during THA surgeries.

One of the most disturbing problems in THR is the wear of polyethylene cup liner. With an increase in number of articulations, a significant volume of material loss occurs. Pyburn and Goswami [20] performed a finite element analysis to determine the stress distribution during the weight-bearing conditions for different stem cross-sections. A stem design with broad lateral areas help transfer more loads during gait, reducing the risk of hip implant failure. Similar finite element studies [21,22] were performed to evaluate the importance of hip stem design for a successful total hip replacement. In a study reported by the author [18\*], several wear

mechanisms were studied to examine the wear behavior leading to prosthetic component loosening leading to hip dislocation. Four major contributing factors included in the study of wear rate were surface roughness, clearance between articulating surfaces of femoral head and acetabular cup liner, coefficient of friction, and sliding distance.

Metal-on-metal combination was widely used throughout the invention era of THR [18]. Excellent mechanical stability and fatigue resistance of metal were the key factors for the preceding use of metals. Further improvements in the material properties led the use of ceramics due to their excellent biocompatibility [18]. Zirconia was observed with lowest wear rate amongst all ceramics [23]. Recently, highly cross-linking of UHMWPE is being experimented to achieve the excellent control of wear rate in total joint arthroplasties.

Long-term performance of a hip implant requires ability to resist dislocation. This behavior is classified in three categories: Preoperative factors, Intraoperative factors, and postoperative factors. Preoperative factors include patient data including age, sex, weight and side of operation along with surgeon's experience, primary causes of dislocation and several surgical approaches. Major contributing parameters to dislocation include femoral and acetabular component defects and depicted as Intraoperative factors. Orientation of prosthetic component was found highly significant affecting the dislocation. Postoperative factors include dislocation mechanisms, time of dislocation, and significance of revision surgery and recurrent dislocations. Dislocation mechanisms include three classified types of dislocation: anterior, superior and posterior dislocation. Time of dislocation was observed as either early or late with respect to time after surgery. Effects of revision surgery causing recurrent dislocations will be discussed as postoperative factors affecting the risk of dislocation.



## **2.1 PREOPERATIVE FACTORS**

Reported significance of preoperative factors affecting dislocation varies from study to study. Patient data including age, sex, weight, and side of operation were found to be less contributing yet significant factors influencing dislocation [24]. However, a reported case study examined femoral bending due to overweight of patient [25]. Surgeon's experience has been reported as a major factor affecting dislocation incidences [3,24,26-29].

Osteoarthritis was found 65.9% significant of all contributing factors amongst recorded incidences of diagnoses [30]. Infection was examined to be 6.6% affecting in the series by Charnley [30]; while there was no evidence of infection reported by Williams [31]. Individual preferences for surgical method include anterior, lateral or posterior approach. Review of literatures shows controversial issue for different surgical approaches; 0.2% higher dislocation rate using posterior approach reported by Ali Khan [15]; in contrast, the advantages using posterior approach reported by Roberts [32]. Review of research performed on dislocation rates efficiently proves multifactorial behavior of dislocation affecting parameters. Table 2.1 [24] describes the evidence of age, sex, side of operation, and diagnosis features.

### **2.1.1 Clinical Perspectives**

It is evident that experience and skill of a surgeon performing THA affects rate of dislocation incidences [24,29]. Continuous examination of presented dislocation incidences can help evaluate the efficiency of a surgeon [29]. Frequency of dislocation cases by inexperienced surgeon was found twice as that of an experienced surgeon showing 50% higher risk by those who undertook occasional THR surgeries [29]. Another reported study [24] showed 76% evidence in

reducing dislocation by an experienced surgeon compared to 10% of those by inexperienced colleague. The same study reported 14% risk of dislocation by surgeons who were intermediate on the scale of experience. The increase in the surgical experience can significantly help reduce the rate of dislocation.

Table 2.1 Patient data for dislocation cases [24]. Age, sex, side of operation and primary causes of dislocation are found significant affecting dislocation statistics. Osteoarthritis was a major contributing factor to all the hip dislocation cases. Mean age of patients with dislocation was reported 70 years ranging from 22 to 94 years. Nearly 67% dislocations were recorded in females; whereas, 33% in males. There was no significance found for the side of operation.

| Factor               | Dislocated THA | Non-dislocated THA | All THA    |
|----------------------|----------------|--------------------|------------|
| Total Cases          | 60             | 118                | 1838       |
| Mean Age (Range)     | 71 (43-89)     | 71 (52-85)         | 70 (22-94) |
| Gender (%)           |                |                    |            |
| Men                  | 33             | 32                 | 30         |
| Women                | 67             | 68                 | 70         |
| Operated Side (%)    |                |                    |            |
| Left                 | 50             | 50                 | 45         |
| Right                | 50             | 50                 | 55         |
| Diagnosis (%)        |                |                    |            |
| Arthritis            | 42             | 43                 | 58         |
| Rheumatoid arthritis | 28             | 25                 | 15         |
| Hip fracture         | 30             | 30                 | 23         |
| Others               | 0              | 2                  | 4          |

### 2.1.2 Primary Causes of Dislocation

In order to understand the mechanisms that cause dislocation, both surgical and design aspects must be bridged. An identified cause can be effectively treated using systematic treatment approaches. For example, the dislocation due to mal-position of acetabular component or femoral component can be treated by

improving their design related or orientation related factors. Design related treatments can efficiently reduce chances of dislocation, and relate to head-neck diameter ratio, allowable range of motion (ROM), head diameter, etc. However, component orientation related factors such as cup inclination or anatomical offset of femoral component can be emphasized during THR surgeries.

There are some profound factors like osteoarthritis and femoral fracture which are considered to be major factors causing dislocation; although, they are difficult to prevent. Major reason for difficulties in their prevention is due to limitation of our knowledge in their causes and effects. McMurray [33] reported his attempts to analyze types of osteoarthritis in a hip joint. Osteoarthritis can be differentiated in two categories: Unilateral and Bilateral. Unilateral osteoarthritis includes a group of patients with some noticeable changes in mechanical relationships between femoral head and acetabular cup. Effective causes include severe injury to the weight-bearing surfaces of femoral head or acetabular cup. Increased joint stiffness can also be a possible feature causing osteoarthritis which reduces ability of ordinary movements during daily activities and increases pain [33]. Bilateral osteoarthritis may be differentiated with mechanical disturbances on both sides which frequently contribute to trauma. The symptoms of bilateral osteoarthritis may include an unequal progress of changes in both joint and occasionally the less affected joint may not be noticed until definite time duration [33].

Prosthetic instability may occur due to mal-positioning [3,26] and also by osteoarthritis, rheumatoid arthritis, and hip fracture [28,30,34-36]. Osteoarthritis

was reported 65.9%; whereas, rheumatoid arthritis with 26.5% affecting hip instability [30]. The same study reported 6.6% evidence of infection amongst all diagnosis factors; whilst there was no evidence of infection found following the treatment of dislocation during a similar study [31]. As an evidence of examined dislocation statistics, Table 2.1 shows 71% effectiveness of osteoarthritis amongst 11% and 14% contribution of rheumatoid arthritis and hip fracture, respectively [24]. All of these studies successfully show increased effectiveness of hip fracture by 8% compared to rheumatoid arthritis [27]. Osteoarthritis is a major contributing factor amongst all identified primary diagnosis.

Oblique osteotomy is reported as one of the successful treatments for osteoarthritis [33]. During oblique osteotomy, a large amount of weight is transferred to the femur shaft instead of pelvis, reducing applied loads on the hip joint; and second is to rotate the femur head such that a new articulating face can contribute during the weight bearing articulations [33].

### **2.1.3 Age, Gender, Weight and Side of Operation**

The rate of dislocation incidences was found to be influenced by patient age, sex, gender, weight and side of operation [3,26,35,37]. Mean age of patients with dislocation was reported 70 years ranging from 22 to 94 years [24,27]. The frequency of dislocation in females was higher than that in males [24,26-28]. Table 2.1 [27] describes the evidence of patient gender for dislocation cases that were recorded as 61 females compared to 39 male patients. Another study reported 70% dislocation cases in females and 30% in males [27]. A reported ratio

of dislocation for women to men was three to one, which is significant enough to conclude that females are more sensitive to dislocation than males [28].

Obesity is also found to be a major influencing factor causing stem bending, component loosening or fracture [25-26]. In a study [25], 6.2% of all 160 patients were observed with component loosening and all were overweight. Side of operation was also found as a significant factor affecting dislocation [27,38-39]. In a study of 1023 patients, the hip replacements in females were found 4.6% higher in right compared to left hip; and in males, the THR was found 6% higher in the left than in the right hips [26]. The ratio of left to right hip replacements was recorded to be 45 to 55 in the literatures [21,24,27].

#### **2.1.4 Surgical Approach**

Several surgical approaches, used for THR surgery, greatly depend on experience of the surgeon and his/her choice. The anterolateral and posterior techniques have been reported to result in hip dislocation [3,26,32,35,40]. A study compared trans-trochanteric approach used in Malmö General Hospital with posterior approach used in Kalmar County Hospital [39]. Nearly equal dislocation statistics were observed with 3.4% for trans-trochanteric and 3.3% for posterior approach. The examined dislocation rate for anterolateral approach was 1.9% compared to 2.1% using posterior approach [41].

Table 2.2 Dislocation statistics for different surgical approaches and their correlation with femoral head diameters. Dislocation rates for posterior were found 3.5% and 2.7% higher than anterior and lateral, respectively. Difference between instabilities in hips using anterior and posterior was found lowest (1.4%) for 32mm head diameters [3].

| Head Diameter (mm) | Surgical Approach (No. of Hips) |     |         |     |           |     | Total |     |
|--------------------|---------------------------------|-----|---------|-----|-----------|-----|-------|-----|
|                    | Anterior                        |     | Lateral |     | Posterior |     | No.   | %   |
|                    | No.                             | %*  | No.     | %   | No.       | %   |       |     |
| 22                 | 571                             | 2.6 | 1251    | 2.7 | 88        | 6.8 | 1910  | 2.9 |
| 28                 | 151                             | 1.3 | 295     | 4.1 | 511       | 6.0 | 957   | 4.7 |
| 32                 | 48                              | 2.7 | 352     | 3.4 | 86        | 3.5 | 486   | 3.3 |
| Total              | 770                             | 2.3 | 1898    | 3.1 | 685       | 5.8 | 3353  | 3.5 |

\* Numbers in % columns show percentages of Total hip instabilities

Woo and Morrey [3] compared dislocation rates for different surgical approaches and their correlation with femoral head diameters in THRs (see Table 2.2). Anterior surgical approach showed average of 2.3% dislocation in hips with 22 mm, 28 mm, and 32 mm head diameters; which was noticed to be comparatively lower than lateral and posterior surgical approaches. Hips that were implanted using posterior approach obtained instability with comparatively higher average rate of 5.8% than both anterior and lateral for all ranges of head diameters. Dislocation rates for posterior were found 3.5% and 2.7% higher than anterior and lateral, respectively. Instability in the hips implanted with lateral approach (37% for all head diameters) was reported to be in between the anterior and posterior approaches. Difference between instabilities in hips using anterior and posterior was found lowest (1.4%) for 32mm head diameters [3]; which indicates that large head diameter reduces dislocation rates.

## 2.2 INTRAOPERATIVE FACTORS

Operative errors can be corrected by emphasizing surgeon's awareness on appropriate placement of prosthetic components; however, the errors introduced due to mechanical failure including defects in prosthetic components need to be corrected by emphasizing on technical details of prosthetic hip designs [42-43]. After THR, several intraoperative factors are responsible that induce prosthetic hip dislocation. Improper selection of geometrical design parameters of femoral component and acetabular component significantly increases the rate of dislocation. Impingement between femoral neck and acetabular cup eventually leads to dislocation, which can be avoided by using appropriate cup anatomical orientation as well as femoral stem orientation [44-46]. Geometrical parameters including head diameter, neck diameter, neck angle, and cup thickness and stable range of motion determine the risk of dislocation.

### 2.2.1 Defects in Acetabular Component

Orientation of acetabular component and its correlation with dislocation rates were discussed [28,36,38,44]. Acetabular cup circumference helps properly hold the femoral head and allows appropriate range of motion by reducing chances of dislocation. Acetabular cup liner thickness was also reported as a significant factor affecting contact stresses and wear between acetabular cup and femoral head surfaces [47-48]. *In vitro* wear of acetabular cup liner is a multi-factorial process which is greatly affected by acetabular design factors as well as its anatomical orientation [49-50]. Cup thicknesses lower than 9 mm showed increased linear wear rate with larger head diameters. Volumetric wear rate was

found to increase with an increase in femoral head diameter for provided cup thickness lower than 11 mm [47,51].

Improper inclination of acetabular cup was found a common cause of dislocation due to its too anteverted or too vertical placement [15]. Table 2.3 shows an analysis of 112 dislocations due to defects in acetabular cup orientation. Amongst all hip instability cases, cups were examined with 31% of too vertical and 29.5% of too retroverted placement. A study [15] reported increase in dislocation chances if the cup was anteverted above  $15\pm 10$  degrees or placed vertical above  $40\pm 10$  degrees.

Table 2.3 Dislocations with Acetabular Component Orientation. Amongst all hip instability cases, cups were examined with 31% of too vertical and 29.5% of too retroverted placement [15].

| Acetabular Cup Placement | Early Dislocations | Late Dislocations | Total |      |
|--------------------------|--------------------|-------------------|-------|------|
|                          |                    |                   | No.   | %*   |
| Loose                    | 8                  | 5                 | 13    | 11.6 |
| Too Anteverted           | 20                 | 13                | 33    | 29.5 |
| Too Retroverted          | 10                 | 3                 | 13    | 11.6 |
| Too Vertical             | 17                 | 18                | 35    | 31.3 |
| Too Superior             | 11                 | 6                 | 17    | 15.2 |
| Too Inferior             | 1                  | 0                 | 1     | 0.9  |
| Total                    | 67                 | 45                | 112   |      |

\*Numbers in % columns show percentages of total dislocation cases

An *in vitro* study [52] examined effects of prosthetic component orientation on offered ROM. With increase in acetabular and femoral anteversion, flexion and



internal rotation movements seem to increase; however, it restricts external rotation and adduction movements with extended hip prosthesis.

As shown in Figure 2.1, amongst all total hip dislocations, 90% of the cases were evaluated with 50 degrees or more inclination angle with horizontal axis for acetabular component [31]. Subsequently, 35% of these cases were examined with the revision dislocations. The cup inclinations showed higher rate of failure for 20 to 60 degrees. Above 60 degrees of cup inclination, the revision dislocations were found less frequent than the primary dislocations. The recommended vertical inclination of cup is  $40$  to  $40 \pm 10$  degrees and anteversion is  $15 \pm 10$  degrees [38].

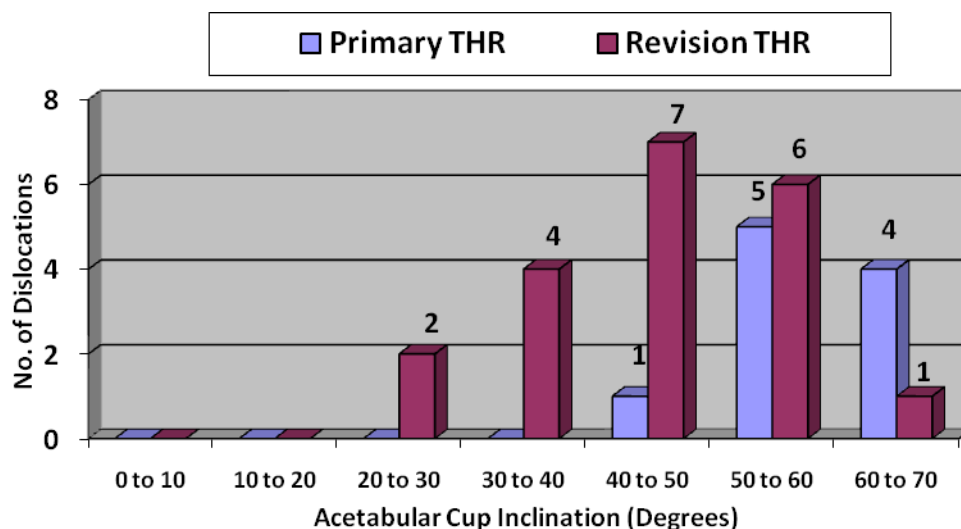


Figure 2.1 Acetabular Cup Inclinations in Primary and Revision THRs. Amongst all total hip dislocations, 90% of the cases were evaluated with 50 degrees or more inclination angle with horizontal axis for acetabular component [31].

## 2.2.2 Defects in Femoral Components

Dislocations due to femoral component defects were found significant in THR. Major factors contributing to femoral component defects include femoral head size, head-neck ratio, proper stem fixation, and stem orientation [53]. Smaller

head diameters were examined to be more significant resulting in not only dislocation but also recurrent dislocation as compared to large head diameters [26,53-54]. Since, larger head diameter increases allowable ROM and needs to travel large amount of distance to get dislocated, it is examined with comparatively less risk of dislocation [11,54-56].

Another study [3] reported the rate of instability in hip implants using several surgical approaches. Prosthetic hip implantation using anterior approach showed 2.6% instability in 22 mm head diameter compared to 1.3% and 1.2% in 28 mm and 32 mm head diameters, respectively. Using posterior approach, less difference was noticed between 22 mm (68% of all dislocations) and 28 mm (60% of all dislocations). However, 32 mm femoral head was examined with 3.5% higher stability compared to other two head diameters [3].

Impingement between neck and acetabular component can be reduced by evaluating appropriate neck length as well as neck diameter [38]. Increase in neck length provided higher ROM reducing chances of primary impingement of neck with the outer rim of acetabular cup [56]. Smaller Neck cross-section was observed with higher ranges of motion and also with reduced possibility of impingement between femoral neck and outer rim of acetabular cup [57].

Conversely, smaller neck diameters may produce higher stresses at contact area between femoral head and neck. Hip implants with higher neck diameters help provide comparatively higher contact area with femoral head reducing contact stresses; however they may limit allowable ROM. Several combinations of femoral neck and head diameters are succinctly examined in the present study.

Femoral stem orientation is proven to be a significant factor affecting dislocation rate. Table 2.4 describes correlation of different stem orientation with dislocation cases [15]. Hip dislocations are found more sensitive to too anteverted or too retroverted stems as compared to stem loosening or femoral shaft fractures. Too anteverted and too retroverted stem orientations were respectively 44.9% and 22.4% contributing to all recorded hip dislocations. Stem loosening with 12.2% and femoral shaft fractures with 14.3% were observed relatively less contributing to all dislocations caused by femoral component defects. An uncommon case was examined with complete femoral stem migration from the femoral shaft due to femoral component loosening [58].

Table 2.4 Dislocations with Femoral Component Orientation. Hip dislocations are found more sensitive to too anteverted or too retroverted stems as compared to stem loosening or femoral shaft fractures [15].

| Femoral Placement      | Early Dislocations | Late Dislocations | Total |      |
|------------------------|--------------------|-------------------|-------|------|
|                        |                    |                   | No.   | %*   |
| Loose                  | 5                  | 1                 | 6     | 12.2 |
| Too Anteverted         | 17                 | 5                 | 22    | 44.9 |
| Too Retroverted        | 10                 | 1                 | 11    | 22.4 |
| Too much Neck removed  | 3                  | 0                 | 3     | 6.1  |
| Femoral Shaft Fracture | 7                  | 0                 | 7     | 14.3 |
| Total                  | 42                 | 7                 | 49    |      |

\*Numbers in % columns show percentages of total dislocation cases

In order to reduce the stresses on the stem area after prosthetic hip implantation, several studies have been reported on the stress analysis of femoral stems [59-60]. Higher stress levels at the proximal stem area may result in fatigue failure of

femoral component [59]. Cyclic stress distribution and body weight plays an important role in fatigue failure of stem [59]. To reduce the risks of dislocation due to femoral stem defects, a study has been reported investigating an innovative design of cervico-trochanteric stemless prosthesis replacing the traditional stem-type prosthesis [61]. A review of unusual case studies [62-64] examined femoral heads completely disengaged from stem necks due to excessive force applied during closed reduction of dislocated femoral components.

Comparison of Table 2.3 and Table 2.4 determines that a series of dislocation cases are less effective to the defects in femoral component compared to acetabular component.

## **2.3 POSTOPERATIVE FACTORS**

A study observed computationally predicted dislocations as more likely to be maneuver dependent [65]. The study showed six times higher risk of dislocation for low-sit-to-stand movement compared to stopping. Significance of recurrent dislocation is a disturbing issue for both patient and surgeon. A review [66] of 39 dislocation cases reported sixteen cases (41%) as single dislocation; whereas, 23 cases (59%) with more than one dislocations. Another study [67] of elevated acetabular liner showed 2.9% primary dislocation as compared to 7% of recurrent dislocations that had revision surgery.

### **2.3.1 Dislocation Features and Mechanisms**

A significant difference in the direction of dislocation was noticed by researchers [3,28]. When patient activity level exceeds the permissible ROM of a prosthetic hip, dislocation occurs. Direction of dislocation depends on the type of

activity causing a hip implant to rotate above its limitations. Three different directions of dislocations were classified (see Figure 2.2): 1. Anterior dislocation, which usually occurs when the leg is externally rotated or abducted too much; 2. Superior dislocation, which may occur due to fracture in acetabular component or complete migration of femoral component disengaging the articulating surfaces other than posteriorly or anteriorly; 3. Posterior dislocation, which occurs when leg is forced to flex during internally rotated or too much abducted position [26].

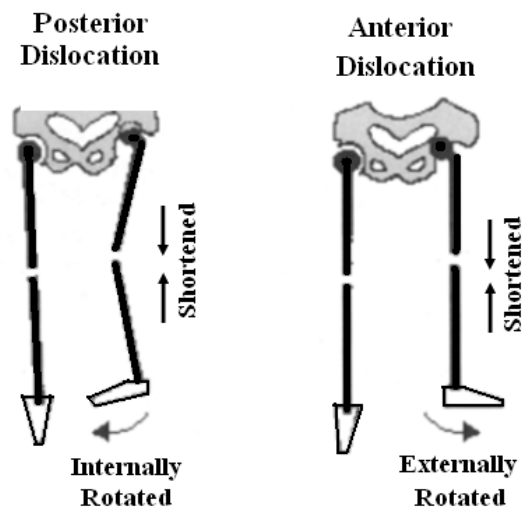


Figure 2.2 Types of Dislocation. Anterior dislocation usually occurs when the leg is externally rotated or abducted too much; whereas, Posterior dislocation, which occurs when leg is forced to flex during internally rotated or too much abducted position [26].

Anterior dislocations were found to occur less frequently (11% of all hip dislocations) than posterior dislocations [68]. Anterior dislocations are often difficult to differentiate from posterior dislocations. Hyper extension, higher external rotation and higher abduction are examined as effective causes of anterior dislocation [26]. Damaged soft tissue often fails to recover the normal hip position after effective ROM which weakens the stability of prosthetic

components, finally causing dislocation [3]. Traumatic dislocations are documented as 7% contributing to all types of anterior dislocations. However, anterior dislocations were observed with 3 to 8% of all hip dislocations [3,28], which is significantly lower than posterior and superior dislocations.

Superior dislocations are often misdiagnosed as anterior or posterior dislocations [68]. Hip implants are usually found hyper extended at the time of dislocations. Fracture of acetabulum can be one of the possible causes that may lead to the hip protrusion into the pelvis. Superior dislocations were observed with 13 to 20% contributing to all types of hip dislocations [3,28].

Most common feature of all hip instabilities is posterior hip dislocation [3,26,28,68]. It usually occurs due to hyper extension, higher adduction or internal rotation. Internally rotated hip when forced to hyper flex, posterior dislocation occurs. Patient getting up from a low chair or bent to pick up an object from the ground are most common activities leading to this type of dislocation [26]. Posterior instabilities are examined to be more than 85% of all hip dislocations [68]. The comparison of cases showed 78% dislocation of total 116 unstable hips [3] and that 77% dislocations of total 23 unstable hips [28] were found posterior in direction.

### **2.3.2 Time of Dislocation**

Based on the time of observation after THR surgery, dislocations can be classified into two categories: Early and Late. Time of dislocation recorded as early and late may vary from study to study. Usually, dislocations within 6 weeks are said as

early, and after 6 weeks as late [26]. A study [35] succinctly described several possible causes affecting early and late dislocations. Instabilities within first three months may occur due to lack of time needed for soft tissue healing or lack of patient education related to hip care. Unless there is mal-positioning of prosthetic components, early dislocations can be easily cured using closed reduction.

Instabilities between 1 to 5 years are usually allocated with a well defined cause of dislocation. Reoperations of these dislocated hip implants are more likely to get success in their intension. Instabilities after five years are usually examined with wear of articulating surfaces as a major factor causing dislocation. Several possible causes of late dislocations include worn out polyethylene liner of the cup or increased range of motion due to weakened tissue tension.

A significant difference between early dislocations and late dislocations has been examined [15,3,24,26]. Reference [15] showed nearly 66% of dislocations reported within first five months of surgery, which is significantly comparable to 70% of dislocations observed within first month of surgery [31]. Another study reported 85% early dislocations (within 6 months) with an average of 4.6 days after THA [26]. The study showed three of seventeen dislocations on the same night they were discharged from hospital.

Table 2.3 and Table 2.4 compare early and late dislocations due to defects in acetabular and femoral components. Hip implants with acetabular defects showed 58.9% (67 cases) as early and 40.1% (45 cases) as late dislocations; whereas, hips with femoral defects showed 85.7% (42 cases) as early and 14.3% (7 cases) as late dislocations [15]. The study depicted significant difference between early and

late dislocations using a bar chart based on reported times of dislocations (see Figure 2.3). Early dislocation period was evaluated as nearly 5 weeks after the surgery. The reported cases of early and late dislocations were 94 and 48, respectively [15]. The reoperation of early dislocated hips achieved stability in 81% (76 cases) of all hip instabilities; whereas, lately dislocated hips achieved 73% (35 cases) stability.

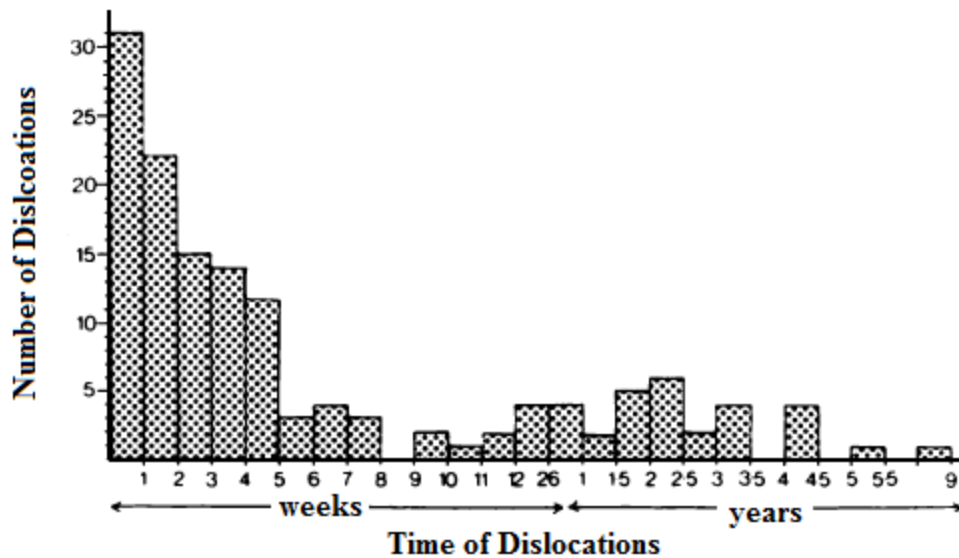


Figure 2.3 Early (within 5 weeks) Dislocations Vs Late Dislocations (within 9 years) [15]

Table 2.5 describes a comparison of early and late dislocations reported within two similar studies. First study [24] was performed on 22 mm head diameter group. The study showed 23 (46%) early of all 50 dislocations within 14 days of surgery compared to 18 (15%) late of all 118 dislocations in Kalmar hospital. Average early dislocations were nearly 59% of all dislocations in both centers; whereas, average of late dislocations was 15.2% of all dislocations. Another study



[3] included a review of total 331 dislocations based on the time of dislocations. Total time observed for all dislocations was nine years. However, 59% of all dislocations were recorded within 3 months and 77% within a year. During 5 years of study, about 16% of total 331 dislocations were observed; whereas, 20 (6%) dislocations were reported between five to nine years after the surgeries were performed.

Table 2.5 Comparison of studies examined for Early Vs Late Dislocations [3,24].

| STUDY 1 [24]         |                    |                 |       | STUDY 2 [3]          |     |     |
|----------------------|--------------------|-----------------|-------|----------------------|-----|-----|
| Time of Dislocations |                    | Hospital Center |       | Time of Dislocations | No. | %*  |
|                      |                    | Kalmar          | Malmö |                      |     |     |
| Early                | Total Dislocations | 83              | 68    | ≤ 1 day              | 17  | 5   |
|                      | ≤ 14 days          | 23              | 8     | ≤ 7 days             | 37  | 11  |
|                      | ≤ 30 days          | 32              | 23    | ≤ 30 days            | 131 | 39  |
|                      |                    |                 |       |                      |     |     |
| Late                 | Total Dislocations | 118             |       | 1 year               | 257 | 77  |
|                      | > 5 years          | 8               | 10    | > 1 year             | 331 | 100 |

\*Numbers in % columns show percentages of total examined dislocation cases

### 2.3.3 Revision Surgery and Recurrent Dislocations

Incessant instability after THR surgery can be painful for a patient and challenging for a surgeon. Reoperation is an ordinary approach to cure the hip instability; although rate of success for reoperation is observed with poor results

after reoperation. After revision surgery, observed rate of recurrent dislocations is always significantly higher as compared to single dislocations [15,24,35,69]. A study [24] of recurrent dislocations and reoperations showed 18 and 23 single dislocations in Kalmar and Malmö, respectively. Multiple dislocations recorded were 32 cases in Kalmar and 45 cases in Malmö; which is 56% and 51% of reported single dislocations, respectively.

Table 2.6 Hip Instability with Previous Surgery and Surgical Approach. Previous hip surgeries, when compared with different surgical approaches (see Table 2.6), showed three folds increase in the frequency of instability with anterior and lateral approaches compared to hip implants without previous surgeries [3].

| Previous Surgery | Surgical Approach (No. of Hips) |     |         |     |           |     | Total |     |
|------------------|---------------------------------|-----|---------|-----|-----------|-----|-------|-----|
|                  | Anterior                        |     | Lateral |     | Posterior |     | No.   | %   |
|                  | No.                             | %*  | No.     | %   | No.       | %   |       |     |
| No               | 630                             | 1.7 | 1241    | 1.7 | 588       | 5.6 | 2459  | 2.6 |
| Yes              | 140                             | 5   | 657     | 5.6 | 97        | 7.2 | 894   | 5.7 |
| Total            | 770                             | 2.3 | 1898    | 3   | 685       | 5.8 | 3353  | 3.5 |

\*% Numbers in % column show percentages of total hip instabilities

Previous hip surgeries, when compared with different surgical approaches (see Table 2.6), showed three folds increase in the frequency of instability with anterior and lateral approaches compared to hip implants without previous surgeries [3]. An increase in frequency of instability after revision surgery with posterior approach was lower; however, posterior approach was found with the highest rate of dislocation independent of prior surgery.

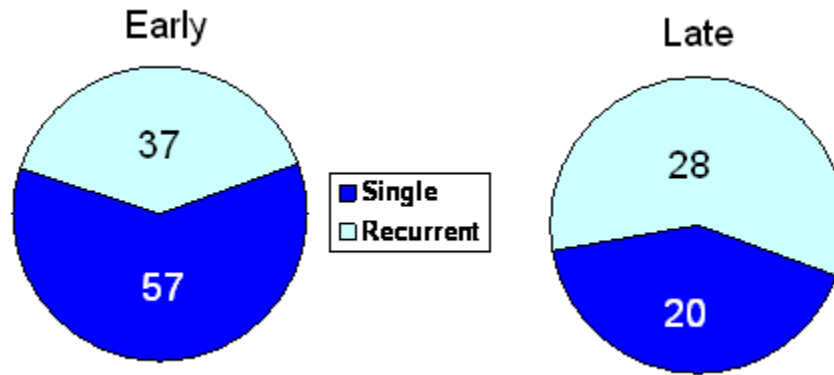


Figure 2.4 Correlation of time of dislocation and rate of recurrence. Higher correlation of recurrent dislocations was observed with late compared to early dislocations [15].

The rate of recurrent dislocations appeared to be correlated with time of dislocations [15]. Figure 2.4 describes higher correlation of recurrent with late dislocations compared to early dislocations. In the case of early, the recurrent dislocations were lower than the single dislocations; although the rate of instability was higher in early as compared to late. Lately occurred recurrent dislocations were reported in 28 cases; whilst single dislocations were examined in 20 cases.

# 3

## **METHODS AND MATERIALS**

This chapter provides details of applied materials, meshing strategies, and different loading conditions that were used to analyze the models. SolidWorks 2008 SP 2.1 was used to create the hip implant models with several design parameters. First, a baseline hip implant was designed and modified to develop twelve different hip models using design and non-design related parameters. Then, 3-D models were imported into ANSYS 11.0. All twelve hip models were analyzed using finite element analysis. The results were then statistically analyzed using JMP 7, an interactive statistical graphical software.

### **3.1 DEVELOPMENT OF 3-DIMENSIONAL SOLID HIP MODELS**

This section illustrates the development of baseline 3-D hip implant model in SolidWorks. Twelve different hip prosthetic models were created with different geometrical parameters. This section enlists the parameters used to design component. A final step to these procedures includes preparation of the developed models to import them into ANSYS 11.0.

#### **3.1.1 Designing of a Baseline Hip Model**

SolidWorks 2008 SP 2.1 is widely used to create complex mechanical models.

Selection of this software basically depended on the ease of manipulating three-dimensional models and even to acquire them for future improvements.

First, three major solid components of a hip implant were created: Femoral Stem, Femoral Head, and Acetabular Cup (see Figure 3.1). A hip implant\* was used to generate dimensions during the designing of this baseline hip model. Approximate stem dimensions in basic hip model included 16 cm of height excluding the neck length of nearly 3.8 cm. Neck length may vary with changes of desired neck angles during further analysis. Neck diameter and neck angle were changeable factors in the developed femoral stem design. Femoral head was designed as a basic model with diameter of 22 mm and a cylindrical cut with radius of 5.5 mm was created to allow stem neck insertion. For femoral head, the changeable parameters were head diameters and the diameter of cylindrical pathway for neck insertion. Acetabular cup was designed with outer radius of 20 mm and inner socket radius with 8 mm. The inner diameter may vary with variation in femoral head diameter. The cup thickness varied between 9 mm to 11 mm based on selection of the design parameters.

All three components were used to design a hip implant assembly. Femoral head was fitted on the top of the neck. Neck diameter was adjusted for proper fixation of the femoral head. This assembly completed a design of a femoral component. The acetabular cup was moved on top of the femoral head to achieve proper socket mechanism between head and cup. The cup orientation angles were defined later based on the classification of different hip implant models.

\*Hip implant was provided from TRIDENT™ Acetabular System by Stryker Howmedica OSTEONICS

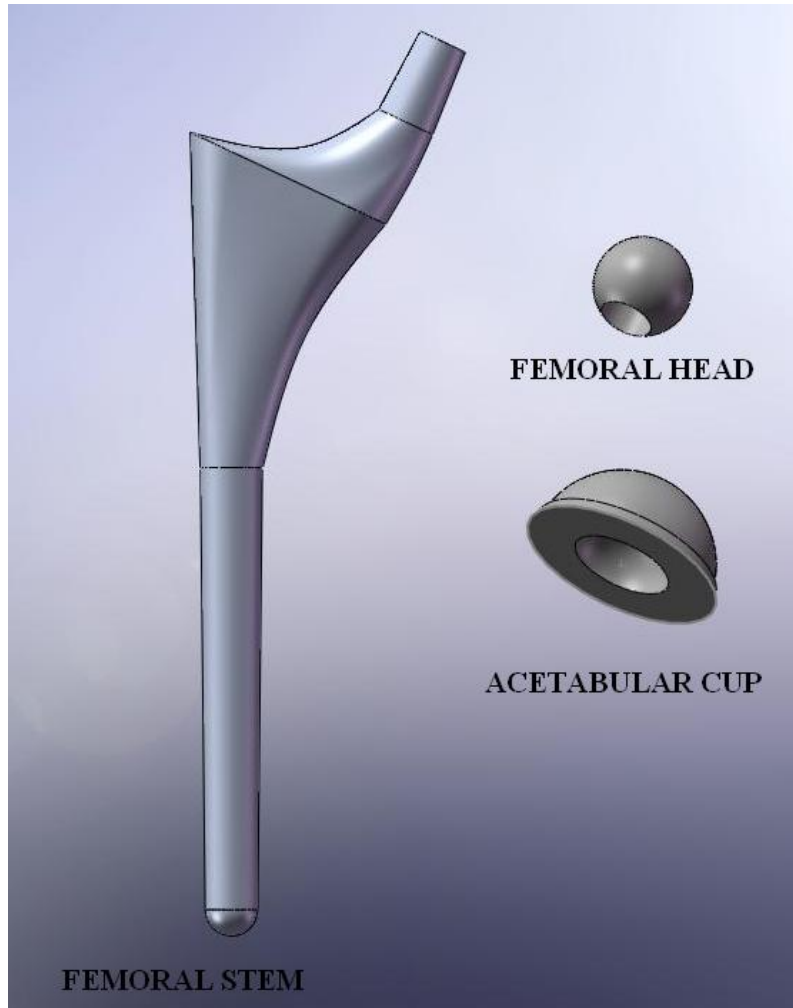


Figure 3.1 Basic components of a Hip Implant in SolidWorks 2008. A complete hip implant assembly was developed using femoral stem, femoral head and acetabular cup.

### 3.1.2 Geometrical Parameters and Classification of Hip Models

Basic hip model was transformed into 12 different hip models according to the selected design parameters of interest. The design parameters in this study were head diameter (HD), neck diameter (ND), head-neck (H-N) ratio, neck angle, cup thickness, cup anatomical inclination, and cup anteversion. Table 3.1 shows all 12 hip models with their design specifications for each model. Importance of the selected geometrical parameters will be discussed later in this section. The ranges

of parameters varied based on reported clinical studies discussed in the previous chapters. The shaded area for model 1, 5 and 9 differentiates a group of three similar models based on the hip design parameter for same head diameter. Cup anatomical angle and cup anteversion angle are the parameters that should be applied during THA surgery. In this study, these two parameters were adjusted while designing the hip model assembly to simulate hip implant stability and dislocations.

Head diameters used in this study were 20 mm, 26 mm, 32 mm and 40 mm in diameters. The head diameters were combined with three other stems to develop all 12 different models. Another femoral component design parameter was neck diameter. Range of neck diameters included 10 mm, 14 mm and 18 mm. H-N ratio was defined as head diameter divided by neck diameter. The selected head and neck diameters defined the H-N ratio from 1.11 to 4. Neck angle was considered as a cause of dislocation when designed with wide ranges. Three different neck angles were used as design parameters of hip models which included 25 degrees, 35 degrees and 50 degrees from vertical axis.

Except design parameters related to femoral component, there were three acetabular component parameters used in the present research. Acetabular cup thicknesses used were 9 mm and 11 mm. Cup thickness was considered secondary to the cup orientation parameters. Figure 3.2 defines different orientation angles of prosthetic components.

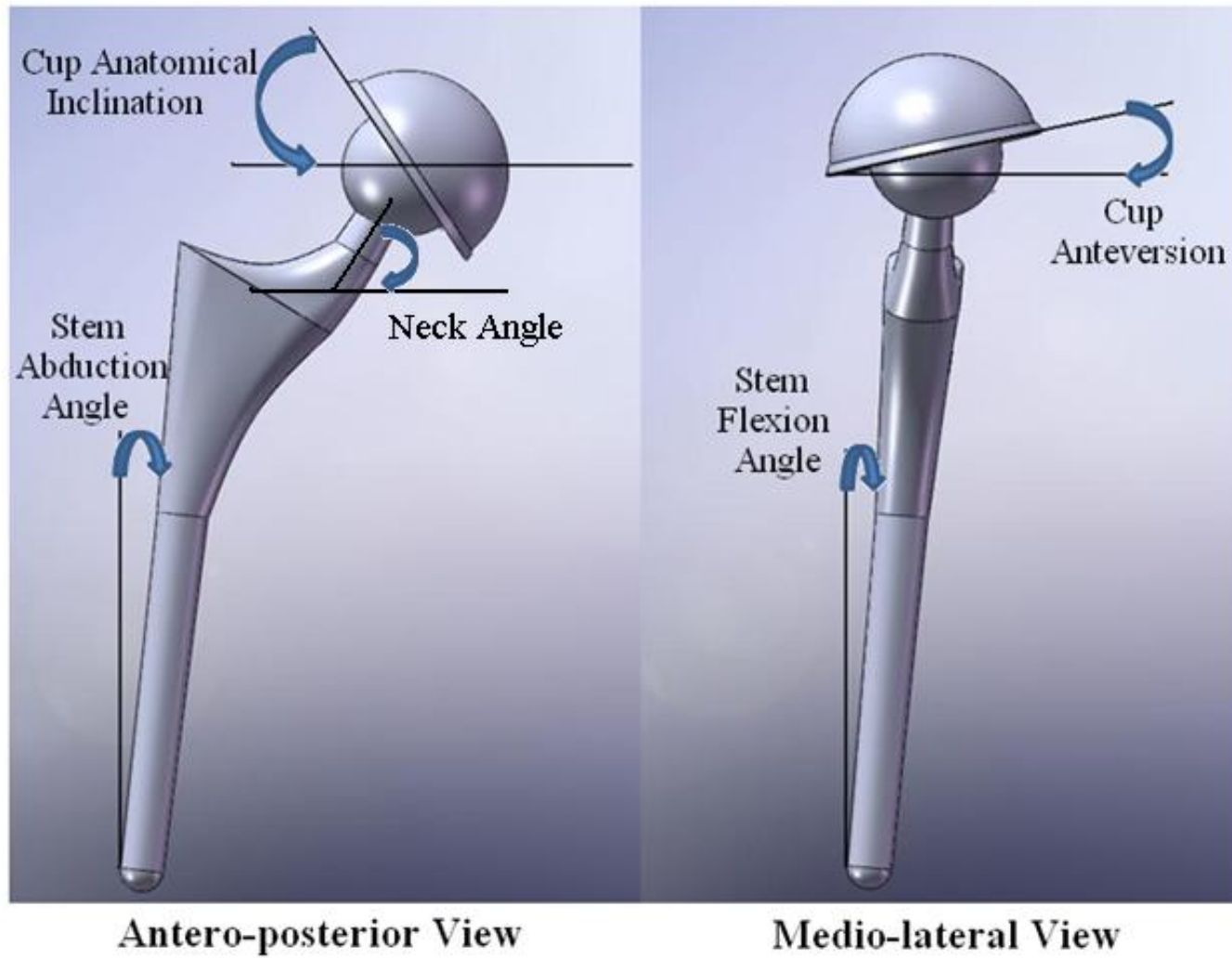


Figure 3.2 Different prosthetic component orientations showed using antero-posterior and medio-lateral views. Femoral component inclinations include stem flexion and stem abduction angles with vertical axis, and neck angle with horizontal axis. Acetabular component orientations include cup anatomical inclination and cup anteversion angle with horizontal plane.



Table 3.1 Classification of Hip Models based on the selected design related as well as non-design related parameters. The ranges for all geometrical parameters are also included. The shaded areas on models 1, 5 and 9 help differentiate between all twelve models.

| <b>Models</b> | <b>Head Diameter (mm)</b> | <b>Neck Diameter (mm)</b> | <b>Head/Neck Ratio</b> | <b>Neck Angle (deg)</b> | <b>Cup Thickness (mm)</b> | <b>Cup Anatomical Inclination (deg)</b> | <b>Cup Ante-version (deg)</b> |
|---------------|---------------------------|---------------------------|------------------------|-------------------------|---------------------------|---|-------------------------------|
| <b>Ranges</b> | <b>20-26-32-40</b>        | <b>10-14-18</b>           | <b>1.11-4</b>          | <b>25-35-50</b>         | <b>9-11</b>               | <b>20-35-50-65</b>                      | <b>5-10-20</b>                |
| <b>1</b>      | 20                        | 10                        | 2                      | 25                      | 9                         | 20                                      | 5                             |
| <b>2</b>      | 26                        | 10                        | 2.6                    | 25                      | 9                         | 35                                      | 5                             |
| <b>3</b>      | 32                        | 10                        | 3.2                    | 25                      | 9                         | 50                                      | 5                             |
| <b>4</b>      | 40                        | 10                        | 4                      | 25                      | 9                         | 65                                      | 5                             |
| <b>5</b>      | 20                        | 14                        | 1.43                   | 35                      | 9                         | 65                                      | 10                            |
| <b>6</b>      | 26                        | 14                        | 1.86                   | 35                      | 9                         | 20                                      | 10                            |
| <b>7</b>      | 32                        | 14                        | 2.29                   | 35                      | 11                        | 35                                      | 10                            |
| <b>8</b>      | 40                        | 14                        | 2.86                   | 35                      | 11                        | 50                                      | 10                            |
| <b>9</b>      | 20                        | 18                        | 1.11                   | 50                      | 11                        | 50                                      | 20                            |
| <b>10</b>     | 26                        | 18                        | 1.44                   | 50                      | 1                         | 65                                      | 20                            |
| <b>11</b>     | 32                        | 18                        | 1.78                   | 50                      | 11                        | 20                                      | 20                            |
| <b>12</b>     | 40                        | 18                        | 2.22                   | 50                      | 11                        | 35                                      | 20                            |

Cup anatomical inclination was studied briefly in this study to reduce the risk of dislocation caused by orientation of acetabular component. Higher the cup anatomical inclinations, higher the chances of anterior or posterior dislocation [15]. The range of cup inclination included 20, 35, 50 and 65 degrees from the horizontal axis. Cup anteversion angle was correlated with cup anatomical inclination. Too anteverted cup shows higher risk of posterior dislocation; whereas, too retroverted cup was found sensitive to anterior dislocation. Cup anteversion angles used in designing present hip implant models were 5, 10 and 20 degrees from the top plane of the hip implant.

### **3.1.3 Preparation for Further Processing into ANSYS 11.0**

All 3-D hip models created into SolidWorks were exported into ANSYS 11.0 using parasolid (.para) format to perform finite element analysis. Parasolid conversion was found more accurate in ANSYS during the present research. Complex geometry of a hip implant assembly appeared to provide higher accuracy with parasolid format. ANSYS could easily import parasolid files into the software database without compromising the accuracy and complexity of 3-D solid geometries. Another way used to import models into ANSYS was IGES (.igs) file format; however, it was not used for analysis due to failure of importing all solid geometries.

## **3.2 DEVELOPMENT OF FINITE ELEMENT MODEL AND FEA**

ANSYS 11.0 is a powerful finite element analysis tool/software widely used for linear/nonlinear structural, thermal or acoustic simulations. It is reliable software extensively used in the industrial, biomedical, automotive and aerospace fields. Finite

element analysis can be used to develop a new geometry and/or analyze the existing model using finite element method. FEA converts the complex geometry into subdivisions and optimizes using mathematical equations. Subdivided geometrical sections are called elements which are achieved by meshing the preferred geometry for FEA analysis. Collective geometrical elements represent an entire geometry to be analyzed. Size of these complex elements is usually selected by user for preferred accuracy of solution. Coarse and/or fine meshing converts a volume into larger or smaller sizes of elements, respectively. Two consecutive elements in the same geometry are connected by common spots, called as *nodes*.

The collection of nodes constructs an element, and a collection of several elements build a complex geometry. Due to applied boundary conditions, the interactions between nodes define nodal solution; whilst, the interaction between elements created by nodal interfaces generate elemental solution. The range of motion for elements is the function of permitted nodal vector constraints, also called as the *degree of freedom* (DOF). Customized degree of freedom combined with loads and solutions controls define the type of finite element analysis. The simulation techniques available in ANSYS help reduce the cost of laboratory experimental set-ups and computational costs. It also saves time required for experimental set-ups and provides results with flexibility and higher accuracy as well.

### **3.2.1 Meshing Strategies and Defining Contact Pairs**

The parasolid (.para) formatted hip assemblies were imported into ANSYS. The higher the geometrical complexity, the lesser will be the chances of perfection for FEA. Figure 3.2 explains the systematic procedure for static analysis to solve the

finite element model after importing into ANSYS. Usually, structural analysis is used for any civil engineering analysis, mechanical parts, aerospace applications or biomechanical applications. Structural analysis can be performed as static, dynamic, modal, buckling, transient dynamic, spectrum or explicit dynamic analysis. The present study includes static and dynamic analysis options which will be explained later in this chapter. Further analysis included classification of volumes to generate specific hip implant geometry.

The volumes imported into ANSYS were considered as some irregular assembly until they were defined using component names. The volumes were selected to provide their specific names as *stem*, *head* and *cup*. An assembly was defined as a *Hip Implant* including all three volumes of stem, head and cup. Defining components make it easy to process their volumes for further analysis. The next step involved element types that were selected for volume mesh.

Present analysis used 10-node 92, 3D Contact 174 and 3D Target 170 elements. Meshing irregular volumetric geometries was successfully performed using 10-node 92 element type. 3D Contact 174 was used to characterize 3D contact or sliding with 3D target element (3D Target 170). A smaller geometry with concave surface was assigned as a contact element and a larger concave geometry was considered as a target element. Head articulating surface were presented as a Contact 174 element and the cup inner articulating surface as a Target 170 element. 3D Target 170 element generates a target surface which consists of several target segments and paired with contact segments of 3D Contact 174 surface.

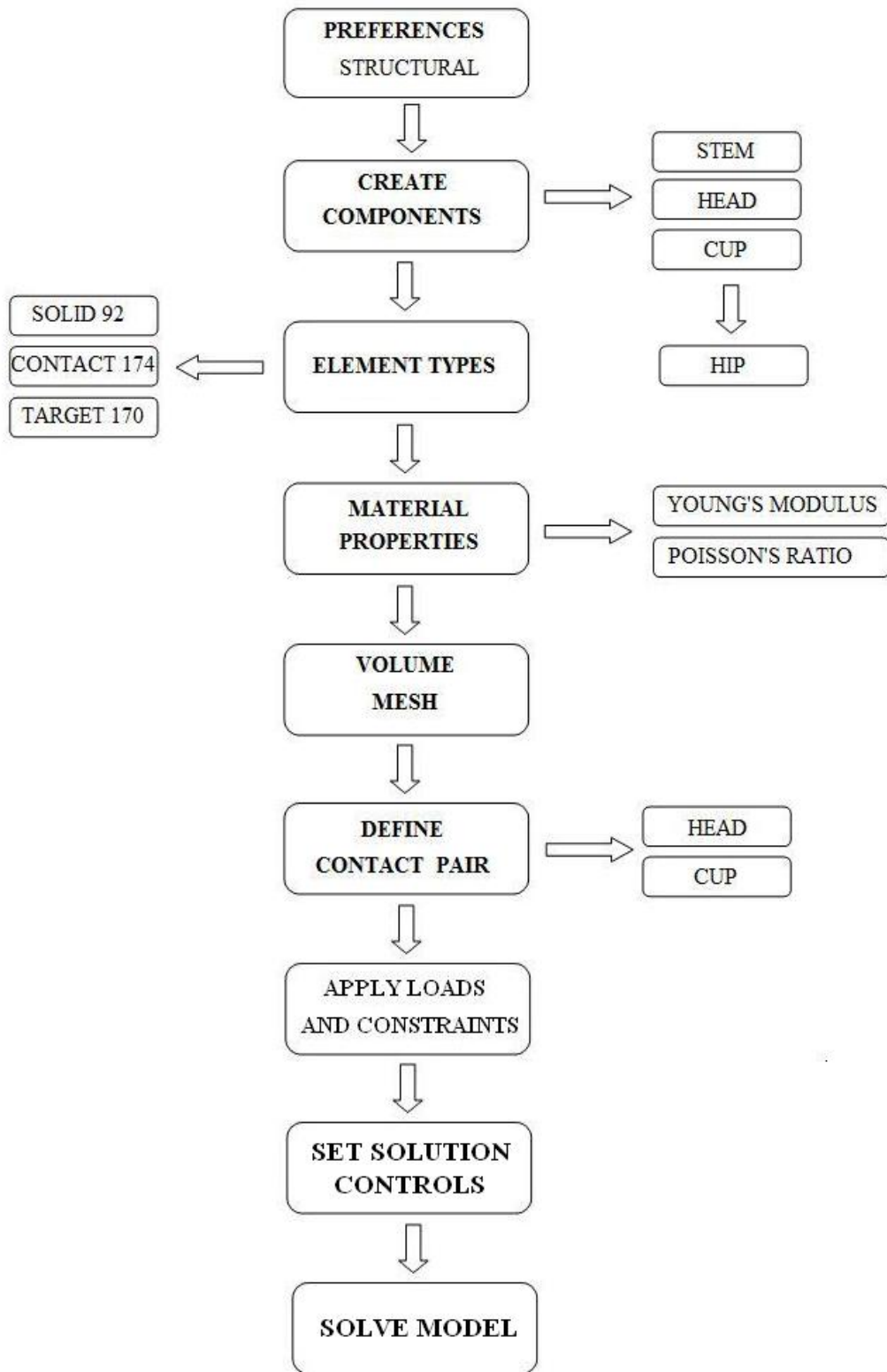


Figure 3.3 Flowchart describing systematic procedures for static analysis in ANSYS.

Material properties define the characteristics of solid geometry to be analyzed. Linear elastic material properties included Young's Modulus and Poisson's Ratio. This study used Young's Modulus of 209 GPa and Poisson's Ratio of 0.3, which defines material characteristics of Stainless Steel 316L. Density of the material was 7800 kg/m<sup>3</sup>.

Volume mesh is important in order to divide large volumes into small elements, which finally defines the accuracy of analysis results. There are three basic steps that need to be followed for a complete volume mesh. 1. Set the element attributes; which allows defining previously added element types to the volumes in order to create volume mesh. During the present study, the stem was defined as 3D Solid 92 element, the head with 3D Contact 174 and the cup with 3D Target 170 in order to create a contact pair. 2. Set mesh controls (optional); which enables user to define smart size level for free meshing. Level of volume mesh ranging from 1 to 10 creates fine to coarse element size, respectively. Present analysis used smart size level of 2. 3. Meshing the model; which permits selections of a volume for free meshing according to the selected element attributes and the smart size level.

Contact surfaces of femoral head and acetabular cup were defined as a contact pair to create accurate results of interactions by articulations during analysis. Contact elements were meshed by selecting the nodes of the upper surface of head and defining element attributes for femoral head. The same method was followed for the target elements by selecting the nodes of the inner surface of cup and meshing them with Target 170. *CNCHECK* command was used to check the

initial contact status between contact and target elements. Subsequent procedures need to define coupled sets to apply DOF, loads and constraints to the nodes.

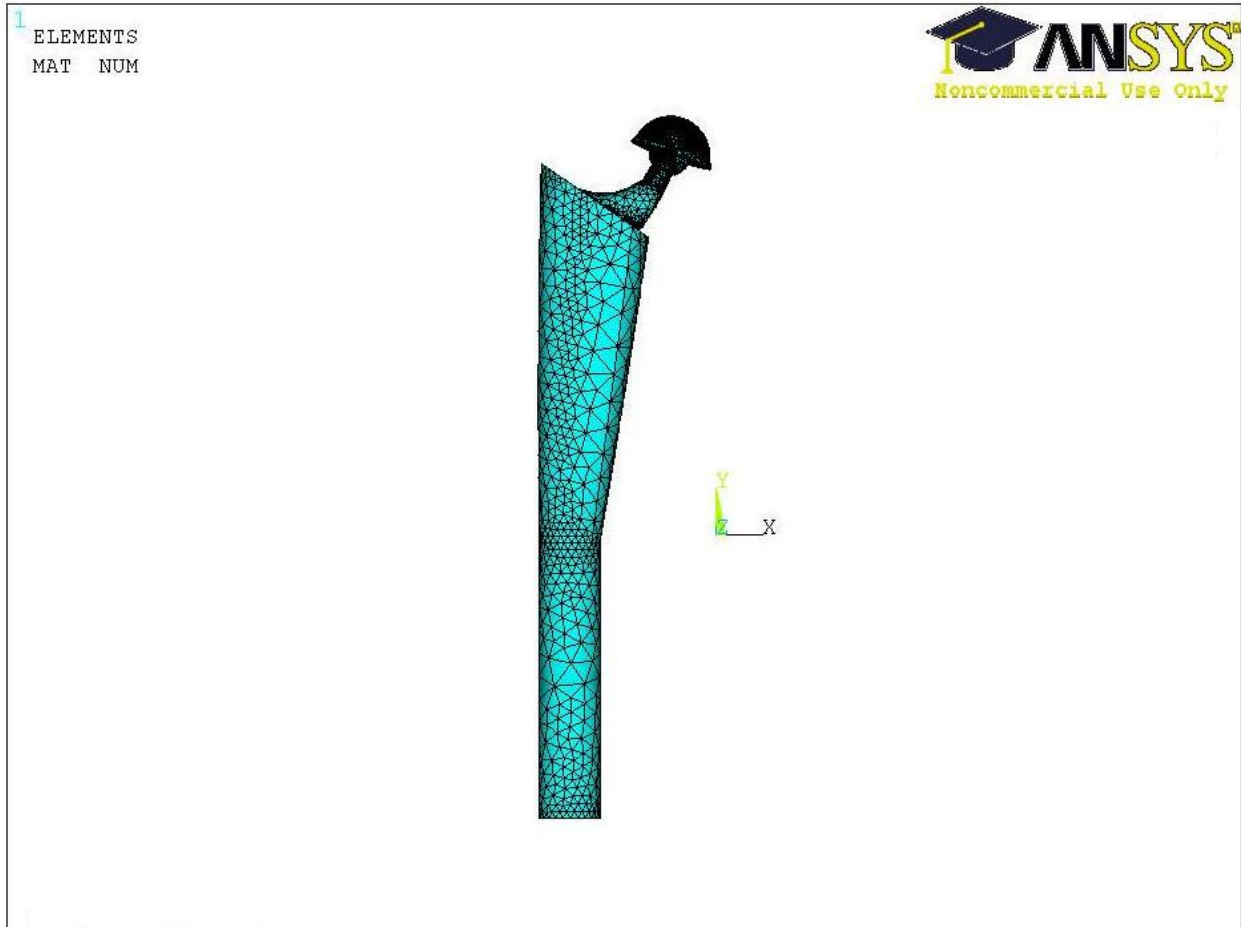


Figure 3.4 Hip Model 1 inserted into Femur with free volume mesh in ANSYS 11.0. A model of femur was developed; however, the static analysis in the present study was performed on the stem without femoral bone.

### 3.2.2 Loads and Constraints

The results show how the entire geometry reacts to the applied loads and constraints. Loads can be displacements, forces, pressures, velocities, thermal, gravity etc. Loadsteps define the load application at certain time intervals. The defined substeps record the results at given time durations in static or dynamic analysis.

Structural loads were applied in order to simulate ROM, and structural constraints to restrict the ROM. Static analysis in the present study needs to simulate loads only in Y-direction and analyze the results for contact stresses and contact penetration between femoral head and acetabular cup. The force of 100 N was applied in Y direction at the nodes of an element located at lower end of the stem. The load applied at the nodes was automatically transferred from nodes and elements. Nodes at the stem area were coupled (using *COUPLE DOFS*) to move at the same pace in all directions and achieve the similar pattern of motion with a stem inserted into a femur. Nodal DOF during analysis was defined into six different ways; UX, UY, UZ, ROTX, ROTY, and ROTZ (DOF in X, Y and Z-direction, and rotations in X, Y, and Z-direction, respectively). The nodes of the outer surface of femoral head were fixed with structural displacement of 0.01 meter; which resisted the stem motion within certain range without allowing femoral component to swing in the space. Nodes at the surface area of acetabular cup were provided zero displacement in all directions in order to fix the cup into acetabulum.

Customized solution controls were used for a static analysis. After load was applied, the analysis type was selected based on the desired simulation characteristics. Static analysis was performed with large static displacements of nodes. Static analysis used in this study was time rate independent; which simply considered time duration as a loadstep counter and recognized the loadsteps and load substeps. The loadstep is a set of loads applied in the given time duration and load substeps defines the time steps within a complete loadstep at which the



solutions were calculated for final display of results. The time at the end of loadstep was kept at 100 seconds with no automatic time stepping. This set up of time applied constant load for 100 seconds with no substeps to be recorded in between 100 seconds. Increase in the load substeps increases the time needed to run complete analysis and calculate results. Current study was performed with no load substeps; however the results after the specified time durations were successfully recorded.

Appendix A shows all twelve hip models analyzed during present study. Hip Model 2 failed during meshing and Hip Model 9 failed to converge during static simulation performed in the present analysis.

### **3.3 STATISTICAL TERMS**

Oneway analysis of variance, also referred as ANOVA, determines the significance of an independent parameter or group within a specified group under examination. A non-significant means using ANOVA for more than one group of experimental data indicates that there is no correlation between individual groups. However, ANOVA fails to determine the specific pair of group which is less significant. To achieve higher accuracy, post Hoc methods are used. To evaluate multiple comparisons between the specified experimental groups, Tukey-Kramer Honestly significant difference (Tukey-Kramer HSD) method was used. Tukey-Kramer HSD significantly correlates multiple groups consisting of equal number of data points with similar variations. Compatibility between parameters of a group using means of their experimental data was analyzed during present analysis. The difference plots between individual mean values of head and neck diameters were successfully analyzed using Tukey-Kramer HSD method.

# 4

## RESULTS

This chapter describes results obtained from static and dynamic analysis during the present study. After completion of the static analysis in ANSYS, results were reviewed by POST1, from the *General Postprocessor* menu. Four significant types of results were recorded from static analysis of all 11 models; one of the twelve models failed while free meshing. In this chapter, results are presented for each of the four categories namely: von Mises stress, contact stress, contact penetration and sliding displacement. The values for stem degree of freedom (DOF) available from the static analysis were also recorded; however, it was not comparable to any geometrical parameters presented in this study.

### 4.1 von Mises Stress

Figure 4.1 shows the von Mises stresses plotted for Hip Model 1 after static analysis with 100 sec of time at the end of a loadstep. The peak intensity of von Mises stresses were examined at the contact area between femoral head and femoral neck for all eleven hip models (see Table 4.1). The range of von Mises stresses recorded was 0.65 MPa to 1.733 MPa.

Majority of peak stress intensities were found at the contact surfaces between the head and the neck. A few models showed that highest stresses generated at the section of the

stem connected with distal portion of the neck. Highest stresses at the stem portion were found in the hip models with higher neck angles. Since, individually recorded stress intensities show maximum stress behavior for entire hip model, it will be referred as *Maximum Stresses* later in this chapter.

Table 4.1 von Mises Stresses acquired from static analysis all hip models.

| HIP MODEL | VON MISES STRESS (MPa) | HIP MODEL | VON MISES STRESS (MPa) |
|-----------|------------------------|-----------|------------------------|
| 1         | 1.71                   | 7         | 1.16                   |
| 2         | N/A                    | 8         | 0.92                   |
| 3         | 1.07                   | 9         | N/A                    |
| 4         | 1.17                   | 10        | 1.733                  |
| 5         | 0.73                   | 11        | 1.728                  |
| 6         | 0.65                   | 12        | 1.725                  |

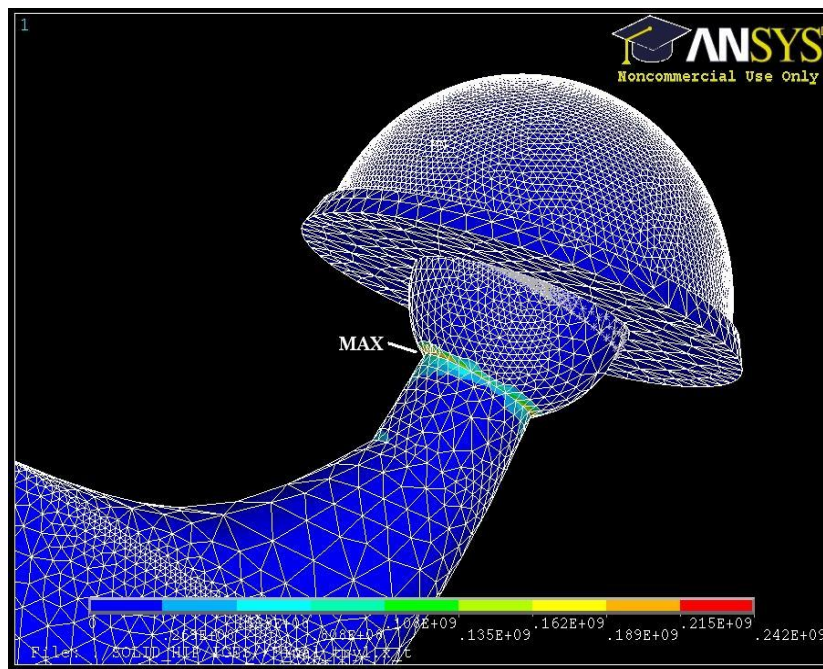


Figure 4.1 von Mises stresses plotted for static analysis of Hip Model 1.

## 4.2 Contact Stress

Forces applied during present static analysis simulate ground reaction forces applied in a hip prosthesis in Y-direction. These forces tend to migrate the femoral component towards acetabular component producing significant contact stresses. Contact pair in the present study was defined as surface-to-surface contact. The forces exerted due to femoral head surfaces on acetabular liner will be enlisted as contact stresses.

Table 4.2 Contact Stresses achieved from static analysis of all hip models.

| <b>HIP MODEL</b> | <b>CONTACT STRESS (MPa)</b> | <b>HIP MODEL</b> | <b>CONTACT STRESS (MPa)</b> |
|------------------|-----------------------------|------------------|-----------------------------|
| 1                | N/A                         | 7                | 1.16                        |
| 2                | N/A                         | 8                | 9.14                        |
| 3                | 9.16                        | 9                | N/A                         |
| 4                | 28.71                       | 10               | 8.32                        |
| 5                | 110.7                       | 11               | 6.92                        |
| 6                | 15.17                       | 12               | 7.49                        |

Contact stresses for all hip models are listed in Table 4.2. The range of recorded contact stresses was from 1.16 MPa to 110.7 MPa; which were significantly higher compared to von Mises stresses listed previously. It was evident higher stress intensities at the contact between femoral head and cup articulating surfaces (Table 4.2).

## 4.3 Contact Penetration

Contact penetration at the acetabular cup surfaces was determined. Penetration was observed between the contact surface of femoral head and the target surface of acetabular cup as shown in Table 4.3.

Table 4.3 Contact penetration achieved from static analysis of all hip models.

| <b>HIP MODEL</b> | <b>CONTACT PENETRATION (mm)</b> | <b>HIP MODEL</b> | <b>CONTACT PENETRATION (mm)</b> |
|------------------|---------------------------------|------------------|---------------------------------|
| 1                | N/A                             | 7                | 0.2                             |
| 2                | N/A                             | 8                | 0.21                            |
| 3                | 0.187                           | 9                | N/A                             |
| 4                | 0.2                             | 10               | 0.21                            |
| 5                | 0.3                             | 11               | 0.14                            |
| 6                | 0.193                           | 12               | 0.191                           |

The highest contact penetration was 0.3 mm to as low as 0.14 mm for all the hip models. Little or no penetration was found at the surface elements of acetabular cup which was unable to interact with contact surface of femoral head. These elements are more likely to be closer to the outer rim of acetabular cup.

#### **4.4 Sliding Displacement**

Vertical forces applied during the static analysis caused the femoral head to slide on the inner surface of the acetabular cup. The higher angles of acetabular cup are more likely to induce higher sliding displacement of femoral contact surfaces. Table 4.4 describes results examined as sliding displacement for all hip models. The range of displacements reported was from 0.15 mm to 0.73 mm. Sliding displacement was believed to be dependent on the co-efficient of friction. The friction co-efficient applied during present static analysis was 0.1; which was believed evident factor producing sliding displacement.

Table 4.4 Sliding Displacement achieved from static analysis of all hip models.

| <b>HIP MODEL</b> | <b>SLIDING DISPLACEMENT (mm)</b> | <b>HIP MODEL</b> | <b>SLIDING DISPLACEMENT (mm)</b> |
|------------------|----------------------------------|------------------|----------------------------------|
| 1                | N/A                              | 7                | 0.73                             |
| 2                | N/A                              | 8                | 0.15                             |
| 3                | 0.1729                           | 9                | N/A                              |
| 4                | 0.172                            | 10               | 0.171                            |
| 5                | 0.172                            | 11               | 0.1709                           |
| 6                | N/A                              | 12               | 0.173                            |

Table 4.5 Stem DOFs Recorded from static analysis of all hip models.

| <b>HIP MODEL</b> | <b>STEM DOF (mm)</b> | <b>HIP MODEL</b> | <b>STEM DOF (mm)</b> |
|------------------|----------------------|------------------|----------------------|
| 1                | 7.9762               | 7                | 2.3664               |
| 2                | N/A                  | 8                | 2.1567               |
| 3                | 5.4491               | 9                | N/A                  |
| 4                | 6.0107               | 10               | 1.0818               |
| 5                | 2.5365               | 11               | 1.0262               |
| 6                | 2.3606               | 12               | 1.0076               |

Stem DOFs used during static analysis for all hip models were tabulated in order to understand the stem migration towards the acetabular component. Table 4.5 shows that Stem DOFs were positive in values during present analysis due to forces applied in the positive Y-direction compared to the origin of all solid hip models. These stem DOFs are vector sum of the displacements recorded in X, Y and Z-directions. These values were

not used during statistical analysis due to stem DOF independency on the design parameters of interest in the present research.

# 5

## DISCUSSION

The design parameters for all the twelve solid hip models were determined based on the review of literature, discussion with industry, and physicians. Design parameters were studied in this research to develop a hip implant model with an ideal combination of head diameter, neck diameter, neck angle, cup anatomical angle, cup anteversion, and head-neck ratio in order to achieve a stable artificial hip joint.

Analytical results were used to develop mathematical prediction models. One such model was developed to predict surface stress; whereas, several other models were developed to predict penetration. This study provides new models to predict new models to predict the wear rates under *in vitro* conditions which may be extended to *in vivo* situations. The results are discussed below for various categories.

### 5.1 EFFECTS OF GEOMETRICAL PARAMETERS ON MAXIMUM STRESS

Head diameters were found to affect significantly the stability of a hip implant. As discussed in chapter 2 [11,54-56], larger head diameters provided higher stability. The present analysis found higher stresses for head diameters above 26 mm. The lowest von Mises stresses were found for 26 mm head diameter designed with 14 mm neck diameter.



Table 4.1 in the previous chapter 4 shows the lowest von Mises stress of 0.65 MPa for hip model 6, which is designed with 26 mm head diameter and 14 mm neck diameter.

von Mises stresses from all hip models are plotted using Oneway Anova (Figure 5.1).

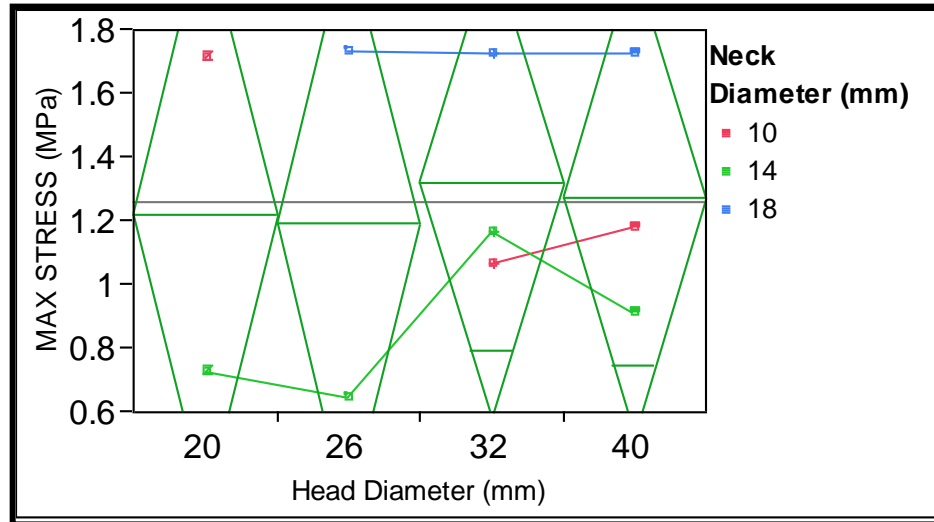


Figure 5.1 Oneway Analysis of Maximum Stress by Head Diameter and Neck Diameter. The lowest von Mises stresses were examined for 26 mm head diameter designed with 14 mm neck diameter.

Figure 5.2 (b) shows a bar chart of mean of maximum stresses with their respective head diameters. Two Hip Models analyzed with 20 mm and 26 mm head diameters showed mean stresses of 1.22 MPa and 1.19 MPa, respectively (refer to Figure 5.2 (a)). Mean stress value for 32 mm head diameter was highest of all analyzed hip models; whereas, the mean stress for 26 mm head diameter was found lowest of all series of hip models. Head diameter of 20 mm showed intermediate value of mean stress.

Hip models with 32 mm and 40 mm head diameters showed 10.9% and 6.7% higher mean stresses compared to hip models with 26 mm head diameters. In hips with 14 mm neck diameter, 26 mm head diameter showed 48.9% lower stresses compared to 32 mm

head diameter. All head diameters showed less than 1% difference of stresses in combination with 18 mm neck diameter. 20 mm head diameters were examined with 1.7% higher mean stresses compared to head diameters of 26 mm.

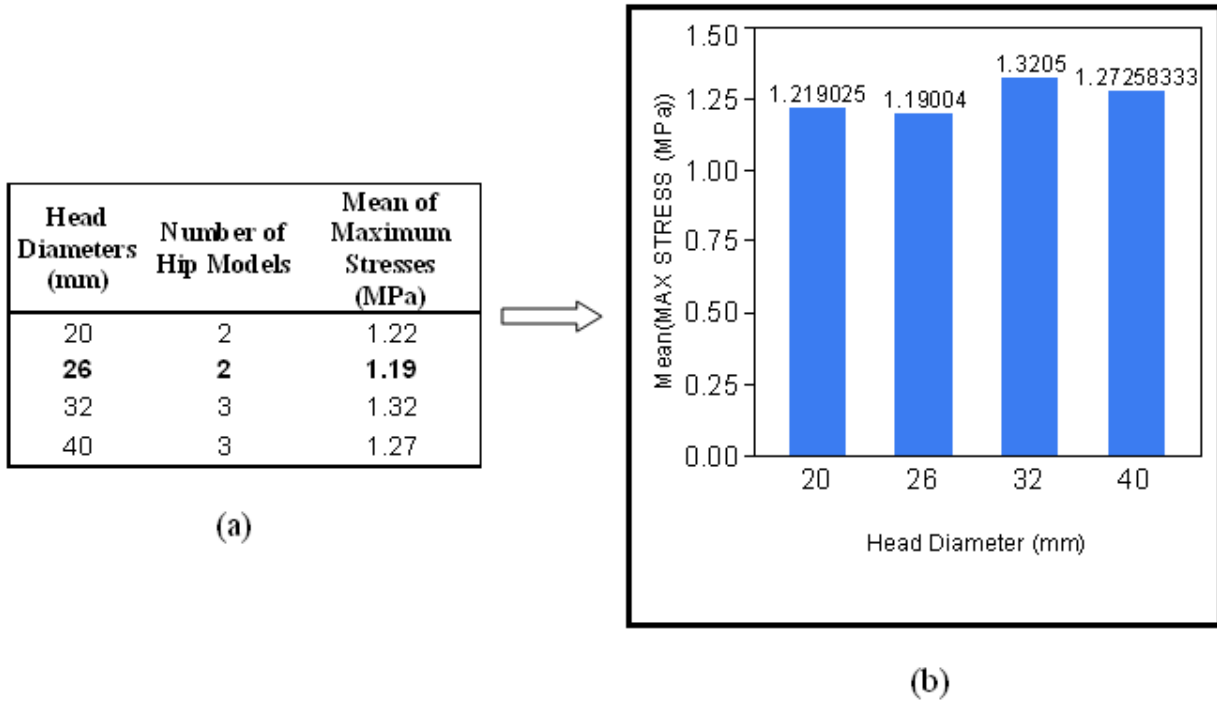


Figure 5.2 Head Diameter Vs Mean of von Mises stress. (a) Tabulated mean of von Mises stresses for all head diameters with analyzed number of hip models (b) Bar chart was plotted using Oneway Anova. Mean stress value for 32 mm head diameter was highest of all analyzed hip models; whereas, the mean stress for 26 mm head diameter was found lowest of all series of hip models.

A significant comparison was found between von Mises stresses for hip models with all neck diameters. Common locations of maximum von Mises stresses for all analyzed hip models were contact area between femoral head and neck. Figure 5.3 compares all neck diameters for their respective means of maximum stresses using Oneway Anova method. Models with 14 mm head diameters were examined with lowest mean stresses compared to 10 mm and 18 mm neck diameters. The comparability plot (Table 5.1(a)) using

Tukey-Kramer HSD method differentiates the means of maximum stresses recorded for all models.

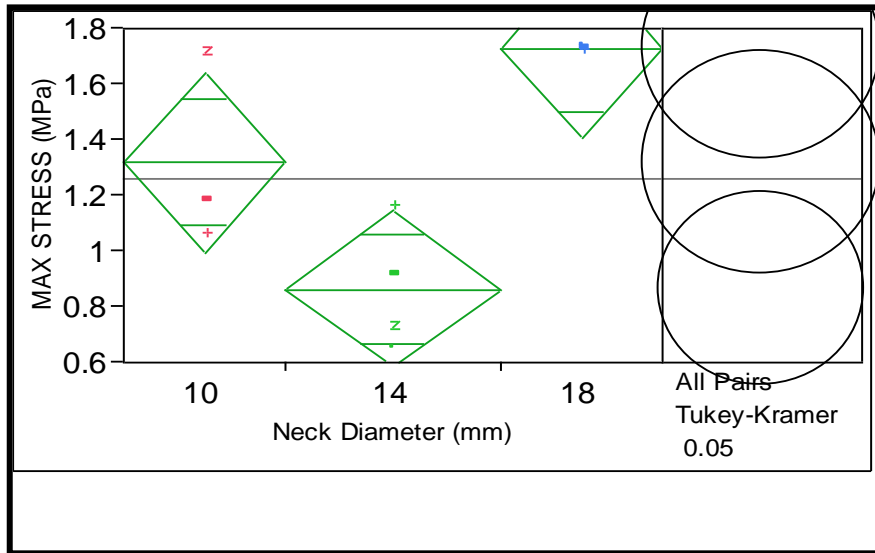


Figure 5.3 Oneway Analysis of Maximum Stress by Neck Diameter. Models with 14 mm head diameters were examined with lowest mean stresses compared to 10 mm and 18 mm neck diameters.

Mean stresses for 18 mm and 10 mm neck diameters were comparable. Similarly, 10 mm and 14 mm neck diameters showed significant comparison for mean stresses; however, there was no comparison found between the range of stresses obtained for 14 mm and 18 mm neck diameters meaning that they are not comparable and design parameters used for 18 mm neck diameter are not viable and should not be used.



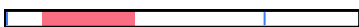
Table 5.1 (b) shows considerable differences in the mean stresses for hip models when correlated with their neck diameters. Three hip models with 18 mm neck diameter showed nearly 100% and 30.3% higher stresses as compared to 14 mm and 10 mm neck diameters, respectively; whereas, mean stresses of four hip models with 14 mm neck diameter was found nearly 50% and 34.6% lower compared to hip models with 18 mm

and 10 mm, respectively. Comparisons between neck diameters and mean stresses were significantly evaluated with a  $R^2$  value of 0.77.

Table 5.1 Comparison of Neck Diameters with Maximum Stresses using Tukey-Kramer HSD method: (a) Neck Diameter comparability of mean of Maximum stresses using Tukey-Kramer HSD method; (b) Neck Diameter comparison using difference in the mean of Maximum stresses.

| Neck Diameter (mm) | Number of Hip Models | Comparability | Mean of Maximum Stresses (MPa) |
|--------------------|----------------------|---------------|--------------------------------|
| 18                 | 3                    | A             | 1.78                           |
| 10                 | 3                    | A             | 1.32                           |
| 14                 | 4                    | B             | 0.86                           |

(a)

| Level of Neck Diameter (mm) | Level of Neck Diameter (mm) | Difference of Mean Stresses | Difference Plot of Mean Stresses   |
|-----------------------------|-----------------------------|-----------------------------|--|
| 18                          | 14                          | 0.87                        |  |
| 10                          | 14                          | 0.46                        |  |
| 18                          | 10                          | 0.41                        |  |

(b)

Maximum stresses when compared with both head and neck diameters, a combination of lower head diameters and higher neck diameters (too low H-N ratio) produced higher stress results (see Figure 5.1). Hip models with higher neck diameters (18 mm in the present study) were found worst meaning higher stresses regardless of the head diameter selection.

Table 5.2 Comparison of Neck Angles with Maximum Stresses using Tukey-Kramer HSD method. Three hip models with 50 degrees were observed with 65.6% higher mean stresses compared to four hip models with 35 degrees of neck angles. Similarly, three hip models with 25 degrees of neck angles showed 52.8% higher mean stresses compared to analyzed four hip models with 35 degrees of neck angles.

| Neck Angle (Degrees) | Number of Hip Models | Comparability | Mean of Maximum Stresses (MPa) |
|----------------------|----------------------|---------------|--------------------------------|
| 50                   | 3                    | A             | 1.73                           |
| 25                   | 3                    | A             | 1.32                           |
| 35                   | 4                    | B             | 0.86                           |

Neck angle showed considerable effects on von Mises stresses ( $R^2 = 0.77$ ). The neck angles were 25 degrees, 35 degrees and 50 degrees. Three hip models with 50 degrees neck angles showed 65.6% higher mean stresses compared to four hip models with 35 degrees of neck angles (Table 5.2). Similarly, three hip models with 25 degrees of neck angles showed 52.8% higher mean stresses compared to analyzed four hip models with 35 degrees of neck angles. Hip implants with 25 degrees of neck angle showed 23.7% lower mean stresses compared to those with 50 degrees. A similar behavior was reported by Latham and Goswami [19]. With an increase in neck angle, the contact stresses were observed to be significantly higher than lower neck angles.

Hip implants with different head diameters and neck angles were plotted simultaneously to find their effective combinations on stress results (Figure 5.4). All hip models with 50 degrees of neck angles showed comparatively higher von Mises stresses regardless of the head diameter sizes combined in those models. Neck angle of 25 degrees were evaluated with intermediate stress values with lowest stresses when combined with 32 mm head diameter and highest when combined with 20 mm head diameter. The best combination

of all hip models was 26 mm head diameter and 35 degrees neck angle with 14 mm neck diameter.

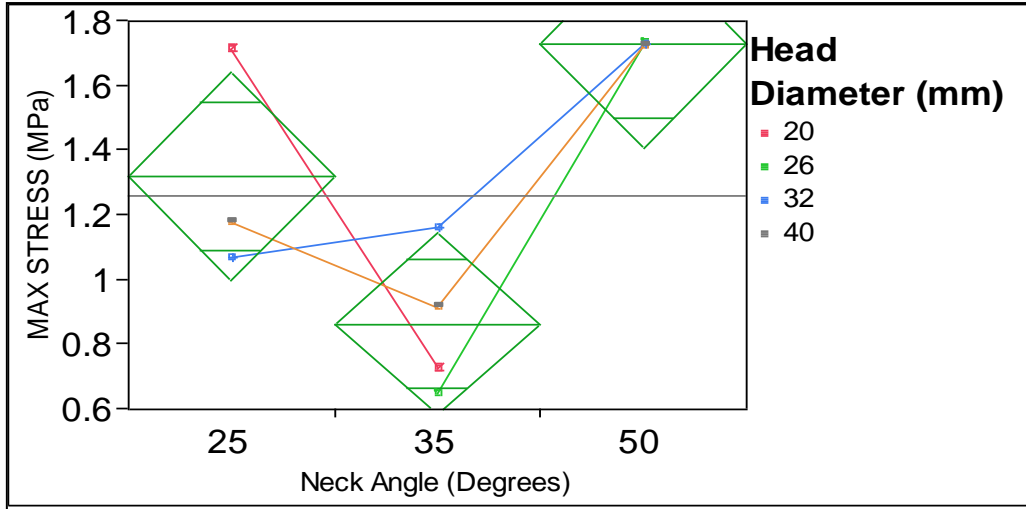


Figure 5.4 Oneway Analysis of Maximum Stress by Neck Angle. All hip models with 50 degrees of neck angles showed comparatively higher von Mises stresses regardless of the head diameter sizes combined in those models. Neck angle of 25 degrees were evaluated with intermediate stress values with lowest stresses when combined with 32 mm head diameter and highest when combined with 20 mm head diameter.

H-N ratio has been studied to find significant correlation between head and neck diameters. During the present study, statistical analysis was performed based on H-N ratio and maximum stresses achieved for all hip models. Figure 5.5 shows that there was no significant correlation observed between H-N ratio and maximum stresses. The lowest peak stress was found for hip model with H-N ratio of 1.86.

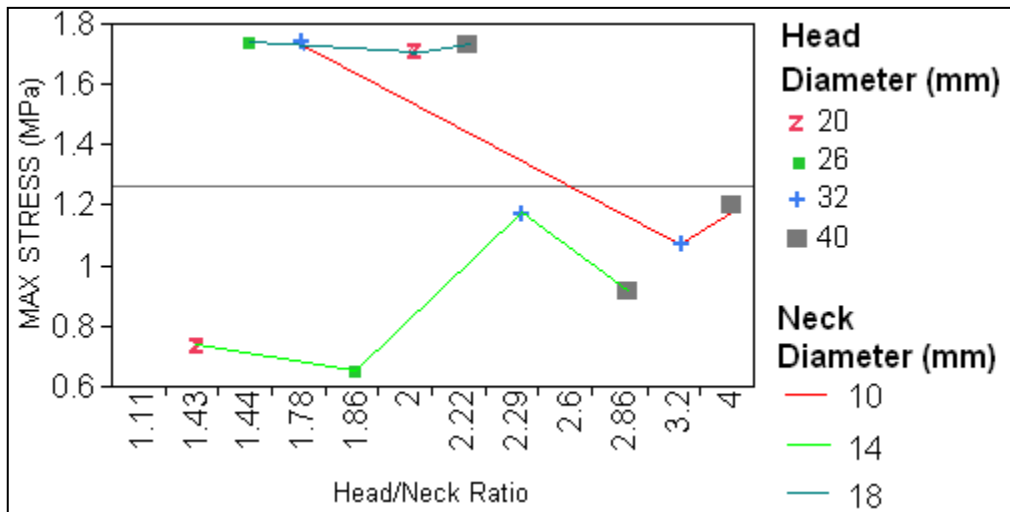


Figure 5.5 Oneway Analysis of Maximum Stresses by H-N Ratio with comparison of Head Diameter and Neck Diameter. There was no significant correlation observed between H-N ratio and maximum stresses. The lowest peak stress was for hip model with H-N ratio of 1.86.

Maximum stress values for the entire range of H-N ratio were compared with different head and neck diameters as shown in Figure 5.5. The lowest stresses with 14 mm neck diameters provide significant evidence to the previous comparisons of neck diameter and maximum stresses. Too high (18 mm) as well as too low (10 mm) neck diameter sizes showed comparatively higher stresses.

## 5.2 EFFECTS OF GEOMETRICAL PARAMETERS ON CONTACT STRESS

Contact stresses on articulating surfaces are significantly affected by the head and cup dimensions as well as their anatomical placements. Since a study of wear rate, by author [18], depicted 0.1 to 0.15 mm as safest range for clearance between articulating surfaces in order to achieve lower linear wear rate, all twelve models designed during the present analysis included 0.1 mm clearance between contact surfaces of femoral head and acetabular cup. Cup liner thicknesses varied from 9 mm to 11 mm for all hip models.

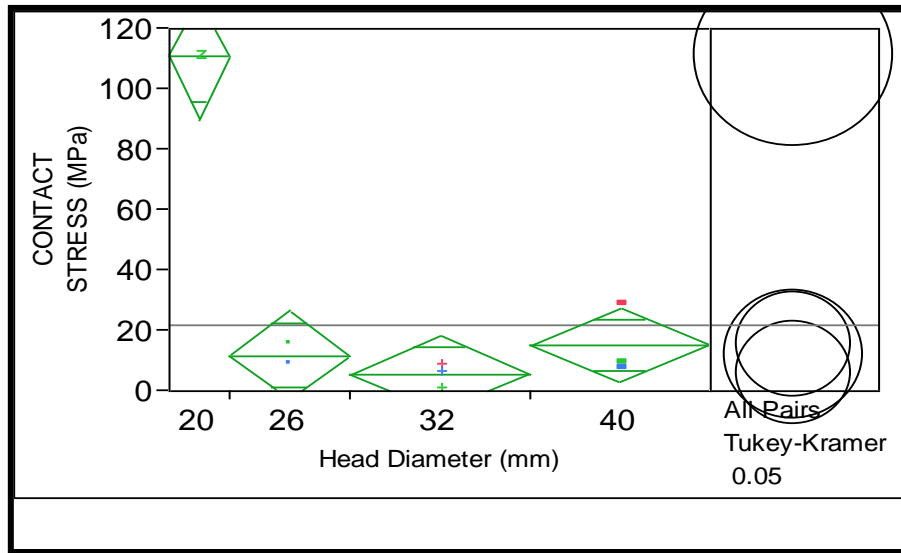


Figure 5.6 Oneway Analysis of Contact Stresses by Head Diameter. Large head diameters showed significantly less contact stresses compared to smaller head diameters ( $R^2 = 0.96$ ).

Head diameters were examined based on contact stresses for all hip models using Oneway Anova method (Figure 5.6). Large head diameters showed significantly low contact stresses compared to smaller head diameters ( $R^2 = 0.96$ ). As shown in Table 5.3, peak contact stress recorded for one hip model with 20 mm head diameter was not found within comparable range of peak contact stresses recorded for rest of the eight hip models with larger head diameters (26 mm to 40 mm). Three hip models with 32 mm heads showed 51% lower mean contact stresses compared to 2 hip models with 26 mm head diameters. Heads with 40 mm diameter showed 28.8% higher stresses compared to heads with 26 mm diameter. Femoral heads with diameters above 40 mm can possibly lead towards higher contact stresses than 26 mm to 40 mm head diameters.



Table 5.3 Comparison of Head Diameters with Mean Contact Stresses using Tukey-Kramer HSD method. Peak contact stress recorded for one hip model with 20 mm head diameter was not found within comparable range of peak contact stresses recorded for rest of the eight hip models with larger head diameters (26 mm to 40 mm).

| Head Diameters (mm) | Number of Hip Models | Comparability | Mean of Contact Stresses (MPa) |
|---------------------|----------------------|---------------|--------------------------------|
| 20                  | 1                    | A             | 110.7                          |
| 40                  | 3                    | B             | 15.1                           |
| 26                  | 2                    | B             | 11.7                           |
| 32                  | 3                    | B             | 5.75                           |

Acetabular component orientation was examined succinctly to observe the relationship of cup anatomical inclination and contact stresses. Figure 5.7 shows the statistical analysis results of contact stresses for hip models with several cup anatomical inclinations. Hip models with 35 degrees of inclination were examined with 60.8% and 52.7% lower mean contact stresses compared to 20 degrees and 50 degrees of cup inclination, respectively. Cup inclination of 20 degrees with horizontal axis showed 20.6% higher mean contact stresses than cup inclination of 50 degrees. Since, mean contact stresses reported for hip models with cup inclination of 65 degrees were not comparable to those below 50 degrees, high cup inclinations are believed to provide less hip stability.

Figure 5.7 also determines the correlation of effects of cup anatomical inclination and cup anteversion associated with contact stresses. Lower peak contact stresses were examined for cup inclination below 50 degrees when combined with 10 degrees and 20 degrees of cup anteversions. Hip models with 5 degrees of cup anteversions failed to provide contact stress results for cup inclinations of 20 degrees and 35 degrees. Hip models with 10

degrees of cup anteversion showed significantly low contact stresses compared to 20 degrees when modeled with 35 degrees of cup inclination. Peak contact stresses seem to increase for hip models with cup inclination above 50 degrees regardless of the provided cup anteversions. Smaller amounts of acetabular and femoral component anteversion seem to provide higher contact area between articulating surface; however, these combinations may restrict the provided ROM [70].

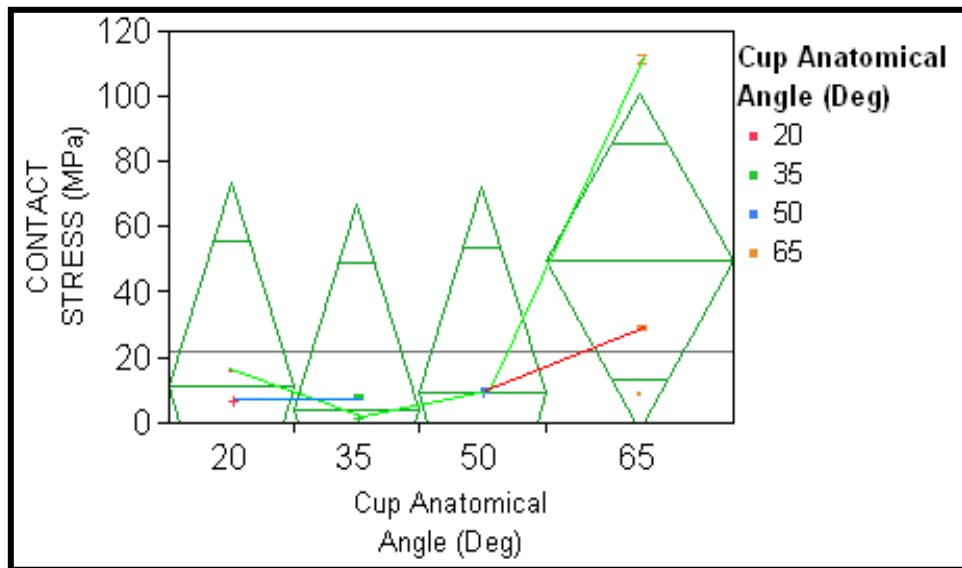


Figure 5.7 Oneway Analysis of Contact Stresses by Cup Anatomical Angle. Lower peak contact stresses were examined for cup inclination below 50 degrees when combined with 10 degrees and 20 degrees of cup anteversions. Hip models with 10 degrees of cup anteversion showed significantly lower contact stresses compared to 20 degrees when modeled with 35 degrees of cup inclination.

Table 5.4 shows the significant difference found for selected range of cup inclinations and their comparability relative to contact stresses. Three hip models with 65 degrees of cup inclinations were successfully analyzed for the present static analysis; whereas, only two hip models completed the FEM runs. Hip models designed with all four cup anatomical inclinations showed comparable results for mean contact stresses.

Table 5.4 Comparison of Cup Anatomical Angle with Mean Contact Stresses using Tukey-Kramer HSD method. Hip models designed with all four cup anatomical inclinations showed comparable mean contact stresses.

| Cup Anatomical Angle (Degrees) | Number of Hip Models | Comparability | Mean of Contact Stresses (MPa) |
|--------------------------------|----------------------|---------------|--------------------------------|
| 65                             | 3                    | A             | 49.25                          |
| 20                             | 2                    | A             | 11.0                           |
| 50                             | 2                    | A             | 9.15                           |
| 35                             | 2                    | A             | 4.33                           |

### 5.3 EFFECTS OF GEOMETRICAL PARAMETERS ON CONTACT PENETRATION

The amount of penetration between femoral head and acetabular cup was recorded for all hip models. Figure 5.8 shows the effects of head diameters on the contact penetration results using Oneway Anova method ( $R^2=0.78$ ). Highest contact penetration was observed in the hip model with 20 mm head diameter which was less significantly

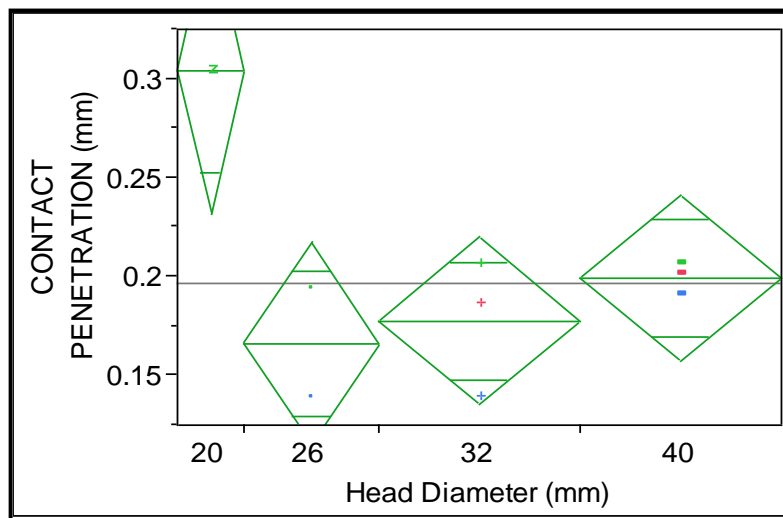


Figure 5.8 Oneway Analysis of Contact Penetration by Head Diameter ( $R^2=0.78$ ). Highest contact penetration was observed in the hip model with 20 mm head diameter which was less significantly compared due to only one successful analyzed hip model with 20 mm head diameter.

compared to only one hip model with 20 mm head diameter. An identical assessment may be performed using two successful hip models with 26 mm head diameter and three successful hip models for each 32 mm and 40 mm head diameters (See Table 5.5).

Table 5.5 Comparison of Head Diameter with Mean Contact Penetrations using Tukey-Kramer HSD method. Mean penetrations showed less significant difference when plotted for 26 mm to 40 mm head diameters; however, there was 7.2% increase in mean penetration observed for 32 mm head diameters compared to 26 mm head diameters.

| Head Diameters (mm) | Number of Hip Models | Comparability | Mean of Contact Penetrations (mm) |
|---------------------|----------------------|---------------|-----------------------------------|
| 20                  | 1                    | A             | 0.304390                          |
| 40                  | 3                    | A             | 0.199247                          |
| 32                  | 3                    | B             | 0.177787                          |
| 26                  | 2                    | B             | 0.165880                          |

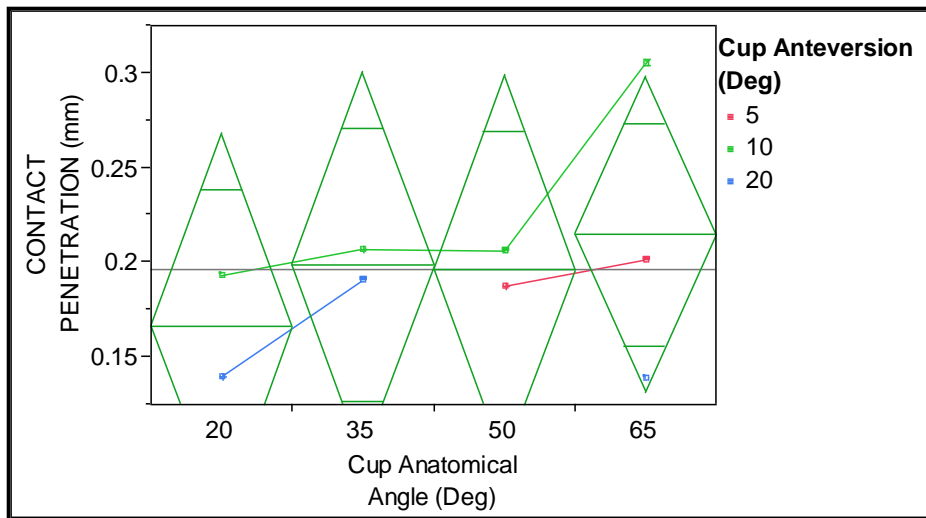


Figure 5.9 Oneway Analysis of Contact Penetration by Cup Anatomical Angle compared with Cup Anteversion. A less significant ( $R^2 = 0.15$ ) correlation was observed between contact penetration and cup anatomical angle with horizontal axis.

Mean penetrations showed similar results when plotted for 26 mm to 40 mm head diameters; however, there was 7.2% increase in mean penetration observed for 32 mm head diameters compared to 26 mm head diameters. Similarly, 40 mm heads showed

12.1% higher mean penetration than 32 mm heads. The effects of head diameters on contact penetration were also observed to be dependent on different cup inclinations.

Figure 5.9 describes correlation ( $R^2 = 0.15$ ) observed between contact penetration and cup anatomical angle with horizontal axis. Table 5.6 describe the relationship observed between all cup anatomical angles and mean contact penetrations with their significant comparability. All four cup inclination angles selected were examined within the comparable range for their observed mean penetrations. Hips with cup angle of 20 degrees showed 16.2% lower mean contact penetration compared to those with 35 degrees. Two hip models with each 35 degrees and 50 degrees were observed with difference for their recorded mean penetrations. Cup inclinations of 65 degrees showed 9.1% and nearly 8% higher mean penetration relative to 50 degrees and 35 degrees of cup inclinations, respectively.

Table 5.6 Comparison of Cup Anatomical Angle with Mean Contact Penetrations using Tukey-Kramer HSD method. All four selected cup inclination angles were examined within the comparable range for their observed mean penetrations.

| Cup Anatomical Angle (Degrees) | Number of Hip Models | Comparability | Mean of Contact Penetrations (mm) |
|--------------------------------|----------------------|---------------|-----------------------------------|
| 65                             | 3                    | A             | 0.214560                          |
| 35                             | 2                    | A             | 0.198655                          |
| 50                             | 2                    | A             | 0.196650                          |
| 20                             | 2                    | A             | 0.166480                          |

Figure 5.9 shows a similar correlation including the combinations of cup anteversions and cup inclinations. A discontinuous behavior was observed for cup anteversions of 5 degrees and 20 degrees. An excellent behavior was examined between all hip models

with 10 degrees of anteversion angle. For 10 degrees of cup anteverted hip models, lowest contact penetration was observed when combined with 20 degrees of cup anatomical inclination; less differentiable yet intermediate behavior for contact penetration was observed with 35 degrees and 50 degrees of cup inclinations; and highest contact penetration was found with cup inclination of 60 degrees.

#### 5.4 EFFECTS OF GEOMETRICAL PARAMETERS ON CONTACT SLIDING DISPLACEMENT

Figure 5.10 describes that there was no significant correlation between contact sliding displacement and head diameters ( $R^2 = 0.25$ ). As shown in Table 5.7, 40 mm head diameter was observed with lowest sliding displacement between the contact surface of femoral head and target surface of acetabular cup. An intermediate behavior without significant difference in displacements was recorded between 20 mm and 26 mm head diameters. Highest mean displacement was found for hip models with 32 mm heads.

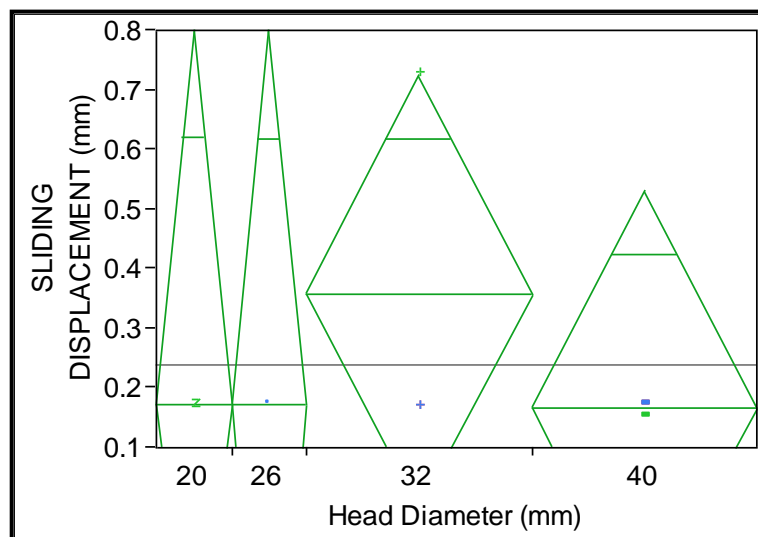


Figure 5.10 Oneway Analysis of Contact Sliding Displacement by Head Diameter. There was no significant correlation found between contact sliding displacement and head diameters ( $R^2 = 0.25$ ).

Reduced accuracy of correlation between head diameter and sliding displacement was believed to be for both head sizes 20 mm and 26 mm in diameters. Provided DOF for head and cup sizes during the static analysis set-up possibly restrict the sliding displacement of the contact surfaces. The sliding displacement was not found correlated to any other design parameters.

Table 5.7 Comparison of Head Diameter with Mean Sliding Displacement using Tukey-Kramer HSD method. 40 mm head diameters were observed with lowest sliding displacement between the contact surface of femoral head and target surface of acetabular cup. An intermediate behavior without significant difference in displacements was recorded between 20 mm and 26 mm head diameters.

| Head Diameters (mm) | Number of Hip Models | Comparability | Mean of Sliding Displacement (mm) |
|---------------------|----------------------|---------------|-----------------------------------|
| 32                  | 3                    | A             | 0.358000                          |
| 20                  | 1                    | A             | 0.172950                          |
| 26                  | 1                    | A             | 0.171350                          |
| 40                  | 3                    | A             | 0.165620                          |

## 5.5 PREDICTION EQUATIONS – CONTACT STRESSES

The wear of acetabular cup liner in hip implants is influenced by the degree of penetration by femoral head during incessant articulations. Penetration in the cup liner is found to be influenced by several geometrical parameters as well as anatomical orientations of the prosthetic components. An attempt was made by Goswami and Alhassan [7] to develop a comprehensive wear rate prediction model for hip and knee implants. Wear rate was predicted based on its primary dependency on femoral head diameter, femoral head roughness, patient body weight and mechanical properties of ultra-high-molecular-weight polyethylene (UHMWPE). The prediction expression

showed that wear rate changes exponentially with surface roughness of femoral head and linearly with body weight and head diameter [7]. The present study was based on further attempts made to correlate these geometrical parameters with linear wear rate of the cup liner based on their effects on penetration. The results, presented in chapter 4, were used to develop an empirical contact stress prediction model using head diameter, neck diameter and cup anatomical inclination. Two separate prediction equations were developed for contact stress prediction. First, a generic equation correlating geometrical parameters to contact stresses using head diameters as a continuous value. Second, a specific equation to predict contact stresses using specific values of head diameters including 20 mm, 26 mm, 32 mm and 40 mm.

### 5.5.1 Generic Equation

A generic equation for contact stress prediction was developed from applied head diameter, neck diameter and cup anatomical inclination angles. During the investigation of a generic equation, the head diameter values were considered as continuous values. Head diameters, neck diameters and cup anatomical angles were separately included to develop prediction. Prediction equation was expressed as follows:

$$CS = 90.002294798 + (- 2.62098999 * HD) + (- 1.196439442 * ND) + (0.733694127 * CI) \dots \dots \dots (1)$$

Where, CS is contact stress in MPa, HD is femoral head diameter in mm, ND is stem neck diameter in mm, CI is cup anatomical inclination in degrees.

Equation (1) has R<sup>2</sup> value of 0.518.



Developed equation can efficiently reproduce the contact stresses for head diameters ranging from 20 mm to 40 mm. Contact stresses were observed decreasing with increase in neck diameter sizes. These effects head and neck diameters on the contact stresses supported a study performed by Latham and Goswami [19]. The effects of geometric parameters were examined on the distribution of stresses in hip implant. The study concluded that increase with both head and neck diameters caused a significant reduction on the stress intensities. A reverse effect was observed while evaluating relationships between contact stresses and cup anatomical inclinations. With increase in cup inclination, stresses increased. A similar behavior was reported for higher stresses with an increase in neck angles [19].

### **5.5.2 Specific Equation**

Head diameters are observed to be significant factors affecting contact stresses. Larger head diameter provides larger contact surfaces with acetabular liner and significantly reduced the contact stresses during articulation. A specific prediction equation was developed to define the relationship between head diameters and contact stresses. Another significant factor affecting contact stresses was neck diameter. Higher neck diameters seem to affect permissible ROM influencing the contact stresses. Cup anatomical inclinations were used as an important parameter affecting contact stresses as well as contact sliding displacements with articulation. Higher cup inclinations are believed to reduce the contact surfaces between femoral head and cup liners which may increase contact stresses with increasing cup inclinations.



Head diameters above 26 mm contribute to a negative effect on the stress calculations. For 20 mm head diameter, the positive value represents comparatively higher stresses.

## 5.6 A NEW WEAR PREDICTION MODEL

The linear wear rate (LWR) can be expressed as rate of depth of penetration (mm) change due to articulations between femoral head and acetabular liner surfaces (shown in Equation (3)). Higher the penetration into the cup liner, higher will be the debris particles removed between weight bearing surfaces producing more wear. Incremental wear rate is observed if the residual debris particles deposited in between the head and cup surfaces. Contact penetration observed during static analysis of the twelve hip models was used during the formation of wear rate prediction equations. Wear rate related to contact penetration was expressed as:

$$LWR = \frac{dP}{d\tau} \dots\dots\dots (3)$$

Where, LWR is Linear Wear Rate (mm/year), P is the contact penetration in mm,  $\tau$  is the unit time (generally in years).

Contact penetration was evaluated using three fundamental parameters: head diameter, contact stress, and contact sliding displacement. Head diameter was considered as a baseline geometrical parameter for generating two different conceptual equations predicting wear rate; Generic Equation and Specific Equation. A generic equation was produced based on the penetration dependency on head diameter, contact stress and sliding displacement; where, head diameter was considered as a continuous parameter. The head diameter values were used as an incremental number form 20 mm to 40 mm;

whereas, a specific equation was developed based on the same phenomena of penetration dependency while considering head diameters as nominal discrete values. Four different head diameter were used. The accuracy of prediction increases for specific equation due to the believed consistency of penetration for each specific head diameter value.

### 5.6.1 Generic Equation

Contact penetration was expressed in terms of head diameter, contact stress and sliding displacement. The three parameters for all twelve hip models were accounted for in the form of their continuous values. Using generic equation, contact penetration (mm) was expressed as follows:

$$CP = 0.03364549 + (0.003082651 * HD) + (0.00170051661 * CS) + (0.098274119 * SD) \dots\dots\dots (4)$$

Where, LWR is linear wear rate, CP is contact penetration in mm, HD is head diameter in mm, CS is contact stress in MPa, SD is sliding displacement in mm.

Equation (4) has R<sup>2</sup> value of 0.9004.

Given Equation (4) can predict contact stresses for the range of head diameter from 20 mm to 40 mm. Contact penetration increased with an increase in head diameter, contact stress and sliding displacement. The multiplier for each significant parameter in the generic equation represents the weight of the individual factor contributing to the predicted contact penetrations. A similar behavior of head diameters on wear rate was predicted by Goswami and Alhassan [7]. Wear rate was observed to be linearly increasing with increasing head diameter sizes.

### 5.6.2 Specific Equation

An attempt was made to develop a comprehensive wear rate equation in terms of contact penetration with an improved  $R^2$  value. Increased weight of the provided head diameter values on the prediction equation shows nearly 3% increase in the accuracy of predicted linear wear rate along with contact penetration. Contact penetration (mm) was expressed as:

$$CP = 0.17668771 + \text{Match [HD]} + (0.00030828 * CS) + (0.080587836 * SD) \dots \dots \dots (5)$$

|          |                                    |
|----------|------------------------------------|
| Include, | Match [HD] = 20 mm » 7.9631936E-02 |
|          | 26 mm » -5.46676E-02               |
|          | 32 mm » -2.95229E-02               |
|          | 40 mm » 4.551721E-03               |

Where, CP is contact penetration in mm, HD is head diameter in mm, CS is contact stress in MPa, and SD is sliding displacement in mm. Equation (5) has  $R^2$  value of 0.9331.

Higher the contact penetration, higher will be the linear wear rate. Specific equation more accurately predicts wear in the terms of contact penetration compared to generic equation. The contribution of each parameter included in the Equation (5) show their effects to penetration and finally linear wear rate.

### 5.7 SAFE ZONES

The range of selected design and non-design related parameters which can be considered within a safe area for developing a hip implant to provide maximum stability is called

the *Safe Zone*. The selected parameters were analyzed using statistical analysis of the FEA results. Based on the performance of these factors, five different safe zones were determined for hip implants which included head diameter, neck diameter and neck angle as design parameters; while, cup anatomical inclination and cup anteversion as non-design parameters.

Several combinations of head and neck diameter sizes were evaluated to define a safe zone in order to reduce the risk of dislocation. Figure 5.11 shows safe zone for all combinations of head and neck diameters. Head diameter below 26 mm and above 32 mm was examined with higher risk of hip instability. Neck diameters above 10 mm as well as below 18 mm showed lowest von Mises stresses. The best performance was for neck sizes of 14 mm in diameters.

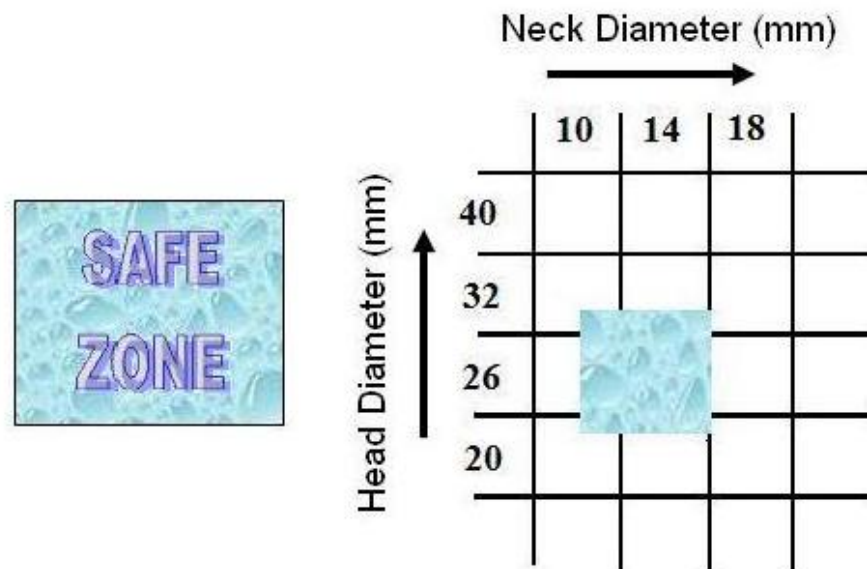


Figure 5.11 Safe Zone for combinations of different Head Diameters and Neck Diameters. Head diameter below 26 mm and above 32 mm was examined with higher risk of hip instability.

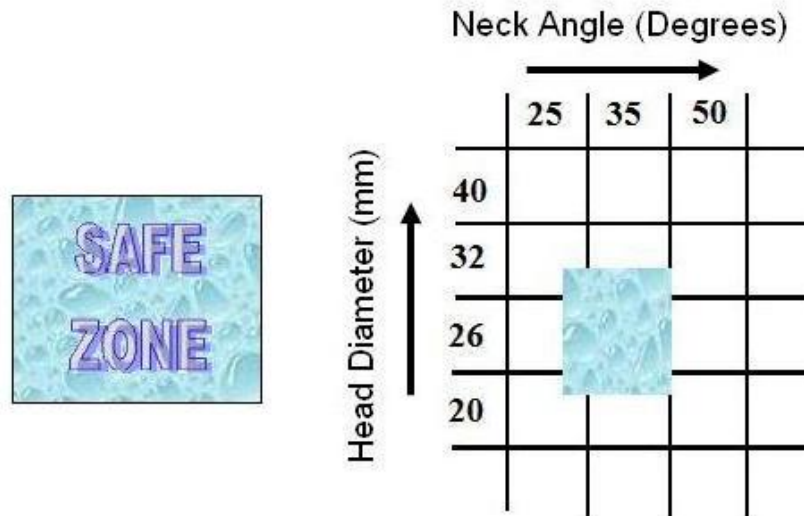


Figure 5.12 Safe Zone for combinations of different Head Diameters and Neck Angles. The safe zone was considered as head diameters from 26 mm to 32 mm, and neck angles between 25 to 35 degrees.

A similar safe zone was examined for combinations of head diameters and neck angles (Figure 5.12). The safe range for head diameters were from 26 mm to 32 mm. The range of examination for neck angle was from 25 degrees to 50 degrees from vertical axis. The safe zone was considered as neck angle between 25 to 35 degrees. The best combination of both design parameters was evaluated as 26 mm of head diameter and 35 degrees of neck angle.

An analysis of ranges of head diameters, neck diameters and neck angles was used to define a safe area which included all three design parameter at the same time.

Figure 5.13 shows the safe zone for all three selected parameters. Head diameters between 26 mm to 32 mm, neck diameters closer to 14 mm, and neck angle between 25 degrees to 35 degrees were examined to be the safest ranges for hip implant designs.

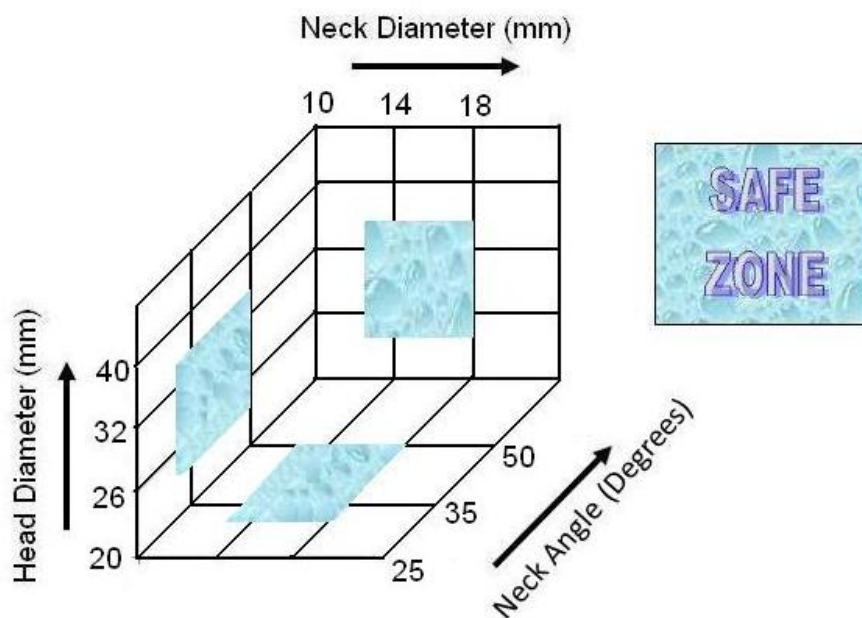


Figure 5.13 Safe Zone for combinations of different Head Diameters, Neck Diameters, and Neck Angles. Head diameters between 26 mm to 32 mm, neck diameters between closer to 14 mm, and neck angle between 25 degrees to 35 degrees were examined to be safest ranges for individual performances of these parameters.

Anatomical orientations of acetabular components were examined to reduce the occurrence of dislocation due to improper fixation angles. Cup anatomical inclination was found to be a significant factor affecting hip stability. Proper inclination of acetabular cup is believed to provide suitable holding of femoral head within the cup socket. Figure 5.14 defines a safe zone for all combinations of head diameters and cup anatomical inclinations. The head diameters between 26 mm to 32 mm were defined as secured region for femoral head designs. A selected range for evaluation of cup anatomical inclination was from 20 degrees to 65 degrees from horizontal axis. The risk area was examined for cup inclinations below 35 degrees as well as above 50 degrees; while, safe zone was described as cup inclination between 35 degrees and 50 degrees. A study by McCollum and Gray [16] determined similar safe range of 30 degrees to 50 degrees for cup inclination.



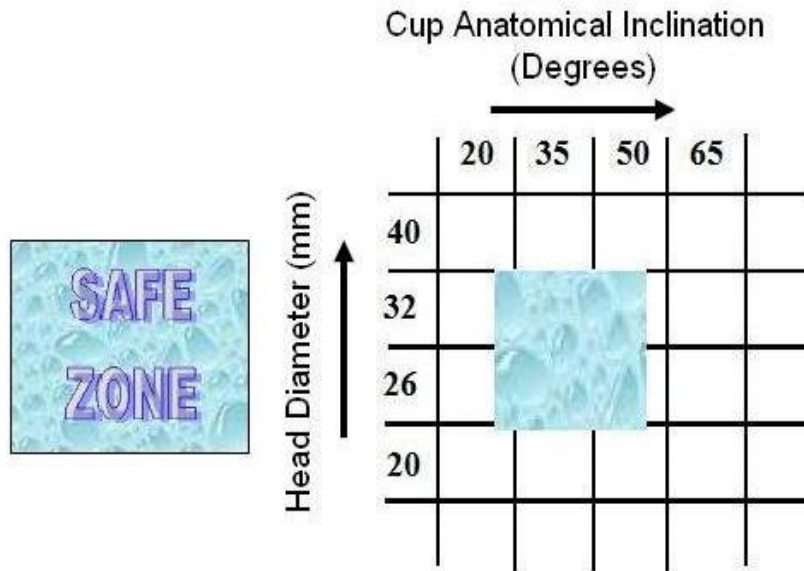


Figure 5.14 Safe Zone for combinations of different Head Diameters and Cup Anatomical Inclinations. The head diameters between 26 mm to 32 mm were defined as secured region for femoral head designs. The risk area was examined for cup inclinations below 35 degrees as well as above 50 degrees; while, safe zone was described as cup inclination between 35 degrees and 50 degrees.

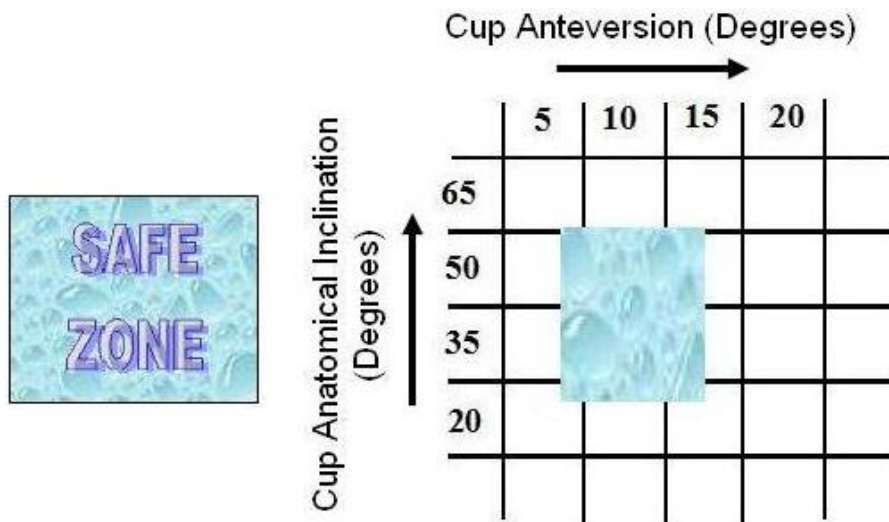


Figure 5.15 Safe Zone for combinations of different Cup anatomical Inclinations and Cup Anteversions. Cup anteversions above 15 degrees was found highly sensitive to dislocation. The safe range of cup anteversion was examined between 5 degrees and 15 degrees.

A significant influence of acetabular component orientation has been attributed to the increased rate of dislocation. Too anteverted or too retroverted cup inclination is more likely to cause anterior and posterior dislocation, respectively. The safe range of cup inclination with horizontal axis was found between 35 degrees and 50 degrees which was similar to safe range of 40 to 45 degrees predicted by Widmer and Zurfluh [44]. Increase in cup inclination above 50 degrees was considered as a risk factor highly increasing the chances of dislocation. Cup anteversion was evaluated in correlation with the cup anatomical inclination in Figure 5.15. Cup anteversions above 15 degrees was found highly sensitive to dislocation. The safe range of cup anteversion was examined between 5 degrees and 15 degrees.

Similar study by Scifert et al. [5] showed 47.6 MPa of von Mises stresses for 60 degrees of cup inclination with 25 degrees of cup anteversion compared to 44.25 MPa of von Mises stresses for 45 degrees of cup inclination and 15 degrees of cup anteversion.

Figure 5.16 was developed to combine the safe areas observed for combinations of hip implant design and non-design related parameters used in this study.


| SAFE ZONE  |    | Neck Diameter (mm) |    |    | Neck Angle (Degrees)      |    |    | Cup Anatomical Inclination (Degrees) |    |    |    |  |
|--|----|--------------------|----|----|---------------------------|----|----|--------------------------------------|----|----|----|--|
|  |    | 10                 | 14 | 18 | 25                        | 35 | 50 | 20                                   | 35 | 50 | 65 |  |
| Head Diameter (mm)   | 40 |                    |    |    |                           |    |    |                                      |    |    |    |  |
|  | 32 |                    |    |    |                           |    |    |                                      |    |    |    |  |
|  | 26 |                    |    |    |                           |    |    |                                      |    |    |    |  |
|  | 20 |                    |    |    |                           |    |    |                                      |    |    |    |  |
|  |    |                    |    |    |                           |    |    |                                      |    |    |    |  |
|  |    |                    |    |    | Cup Anteversion (Degrees) |    |    |                                      |    |    |    |  |
|  |    |                    |    |    |                           |    |    | 5                                    |    |    |    |  |
|  |    |                    |    |    |                           |    |    | 10                                   |    |    |    |  |
|  |    |                    |    |    |                           |    |    | 15                                   |    |    |    |  |
|  |    |                    |    |    |                           |    |    | 20                                   |    |    |    |  |

Figure 5.16 Safe Zones for combinations of hip design and non-design related parameters. For head diameters from 26 mm to 32 mm, neck diameters closer to 14 mm and below 18 mm, neck angles between 25 degrees to 35 degrees, cup anatomical inclination from 35 degrees to 50 degrees and cup anteversion below 20 degrees were found within safe ranges for a stable hip implant design.

## 6

# CONCLUSION

Geometrical design parameters of hip implant are major factors affecting the rate of dislocation. Secondary to geometrical parameters, anatomical orientation of prosthetic components were also found significantly affecting the hip stability in THR. von mises stresses, contact stresses, contact penetration, and sliding displacement were correlated with the selected geometrical factors as well as their different combinations along with anatomical orientations of prosthetic components.

- Geometrical parameters were optimized for 12 hip models.
- Several combinations of geometrical parameters were evaluated to define safe zones in order to reduce the risk of dislocation. Safe zones were efficiently defined based on the performances of the design related as well as acetabular component orientation related factors.
- Head sizes with 26 mm or larger diameters were found within safe range when examined for contact stresses.
- Head diameters between 26 mm to 32 mm, neck diameters closer to 14 mm, and neck angle between 25 degrees to 35 degrees were examined to be the safest ranges for hip implant designs.

- The preeminent stress results were found with combination of 26 mm head and 14 mm neck diameters designed with 35 degrees of neck angle.
- Head diameters lower than 26 mm showed highest contact penetration.
- Proper inclination of acetabular cup is believed to provide suitable holding of femoral head within the cup socket. The risk area was examined for cup inclinations below 35 degrees as well as above 50 degrees.
- The safe combination for cup orientation was observed with cup anatomical inclination from 35 degrees to 50 degrees with cup anteversion below 20 degrees.
- The linear wear rate was estimated using both generic as well as specific prediction equations. LWR was expressed as rate of depth of penetration (mm) change due to articulations between femoral head and acetabular liner surfaces. Higher the penetration into cup liner, higher will be the debris particles removed between weight bearing surfaces.
- Contact penetration was evaluated using three fundamental parameters: head diameter, contact stress, and contact sliding displacement with head diameter as a primary parameters specifying generic and specific equation predicting linear wear rate.

Future work will be needed to derive more accurate contact stress prediction models. Parameters such as femoral stem orientation, clearance, surface roughness and subject body weight may be included to predict linear wear rate for higher accuracy. Future research will include investigation of wear rate using dynamic simulation of gait pattern to estimate the lifespan of the hip implant.

# 7

## REFERENCES

1. Buford A., Goswami T. Review of wear mechanisms in hip implants: Paper I – General. *Materials and Design*. 25: p. 385-393. 2004.
2. Edidin A.A., Kurtz S.M. The evolution of paradigms for wear in total joint arthroplasty: the role of design, material, and mechanics. Available from [www. uhmwpe.org](http://www.uhmwpe.org). p. 1-15. 2000.
3. Woo R.Y.G., Morrey B.F. Dislocations After Total Hip Arthroplasty. *Journal of Bone and Joint Surgery*. 64A(9): p. 1295-1306. 1982.
4. Grigoris P., Grecula M.J., Amstutz H.C. Dislocation of a Total Hip Arthroplasty Caused by Iliopsoas Tendon Displacement. *Clinical Orthopaedics and Related Research*. 306: p. 132-135. 1994.
5. Scifert C.F., Brown T.D., Pedersen D.R., Callaghan J.J. Finite Element Analysis of Factors Influencing Total Hip Dislocation. *Clinical Orthopaedics and Related Research*. 355: p. 152-162. 1998.
6. Fackler C.D., Poss R. Dislocation in Total Hip Arthroplasties. *Clinical Orthopaedics and Related Research*. 151: p. 169-178. 1980.
7. Goswami T., Alhassan S. Wear rate model for UHMWPE in total hip and knee arthroplasty. *Materials and Design*. 29: p. 289-296. 2008.
8. Scifert C.F. A Finite Element Investigation into the Biomechanics of Total Artificial Hip Dislocation. The University of Iowa, IA. Biomedical Engineering department. May 1999.
9. Ritter M.A. Dislocation and Subluxations of the Total Hip Replacement. *Clinical Orthopaedics and Related Research*. 121: p. 92-94. 1976.
10. Yamaguchi M., Akisue T., Bauer T.W., Hashimoto Y. The Spatial Location Impingement in Total Hip Arthroplasty. *The journal of Arthroplasty*. 15 (3): p. 305-313. 2000.

11. Nicholas R.M., Orr J.F., Mollan R.A.B., Calderwood J.W., Nixon J.R., Watson P. Dislocation of Total Hip Replacements: A Comparative Study of Standard, Long Posterior Wall and Augmented Acetabular Components. *Journal of Bone and Joint Surgery*. 72B(3): p. 418-422. 1990.
12. Murray D.W. Impingement and Loosening of the Long Posterior Wall Acetabular Implant. *Journal of Bone and Joint Surgery*. 74B(3): p. 377-379. 1992.
13. Pierchon F., Pasquier G., Cotton A., Fontaine C., Clarisse J., DuQuennoy A. Causes of Dislocation of Total Hip Arthroplasty. *Journal of Bone and Joint Surgery*. 76B: p. 45-48. 1994.
14. Yoshimine F., Ginbayashi K. A Mathematical Formula to Calculate the Theoretical Range of Motion for Total Hip Replacement. *Journal of Biomechanics*. 35: p. 989-993. 2002.
15. Ali Khan M.A., Brakenbury P.H., Reynolds I.S.R. Dislocation Following Total Hip Replacement. *Journal of Bone and Joint Surgery*. 63B(2): p. 214-218. 1981.
16. McCollum D.E., Gray W.J. Dislocation After Total Hip Arthroplasty: Causes and Prevention. *Clinical Orthopaedics and Related Research*. 261: p. 159-169. 1990.
17. Olerud S., Karsltrom G. Recurrent Dislocation After Total Hip Replacement: Treatment by Fixing an Additional Sector to the Acetabular Component. *Journal of Bone and Joint Surgery*. 67B(3): p. 402-405. 1985.
18. Bhatt H., Goswami T. Implant Wear Mechanisms – Basic Approach. *Biomedical Materials*. 3: p. 1-9. 2008.
19. Latham B., Goswami T. Effect of geometric parameters in the design of hip implants paper IV. *Materials and Design*. 25: p. 715-722. 2004.
20. Pyburn E., Goswami T. Finite element analysis of femoral components paper III – hip joints. *Materials and Design*. 25. p. 705-713. 2004.
21. Sabatini A.L., Goswami T. Hip implants VII: Finite element analysis and optimization of cross-sections. *Materials and Designs*. 29: p. 1438-1446. 2008.
22. Bennett D., Goswami T. Finite element analysis of hip stem designs. *Materials and Designs*. 29: p. 45-60. 2008.
23. Slonaker M., Goswami T. Review of wear mechanisms in hip implants: Paper II – ceramics IG004712. *Materials and Design*. 25: p. 395-405. 2004.
24. Hedlundh U., Ahnfelt L., Hybbinette C., Wallinder L., Weckstrom J., Fredin H. Dislocations and the Femoral Head Size in Primary Total Hip Arthroplasty. *Clinical Orthopaedics and Related Research*. 333: p. 226-233. 1996.

25. Marmor L. Femoral Loosening in Total Hip Replacement. *Clinical Orthopaedics and Related Research*. 121: p. 116-119. 1976.
26. O'Brien S., Engela D.W., Leonard S., Kernohan W.G., Beverland D.E. Prosthetic Dislocation in Customized Total Hip Replacement: A Clinical and Radiographic Review. *Journal of Orthopaedic Nursing*. 1: p. 4-10. 1997.
27. Hedlundh U., Fredin H. Patient Characteristics in Dislocations After Primary Total Hip Arthroplasty. *Acta Orthopaedica Scandinavica*. 66(3): p. 225-228. 1995.
28. Coventry M.B. Late Dislocations in Patients with Charnley Total Hip Arthroplasty. *Journal of Bone and Joint Surgery*. 67A(6): p. 833-841. 1985.
29. Hedlundh U., Ahnfelt L., Hybbinette C., Weckstrom J., Fredin H. Surgical Experience Related to Dislocations After Total Hip Arthroplasty. *Journal of Bone and Joint Surgery*. 78B(2): p. 206-209. 1996.
30. Charnley J., Cupic Z. The nine and ten year results of the low-friction arthroplasty of the hip. *Clinical Orthopaedics and Related Research*. 95: p. 9-25. 1973.
31. Williams J.F., Gottesman M.J., Mallory T.H. Dislocation After Total Hip Arthroplasty: Treatment With an Above the Knee Hip Spica Cast. *Clinical Orthopaedics and Related Research*. 171: p. 53-58. 1982.
32. Roberts J.M., Fu F.H., McClain E.J., and Ferguson A.B., Jr. A comparison of the posterolateral and anterolateral approaches to total hip arthroplasty. *Clinical Orthopaedics and Related Research*. 187: p. 205-10. 1984.
33. McMurray T.P. Osteoarthritis of the Hip Joint. *Journal of Bone and Joint Surgery*. 21(1): p. 3-10. 1939.
34. Ekelund A., Rydell N., Nilsson O.S. Total Hip Arthroplasty in Patients 80 Years of Age and Older. *Clinical Orthopaedics and Related Research*. 281: p. 101-106. 1992.
35. Daly P.J., Morrey B.F. Operative Correction of an Unstable Total Hip Arthroplasty. *Journal of Bone and Joint Surgery*. 74A(9): p. 1334-1343. 1992.
36. Garcia-Cimbrello E., Munuera L. Dislocation in Low-friction Arthroplasty. *Journal of Arthroplasty*. 7(2): p. 149-155. 1992.
37. Paterno S.A., Lachiewicz P.F., Kelley S.S. The Influence of Patient-Related Factors and the Position of the Acetabular Component on the Rate of Dislocation After Total Hip Replacement. *Journal of Bone and Joint Surgery*. 79(A): p. 1202-1210. 1997.
38. Turner R.S. Postoperative Total Hip Prosthetic Femoral Head Dislocations. *Clinical Orthopaedics and Related Research*. 301: p. 196-204. 1994.

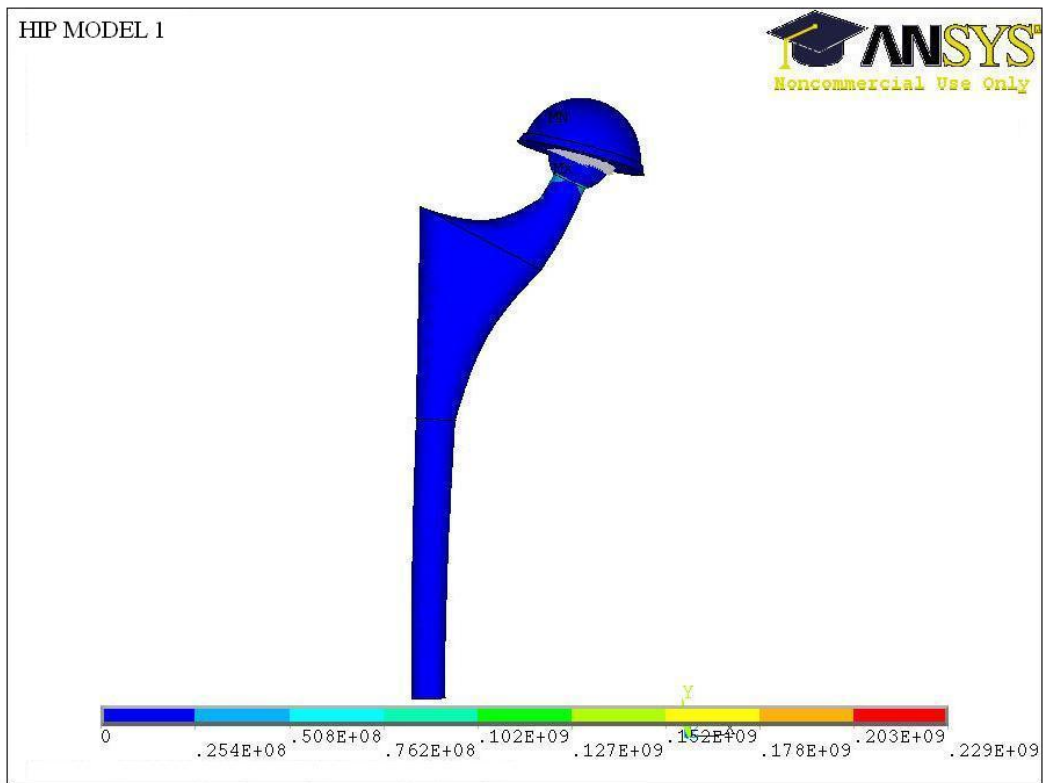


39. Hedlundh U., Hybbinette C., Fredin H. Influence of Surgical Approach on Dislocations After Charnley Hip Arthroplasty. *Journal of Arthroplasty*. 10(5): p. 609-614. 1995.
40. Gore D.R., Murray M.P., Sepic S.B., Gardner G.M. Anterolateral Compared to Posterior Approach in Total Hip Arthroplasty. *Clinical Orthopaedics and Related Research*. 165: p. 180-187. 1982.
41. Maric Z., Karpman R.R. Early Failure of Noncemented Porous Coated Anatomic Total Hip Arthroplasty. *Clinical Orthopaedics and Related Research*. 27(B): p. 116-120. 1992.
42. Carlsson A.S., Gentz C.F. Postoperative dislocation in the Charnley and Brunswik total hip arthroplasty. *Clinical Orthopaedics and Related Research*. 125: p. 177-82. 1977.
43. Barrack R.L., Burke D.W., Cook S.D., Skinner H.B., Harris W.H. Complications Related to Modularity of Total Hip Components. *Journal of Bone and Joint Surgery*. 75B: p. 688-692. 1993.
44. Widmer K.-H., Zurfluh B. Compliant positioning of total hip components for optimal range of motion. *Journal of Orthopaedic Research*. 22: p. 815-821. 2004.
45. Watson P., Nixon J.R., Mollan R.A.B. A Prosthesis Augmentation Device for the prevention of Recurrent Hip Dislocation. *Clinical Orthopaedics and Related Research*. 267: p. 79-84. 1991.
46. Cameron H.U., Hunter G.A., Welsh R.P. Dislocation Requiring Revision in Total Hip Arthroplasty. *Archives of Orthopaedic and Trauma Surgery*. 95: p. 265-266. 1979.
47. Oonishi N., Tsuji E., Kim Y.Y. Retrieved total hip prosthesis: Part I The effects of cup thickness, head sizes and fusion defects on wear. *Journal of Materials Science: Materials In Medicine*. 9: p. 393-401. 1998.
48. Korhonen R.K., Koistinen A., Konttinen Y., Santavirta S.S., Lappalainen R. The effect of geometry and abduction angle on the stresses in cemented UHMWPE acetabular cups- finite element simulations and experimental tests. *BioMedical Engineering OnLine*. 4(32): p. 1-14. 2005.
49. Maxian T.A., Brown T.D., Pedersen D.R., McKellop H.A., Lu B., Callaghan J.J. Finite element analysis of acetabular wear. Validation, and backing and fixation effects. *Clinical Orthopaedics and Related Research*. 344: p. 111-7. 1997.
50. Maxian T.A., Brown T.D., Pedersen D.R., Callaghan J.J. The Frank Stinchfield Award. 3-Dimensional sliding/contact computational simulation of total hip wear. *Clinical Orthopaedics and Related Research*. 333: p. 41-50. 1996.
51. Shaju K.A., Hasan S.T., D'Souza L.G., McMahon B., Masterson E.L. The 22-mm vs the 32-mm Femoral Head in Cemented Primary Hip Arthroplasty: Long-term Clinical and Radiological Follow-up Study. *The Journal of Arthroplasty*. 20(7): p. 903-908. 2005.

52. Amstutz H.C., Ludwig R.M., Schurman D.J., Hodgson A.G. Range of Motion Studies For Total Hip Replacements: A Comparative Study With a New Experimental Apparatus. *Clinical Orthopaedics and Related Research*. 111: p. 124-130. 1975.
53. Burroughs B.R., Hallstrom B., Golladay G.J., Hoeffel D., Harris W.H. Range of Motion and Stability in Total Hip Arthroplasty With 28-,32-,38-, and 44-mm Femoral Head Sizes: An In Vitro Study. *The Journal of Arthroplasty*. 20(1): p. 11-19. 2005.
54. Cuckler J.M., Moore D., Lombardi A.V., McPherson E., Emerson R. Large Versus Small Femoral Heads in Metal-on-Metal Total Hip Arthroplasty. *The Journal of Arthroplasty*. 19(8 suppl.3): p. 41-44. 2004.
55. Herrera L., Lee R., Longaray R., Essner A., Wang A. Hip Simulator evaluation of the effect of femoral heas size on sequentially cross-linked acetabular liners. *Wear*. 263: p. 1034-1037. 2007.
56. Chandler D.R., Glousman R., Hull D., McGuire P.J., Kim I.S., Clarke I.C., Sarmiento A. Prosthetic Hip Range of Motion and Impingement: The Effects of Head and Neck Geometry. *Clinical Orthopaedics and Related Research*. 166: p. 284-291. 1982.
57. Brien W.W., Salvati E.A., Wright T.M., Burstein A.H. Dislocation Following THA: Comparison of Two Acetabular Component Designs. *Orthopedics*. 16(8): p. 869-872. 1993.
58. Volpin G., Grimberg B., Daniel M. Complete Displacement of the Femoral Stem During Dislocation of a THR. *Journal of Bone and Joint Surgery*. 79B(4): p. 616-617. 1997.
59. Andriacchi T.P., Galante J.O., Belytschko T.B., Hampton S. A stress analysis of the femoral stem in total hip prostheses. *Journal of Bone and Joint Surgery*. 58A(5): p. 618-24. 1976.
60. Crowninshield R.D., Brand R.A., Johnston R.C., Milroy J.C. An analysis of femoral component stem design in total hip arthroplasty. *Journal of Bone and Joint Surgery*. 62A(1): p. 68-78. 1980.
61. Tai C-L., Shih C-H., Chen W-P., Lee S-S., Liu Y-L., Hsieh P-H., Chen W-J. Finite element analysis of the cervico-trochanteric stemless femoral prosthesis. *Clinical Biomechanics*. 18: p. S53-S58. 2003.
62. Woolson S.T., Pottorff G.T. Disassembly of a Modular Femoral Prosthesis After Dislocation of the Femoral Component. *Journal of Bone and Joint Surgery*. 72A(4): p. 624-625. 1990.
63. Pellicci P.M., Hass S.B. Disassembly of a Modular Femoral Component During Closed Reduction of the Dislocated Femoral Component. *Journal of Bone and Joint Surgery*. 72A(4): p. 619-620. 1990.

64. Star M.J., Colwell C.W., Donaldson W.F.I. Dissociation of Modular Hip Arthroplasty: A Report of Three Cases at Differing Dissociation Levels. *Clinical Orthopaedics and Related Research*. 278: p. 111-115. 1992.
65. Nadzadi M.E., Pedersen D.R., Yack H.J., Callaghan J.J., Brown T.D. Kinematics, kinetics, and finite element analysis of commonplace maneuvers at risk for total hip dislocation. *Journal of Biomechanics*. 36: p. 577-591. 2003.
66. Dorr L.D., Wolf A.W., Chandler R., Conaty J.P. Classification and Treatment of Dislocations of Total Hip Arthroplasty. *Clinical Orthopaedics and Related Research*. 173: p. 151-158. 1983.
67. Cobb T.K., Morrey B.F., Ilstrup D.M. The Elevated - Rim Acetabular Liner in Total Hip Arthroplasty: Relationship to Postoperative Dislocation. *Journal of Bone and Joint Surgery*. 78A(1): p. 80-86. 1996.
68. Phillips A.M., Konchwalla A. The Pathologic Features and Mechanism of Traumatic Dislocation of the Hip. *Clinical Orthopaedics and Related Research*. 377: p. 7-10. 2000.
69. Chandler R.W., Dorr L.D., Perry J.P. The Functional Cost of Dislocation Following Total Hip Arthroplasty. *Clinical Orthopaedics and Related Research*. 168: p. 168-171. 1982.
70. Robinson R.P., Simonian P.T., Gradisar I.M., Ching R.P. Joint Motion and Surface Contact Area Related to Component Position in Total Hip Arthroplasty. *Journal of Bone and Joint Surgery*. 79B(1): p. 140-146. 1997.

# APPENDIX A



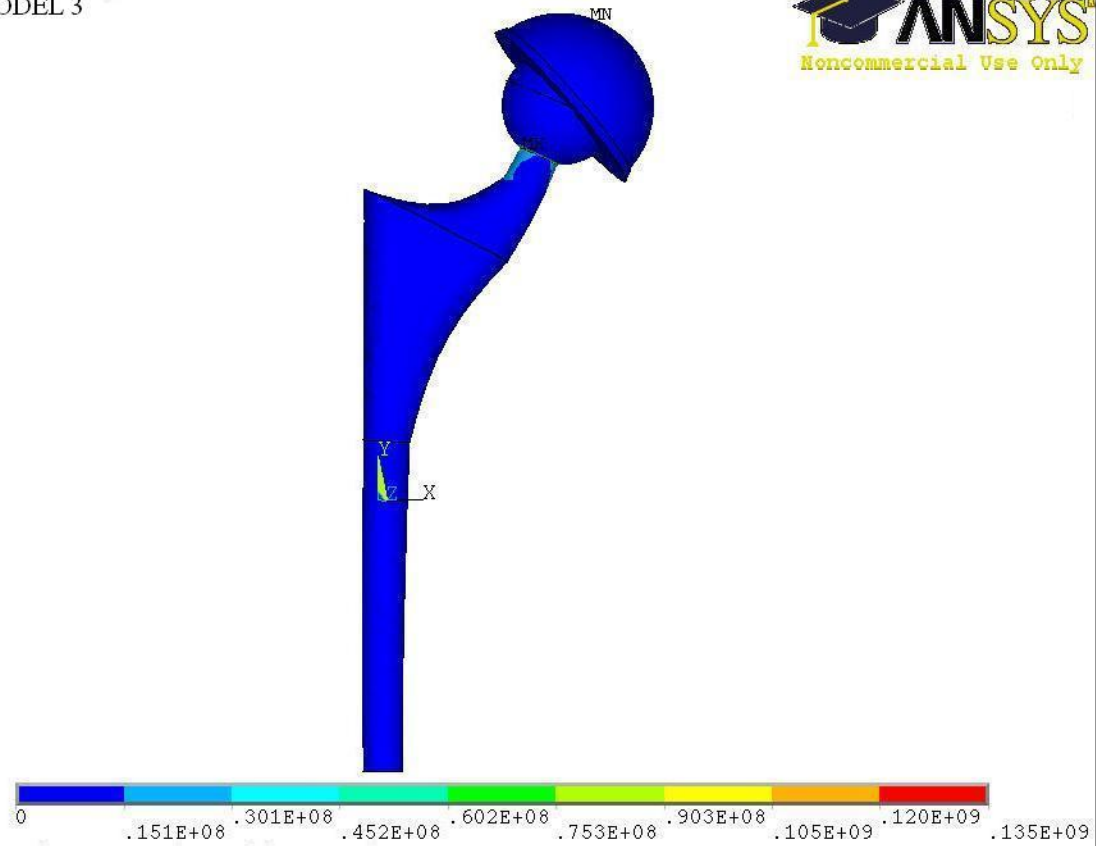
|                                     |    |
|-------------------------------------|----|
| HIP MODEL                           | 1  |
| Head Diameter<br>(mm)               | 20 |
| Neck Diameter<br>(mm)               | 10 |
| Head/Neck Ratio                     | 2  |
| Neck Angle<br>(deg)                 | 25 |
| Cup Thickness<br>(mm)               | 9  |
| Cup Anatomical<br>Inclination (deg) | 20 |
| Cup Ante-version<br>(deg)           | 5  |

HIP MODEL 2



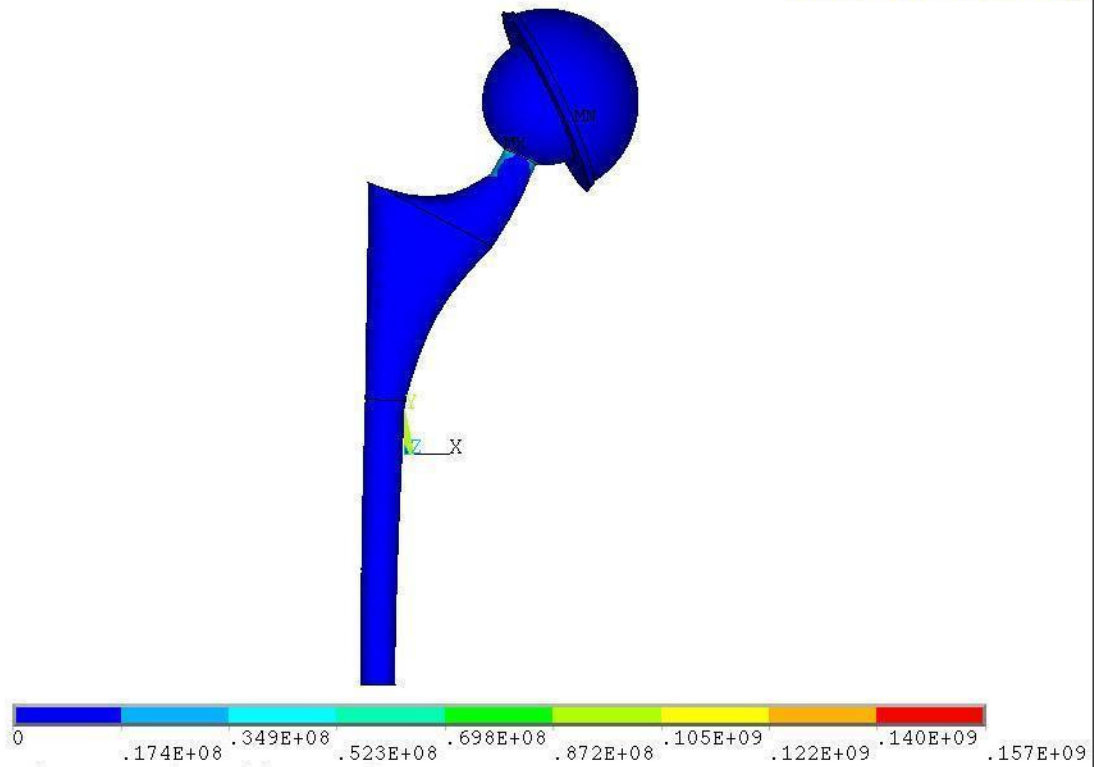
|                                     |     |
|-------------------------------------|-----|
| HIP MODEL                           | 2   |
| Head Diameter<br>(mm)               | 26  |
| Neck Diameter<br>(mm)               | 10  |
| Head/Neck Ratio                     | 2.6 |
| Neck Angle<br>(deg)                 | 25  |
| Cup Thickness<br>(mm)               | 9   |
| Cup Anatomical<br>Inclination (deg) | 35  |
| Cup Ante-version<br>(deg)           | 5   |

HIP MODEL 3



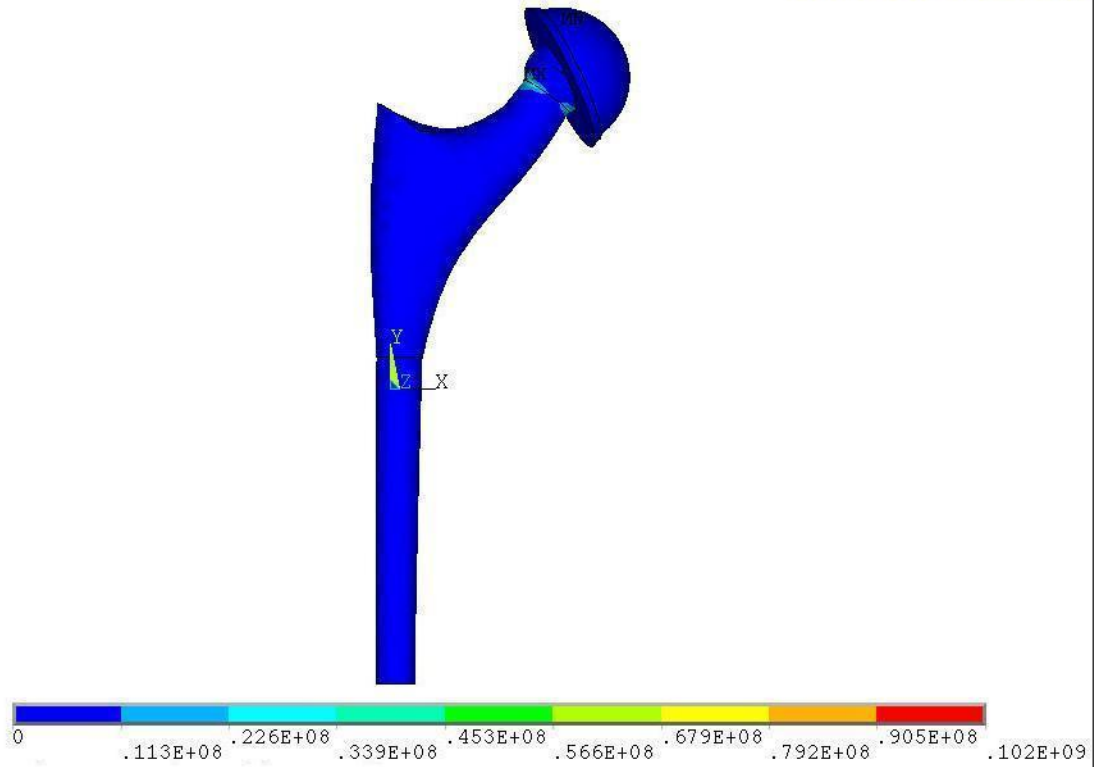
|                                     |     |
|-------------------------------------|-----|
| HIP MODEL                           | 3   |
| Head Diameter<br>(mm)               | 32  |
| Neck Diameter<br>(mm)               | 10  |
| Head/Neck Ratio                     | 3.2 |
| Neck Angle<br>(deg)                 | 25  |
| Cup Thickness<br>(mm)               | 9   |
| Cup Anatomical<br>Inclination (deg) | 50  |
| Cup Ante-version<br>(deg)           | 5   |

HIP MODEL 4



|                                  |    |
|----------------------------------|----|
| HIP MODEL                        | 4  |
| Head Diameter (mm)               | 40 |
| Neck Diameter (mm)               | 10 |
| Head/Neck Ratio                  | 4  |
| Neck Angle (deg)                 | 25 |
| Cup Thickness (mm)               | 9  |
| Cup Anatomical Inclination (deg) | 65 |
| Cup Ante-version (deg)           | 5  |

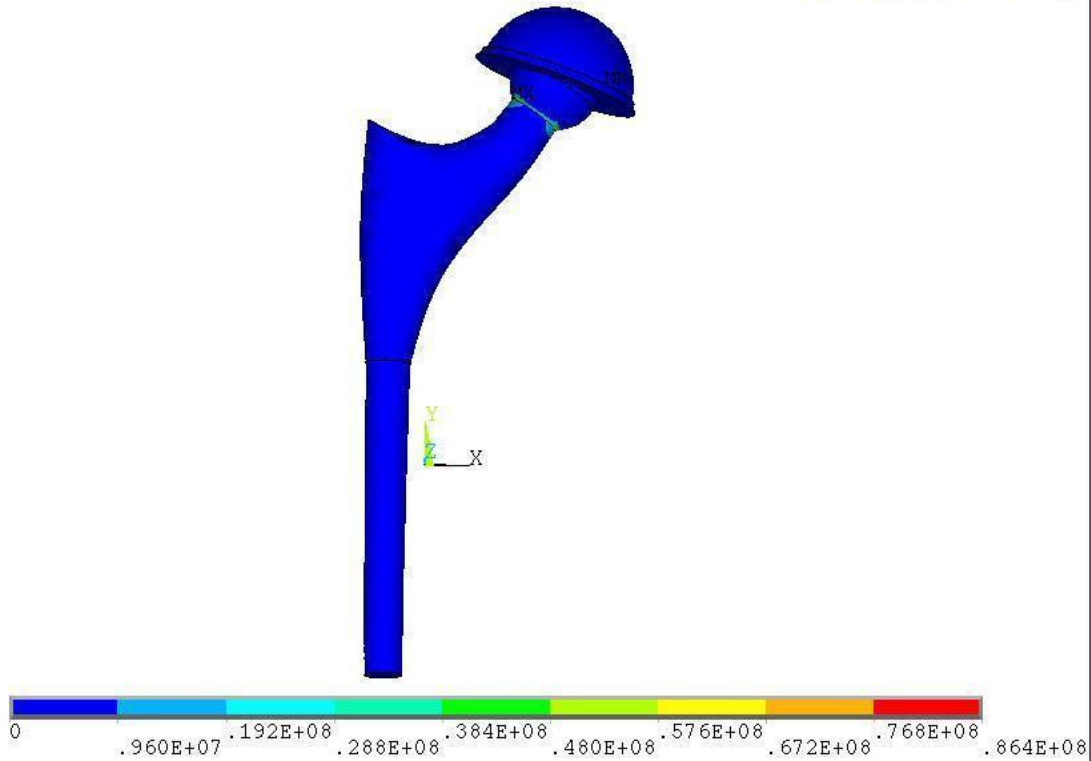
HIP MODEL 5



|                                  |      |
|----------------------------------|------|
| HIP MODEL                        | 5    |
| Head Diameter (mm)               | 20   |
| Neck Diameter (mm)               | 14   |
| Head/Neck Ratio                  | 1.43 |
| Neck Angle (deg)                 | 35   |
| Cup Thickness (mm)               | 9    |
| Cup Anatomical Inclination (deg) | 65   |
| Cup Ante-version (deg)           | 10   |

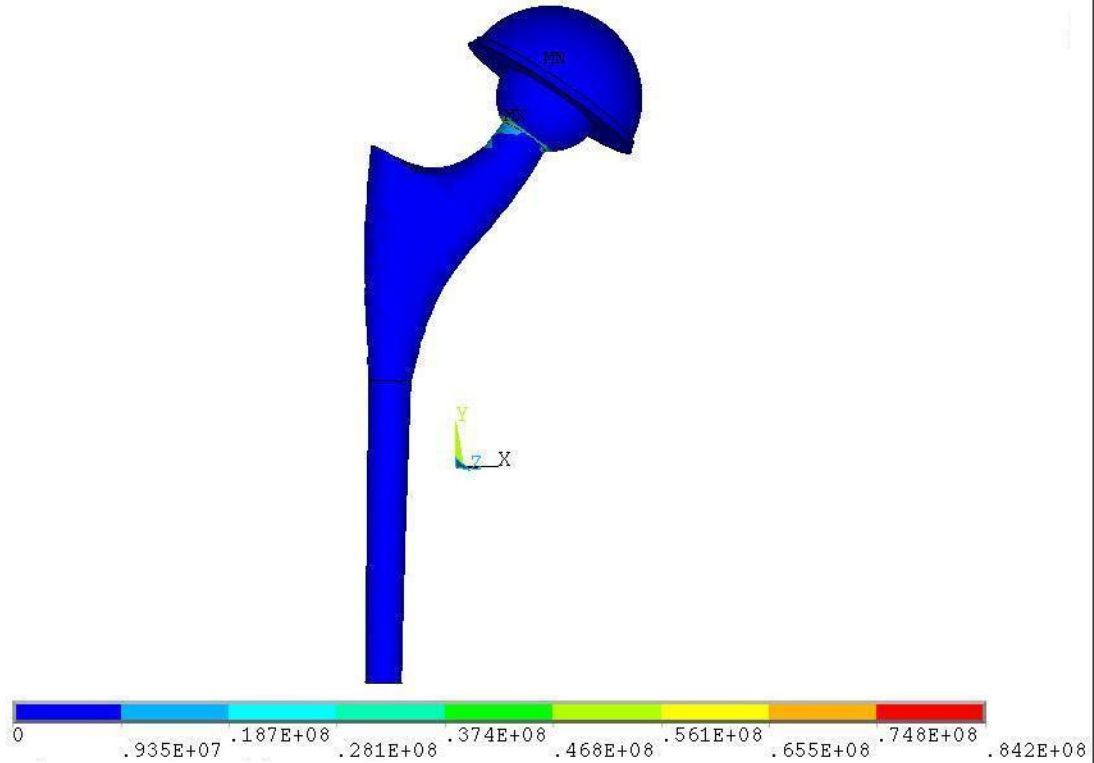


HIP MODEL 6



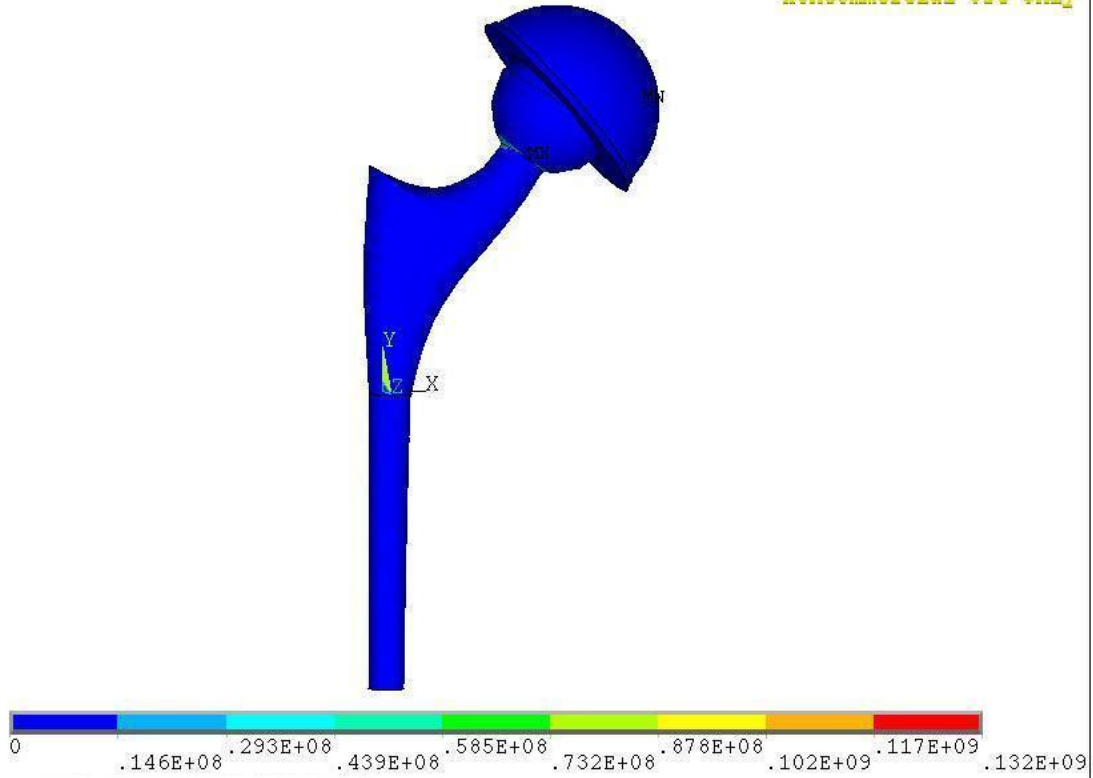
|                                     |      |
|-------------------------------------|------|
| HIP MODEL                           | 6    |
| Head Diameter<br>(mm)               | 26   |
| Neck Diameter<br>(mm)               | 14   |
| Head/Neck Ratio                     | 1.86 |
| Neck Angle<br>(deg)                 | 35   |
| Cup Thickness<br>(mm)               | 9    |
| Cup Anatomical<br>Inclination (deg) | 20   |
| Cup Ante-version<br>(deg)           | 10   |

HIP MODEL 7



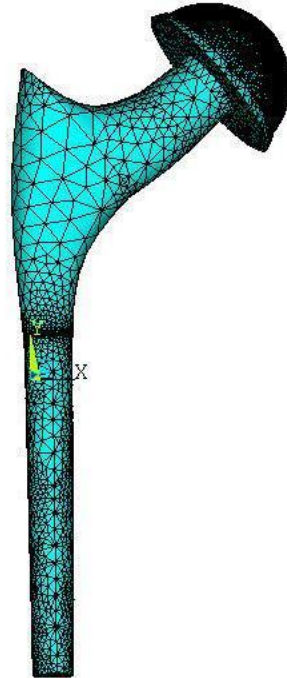
|                                  |      |
|----------------------------------|------|
| HIP MODEL                        | 7    |
| Head Diameter (mm)               | 32   |
| Neck Diameter (mm)               | 14   |
| Head/Neck Ratio                  | 2.29 |
| Neck Angle (deg)                 | 35   |
| Cup Thickness (mm)               | 11   |
| Cup Anatomical Inclination (deg) | 35   |
| Cup Ante-version (deg)           | 10   |

HIP MODEL 8



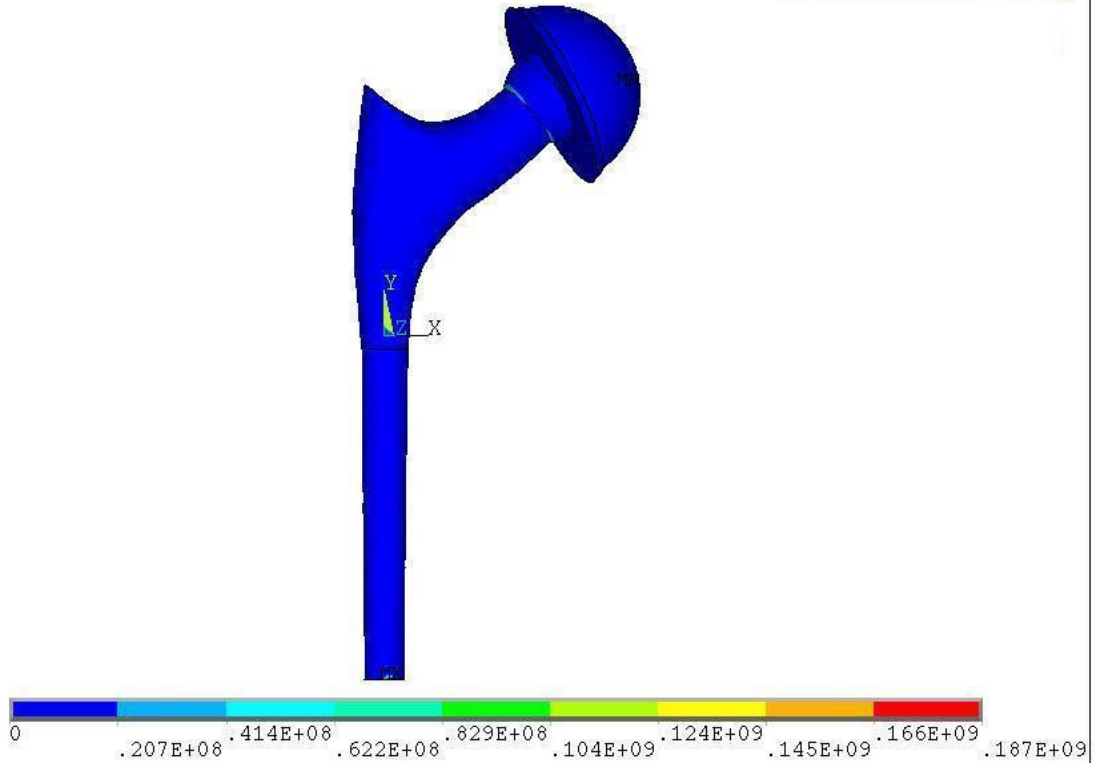
|                                     |      |
|-------------------------------------|------|
| HIP MODEL                           | 8    |
| Head Diameter<br>(mm)               | 40   |
| Neck Diameter<br>(mm)               | 14   |
| Head/Neck Ratio                     | 2.86 |
| Neck Angle<br>(deg)                 | 35   |
| Cup Thickness<br>(mm)               | 11   |
| Cup Anatomical<br>Inclination (deg) | 50   |
| Cup Ante-version<br>(deg)           | 10   |

HIP MODEL 9



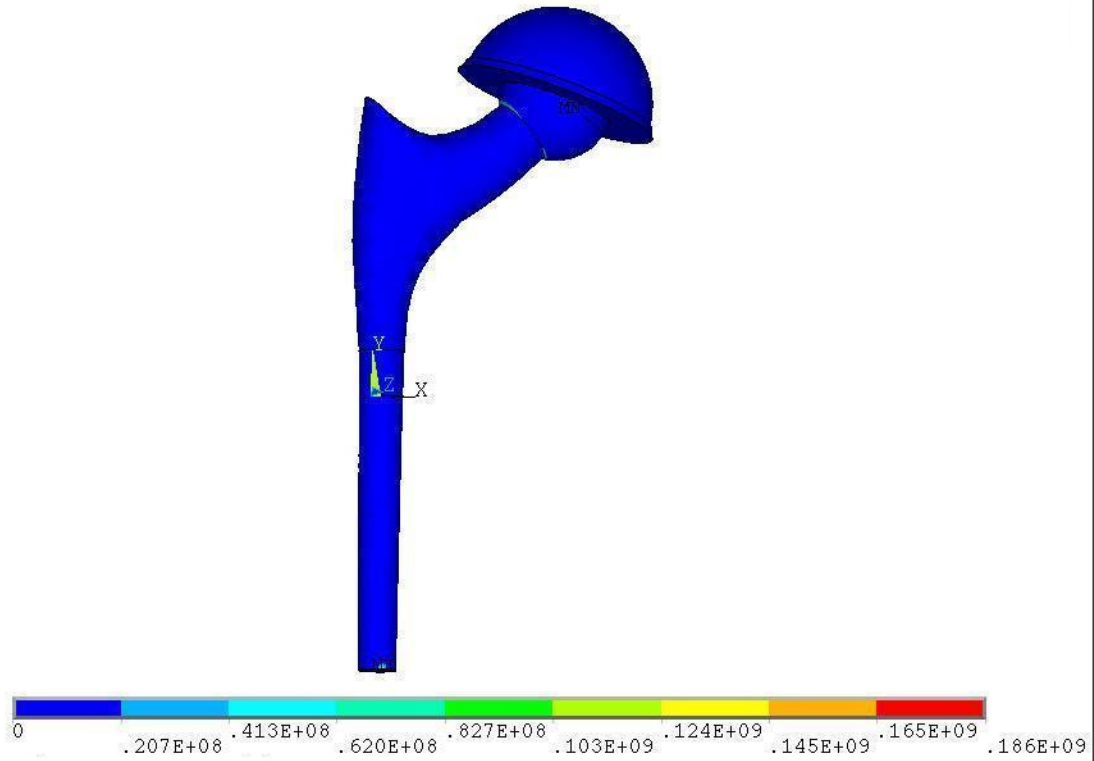
|                                     |      |
|-------------------------------------|------|
| HIP MODEL                           | 9    |
| Head Diameter<br>(mm)               | 20   |
| Neck Diameter<br>(mm)               | 18   |
| Head/Neck Ratio                     | 1.11 |
| Neck Angle<br>(deg)                 | 50   |
| Cup Thickness<br>(mm)               | 11   |
| Cup Anatomical<br>Inclination (deg) | 50   |
| Cup Ante-version<br>(deg)           | 20   |

HIP MODEL 10



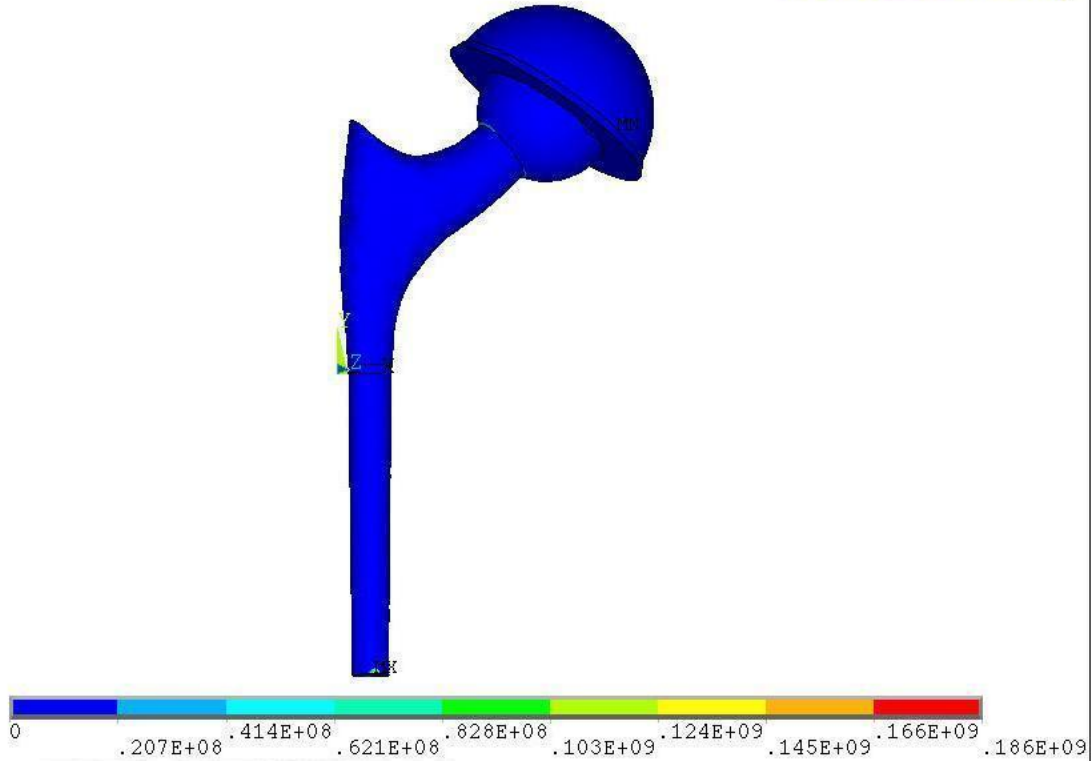
|                                     |      |
|-------------------------------------|------|
| HIP MODEL                           | 10   |
| Head Diameter<br>(mm)               | 26   |
| Neck Diameter<br>(mm)               | 18   |
| Head/Neck Ratio                     | 1.44 |
| Neck Angle<br>(deg)                 | 50   |
| Cup Thickness<br>(mm)               | 11   |
| Cup Anatomical<br>Inclination (deg) | 65   |
| Cup Ante-version<br>(deg)           | 20   |

HIP MODEL 11



|                                  |      |
|----------------------------------|------|
| HIP MODEL                        | 11   |
| Head Diameter (mm)               | 32   |
| Neck Diameter (mm)               | 18   |
| Head/Neck Ratio                  | 1.78 |
| Neck Angle (deg)                 | 50   |
| Cup Thickness (mm)               | 11   |
| Cup Anatomical Inclination (deg) | 20   |
| Cup Ante-version (deg)           | 20   |

HIP MODEL 12



|                                     |      |
|-------------------------------------|------|
| HIP MODEL                           | 12   |
| Head Diameter<br>(mm)               | 40   |
| Neck Diameter<br>(mm)               | 18   |
| Head/Neck Ratio                     | 2.22 |
| Neck Angle<br>(deg)                 | 50   |
| Cup Thickness<br>(mm)               | 11   |
| Cup Anatomical<br>Inclination (deg) | 35   |
| Cup Ante-version<br>(deg)           | 20   |

## APPENDIX B

A publication by author is attached with approved Copy rights by publisher.





09/12/2008 11:13

To [redacted]  
cc Permissions/IOPP@IOPP  
bcc  
Subject Re: Fw: Requesting Copyrights



Himanshu Bhatt  
<bhatt.6@wright.edu>  
08/12/2008 22:29

To bmm@iop.org  
cc  
Subject Requesting Copyrights

Respected Sir/Madam,

I am a Masters Student at Wright State University, Dayton, Ohio. I recently completed my research, "Finite Element Optimization of Hip Implant Geometrical Parameters to Determine Safe Zones and Resist Dislocation", in Fall quarter, 2008. I am requesting for your permission to attach a copy of my paper, "Bhatt, H., Goswami, T. Implant wear mechanisms-basic approach. Biomedical Materials 3 (2008): 1-9" (doi: 10.1088/1748-6041/3/4/042001). I will be pleased to get your permission to attach this article in the Appendix of my thesis. I look forward to hear from you. Thank you.

Sincerely,  
Himanshu Bhatt  
3640 Colonel Glenn Highway  
Department of Biomedical, Industrial and Human Factors Engineering  
Wright State University, Dayton, OH-45435, USA

PERMISSION TO REPRODUCE AS REQUESTED  
IS GIVEN PROVIDED THAT:

- (a) the consent of the author(s) is obtained
- (b) the source of the material including author/editor, title, date and publisher is acknowledged. ©

IOP Publishing Ltd  
Dirac House  
Temple Back  
BRISTOL  
BS1 6BE

9/12/08 [Signature]  
Date Rights & Permissions

© Please include the IOP copyright line, mention the journal's homepage at: [www.iop.org/journals/bmm](http://www.iop.org/journals/bmm) and provide a link back to the article's abstract on our website from the electronic version of your thesis (if applicable).  
Thank you!

## TOPICAL REVIEW

# Implant wear mechanisms—basic approach

Himanshu Bhatt<sup>1</sup> and Tarun Goswami<sup>1,2</sup>

<sup>1</sup> Department of Biomedical, Industrial and Human Factors Engineering, Wright State University, Dayton, OH 45435, USA

<sup>2</sup> Departments of Orthopedic Surgery and Sports Medicine, Wright State University, Dayton, OH 45435, USA

Received 2 May 2008

Accepted for publication 2 July 2008

Published 25 September 2008

Online at [stacks.iop.org/BMM/3/042001](http://stacks.iop.org/BMM/3/042001)

## Abstract

Numerous parameters control the long-term performance of a total hip joint arthroplasty. The articulating motions between the femoral and the acetabular components produce wear debris in a hip implant. Surface roughness, clearance, coefficient of friction and sliding distance are found to be contributing parameters that affect wear rates. Wear produced in a hip implant leads to the loosening of a hip prosthesis and thus failure of the hip implant.

Ultra-high-molecular-weight polyethylene (UHMWPE) has been successfully used as an acetabular weight bearing component in the THR applications. Cross-linked UHMWPE was found to improve the lifespan of an artificial hip. A gradient cross-linking of UHMWPE has been observed to be a recent development in implant bearing materials. During *in vitro* studies, gradient cross-linked UHMWPE showed nearly undetectable wear rates.

## 1. Introduction

In the 1960s, Sir John Charnley developed modern versions of total hip replacement (THR) models [1]. By the year 2000, the number of THR surgeries performed in the United States had increased to approximately 500 000 [2]. Wear has been the primary failure mode affecting the long-term performance of artificial hip and other prostheses. Metal-on-metal was the most prominent bearing combination used throughout the early invention era. The reported failures of the metal hip prosthesis due to ions, osteolysis and aseptic loosening resulted in a decline of usage of the metal-on-metal articulating surfaces [3]. In order to reduce the risk of hip implant failure, different weight bearing configurations that also affect the wear rate were examined. Due to the wear resistance and the ease of alignment of polyethylene, it has been the material of choice for the past 40 years [4, 5]. Metals articulating with metals, polyethylene and ceramics were all used in the earlier designs. However, the current trends are metals articulating with polyethylene liners.

During the earlier designs of artificial hips, metals were widely used in THR applications because of their excellent

mechanical characteristics and fatigue performance. Further improvements in the material properties geared toward the use of ceramics were explored because of their high strength and excellent biocompatibility. Alumina and zirconia are the most preferable ceramics in THR applications. Technological advancement and material processing carved the new path for the use of UHMWPE. Polyethylene has been used recently in high stress applications, such as total hip and knee replacements, due to its superior wear resistance and ease of availability.

Goswami *et al* [6] reported the wear mechanisms and the parameters affecting wear rate in hip designs. Goswami and Alhassan [7] attempted to predict the wear rate of UHMWPE in THR and TKR by an *in vitro* wear rate model. The primary parameters influencing the wear rate in their prediction model were: head diameter (HD), body weight (BW) and head surface roughness (Ra). The *in vitro* wear rate model was used efficiently to predict the wear rate in the hip implants as a function of the geometrical and mechanical parameters. The articulating motion between the acetabular cup and femoral head generates roughness, and wear debris, which induces an immune response and implant loosening

leading to osteolysis. The failure of the artificial hip implant then requires revision. This study reviews the parameters that influence wear mechanisms and wear rates in hip implants.

## 2. Background

A collection of literature [2, 6–14] provides an overview of the different combinations used for articulating surfaces. During articulations, the interactions between the acetabular cup surface and the femoral head surface cause wear debris which results in bone loss and the periprosthetic osteolysis. Different combinations of metal, ceramic and polyethylene materials were attempted to reduce the risk of osteolysis. Slonaker and Goswami [6] reported the lower wear rates in ceramic materials over metal-on-metal and metal-on-polyethylene combinations. An *in vitro* study by Howling *et al* [15] experimented with the ceramic-on-ceramic combination, which showed a lower wear factor (weight loss divided by the product of load and sliding distance) compared to the metal-on-metal and the metal-on-polyethylene combinations. Ceramic-on-ceramic combinations showed lower wear rates in the long-term performance of hip implants. An *in vitro* study by Wang and Essner [14] compared the third-body wear performance of ceramic-on-polyethylene and metal-on-polyethylene. In the presence of PMMA particles in serum, ceramic femoral heads showed higher wear resistance with UHMWPE compared to metal femoral heads with UHMWPE.

Park *et al* [16] discussed the advantages of UHMWPE as a weight bearing surface which helps to achieve higher wear resistance. The lower friction coefficient, higher biocompatibility and toughness are major contributing factors for the excellent performance of UHMWPE. Radiation cross-linking of UHMWPE has proven higher wear resistance compared to the conventional UHMWPE [13, 17–21]. Muratoglu *et al* [17] reported that the increase in the dose level from 0 to 300 kGy showed nearly 98% reduction in pin-on-disk (POD) wear rate while reducing the mechanical properties, such as 41.3% and 5% reduction in ultimate tensile and yield strength, respectively. A slight reduction in hardness and elastic modulus was also documented. The reduction in mechanical properties necessitates improvements in the process of cross-linking. The enhanced cross-linking process widely used is referred to as the *gradient cross-linking process*. The limited irradiation of the electron beam results in the gradient cross-linking and improves wear resistance as well as maintains the mechanical properties of UHMWPE. Oral *et al* [22] reported the effect of  $\alpha$ -tocopherol (vitamin E) on the oxidation and the decay of free radicals in the irradiated UHMWPE. Another study by Oral *et al* [23] showed that the vitamin E doped UHMWPE has better oxidation resistance and is more likely to maintain the mechanical properties of the irradiated UHMWPE used in THR.

### 2.1. Parameters affecting wear rate

Buford and Goswami [2] described different factors influencing the wear mechanisms including contact stresses, lubricant and clearance, surface hardness and roughness,

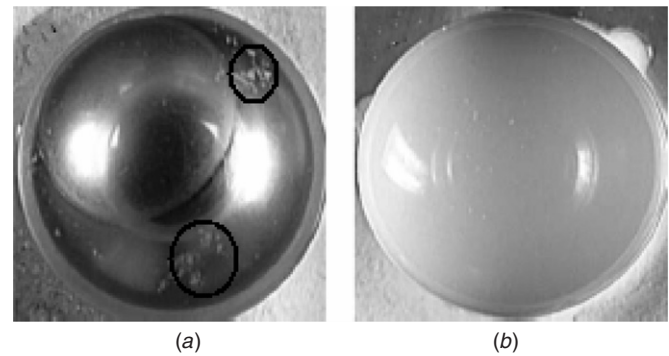


**Figure 1.** (a) CoCr femoral head with marked discrete patches and damage on the ball surface. (b) Alumina femoral head with smooth ball surface and no damage. After *in vitro* testing with PMMA concentration of  $10 \text{ g l}^{-1}$  in the lubricant [14].

different types of articulation due to motion, number of cycles, particle count and distribution and oxidative wear. The contact stresses due to rolling were found to be higher than those produced by sliding and gliding. The present study emphasizes the third-body wear phenomenon, surface roughness, clearance between femoral and acetabular components, friction coefficient and sliding distance as the primary parameters influencing wear rate. An ideal combination of these test parameters can effectively reduce the wearing out of the hip components and may help the design processes.

**2.1.1. Third-body wear phenomenon.** The third-body wear acts as a principal parameter affecting the long-term performance of an artificial hip implant [13]. The third-body particles can be either PMMA for the cemented hip prosthesis or pulled-out grain particles of the articulating surfaces as a result of wear. Wang and Essner [14] reported three possible phenomena by which third-body particles in serum may cause damage to the polyethylene acetabular cup and the metal or ceramic femoral head surfaces during clinical use.

The first phenomenon illustrates how serum particles may get collected on the superficial layer of the acetabular component which reduces the contact between the femoral head and the acetabular cup surface. In the case of the ceramic femoral head, PMMA particles cannot scratch the ceramic head and the reduced contact stress area may help lower the wear in the acetabular component surface. In the metallic femoral head, PMMA particles may damage the head surface and develop unfavorable wear results due to weight loss at higher concentrations of PMMA particles in serum. In figure 1, CoCr and alumina femoral heads that were removed from a hip simulator after being tested with the concentration of  $10 \text{ g l}^{-1}$  of PMMA particles in serum. The metallic head shows significant scratching, whereas the ceramic head was found without any damage [14].

The second phenomenon shows how the PMMA particles may attach on the femoral head surface which can plough through the interior of the polyethylene cup increasing the wear rate. PMMA particles are found to adhere to the metal head surface. However, the ceramic head does not have as many

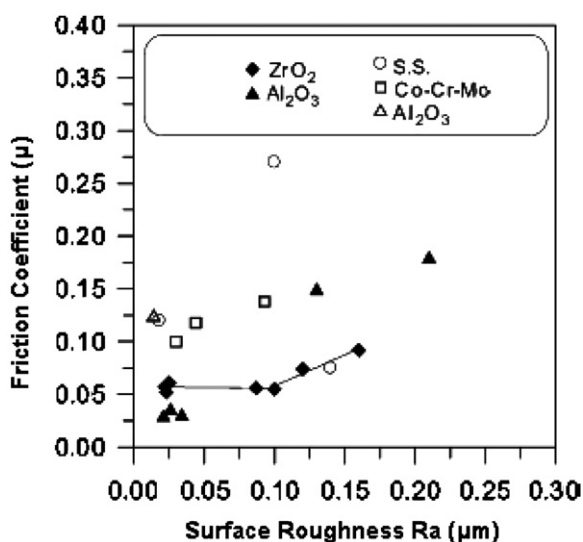


**Figure 2.** The effect of surface roughness of the ceramics (alumina, zirconia) and metals (stainless steel (S.S.), Co–Cr–Mo) on the friction coefficient [8].

PMMA particles on its surface. The higher the concentration of the PMMA particles in serum, the higher the wear rate of UHMWPE surface [14].

The third phenomenon describes how the PMMA particles can roll in between the articulating surfaces instead of sticking to the femoral head or the acetabular cup surfaces. The rolling free particles between the surfaces come into contact and produce the third-body wear rate [14]. Wang and Essner [14] founded this phenomenon to be less effective in the generation of wear rate because of the lower severity of rolling abrasive wear than sliding abrasive wear.

**2.1.2. Surface roughness.** The wear behavior of UHMWPE rings sliding on  $ZrO_2$  and  $Al_2O_3$  was investigated by Cho *et al* [8] using a ring-on-disc reciprocal wear test. The friction coefficient and the wear factor were evaluated in correspondence to the surface roughness and were found to be controlled by the surface roughness [8]. The ceramic ball and UHMWPE liners showed an ideal combination for a hip prosthesis. Zirconia and alumina are the most preferred choices for the ceramic femoral head, of which zirconia showed the lower coefficient of friction and the higher toughness. Amongst all the tested materials, zirconia showed the lowest surface roughness with the critical value of  $0.10 \mu\text{m}$  [8]. Cho *et al* [8] tested a UHMWPE ring on an  $Al_2O_3$  disc. The wear behavior of UHMWPE was found to be either surface fatigue wear or abrasive wear, when surface roughness was deflected from the critical value of  $0.10 \mu\text{m}$ .

The coefficient of friction for zirconia increases steadily as the surface roughness increases from  $0.10 \mu\text{m}$  to  $0.20 \mu\text{m}$ . In figure 2, the friction coefficient of ceramics for roughness less than  $0.10 \mu\text{m}$  produces a stable value (0.06). Stainless steel showed the highest coefficient of friction at  $0.10 \mu\text{m}$  of surface roughness. The friction coefficient for Co–Cr–Mo continuously increases with the increase in surface roughness. However, a limited amount of data were found

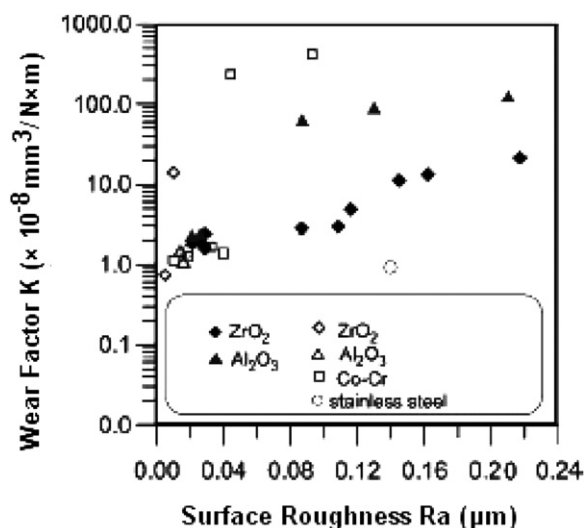


**Figure 3.** The wear factor of ceramic ( $ZrO_2$ ,  $Al_2O_3$ ) and metallic (Co–Cr, stainless steel) materials versus surface roughness (Ra) [8].

in the literature to develop a trend or any of the rate equations. Figure 3 shows the dependence of the wear factor on surface roughness for ceramic and metal surfaces [8]. The wear factor shows a very similar behavior to the friction coefficient in correspondence with the surface roughness. Zirconia showed the lowest wear factor amongst all the materials with the same trend as the friction coefficient. For zirconia, the roughness below  $10 \mu\text{m}$  shows a slight effect in the wear factor starting from  $1.56 \times 10^{-8}$  to  $2.97 \times 10^{-8} \text{mm}^3 \text{N}^{-1} \text{m}^{-1}$ . As the roughness increases above a critical value of  $0.10 \mu\text{m}$ , the wear factor increases up to  $21.5 \times 10^{-8} \text{mm}^3 \text{N}^{-1} \text{m}^{-1}$  for  $0.22 \mu\text{m}$  of roughness. The higher friction coefficient and wear factor of alumina were examined because of the grain pull-out defect on the alumina surface. Co–Cr showed a higher wear factor than ceramics for the surface roughness below  $0.10 \mu\text{m}$ .

**2.1.3. Clearance.** The clearance between the femoral head and the acetabular cup liners plays a vital role in the wear rate behavior of an artificial hip [9]. The wear rate has a remarkable increase for too small or too large clearance values. The clearance near zero and above  $0.5 \text{mm}$  shows the highest volumetric wear rate. The linear wear rate is less sensitive to the change in clearance. An ideal range for the clearance is between  $0.5 \text{mm}$  and  $0.15 \text{mm}$  [9].

Table 1 compiles the wear rates of a  $32 \text{mm}$  diameter CoCrMoC femoral head and the UHMWPE acetabular cup articulating surfaces. The interference between the two articulating surfaces was highest for both extremes of the clearance resulting in the highest volumetric wear rate. The clearance value between  $0.1 \text{mm}$  and  $0.15 \text{mm}$  showed the highest wear resistance, where the linear wear rate was  $0.1 \text{mm yr}^{-1}$  and the volumetric wear rate was  $55 \text{mm}^3 \text{yr}^{-1}$  [9]. Figure 4 compares the results of the clinical data for different clearance values with the highest wear rate for  $0.5 \text{mm}$  and  $0.001 \text{mm}$  clearance with an increase in the implantation time. For  $0.2 \text{mm}$  clearance and no friction, the predicted linear wear rate was  $0.120 \text{mm yr}^{-1}$  [9].

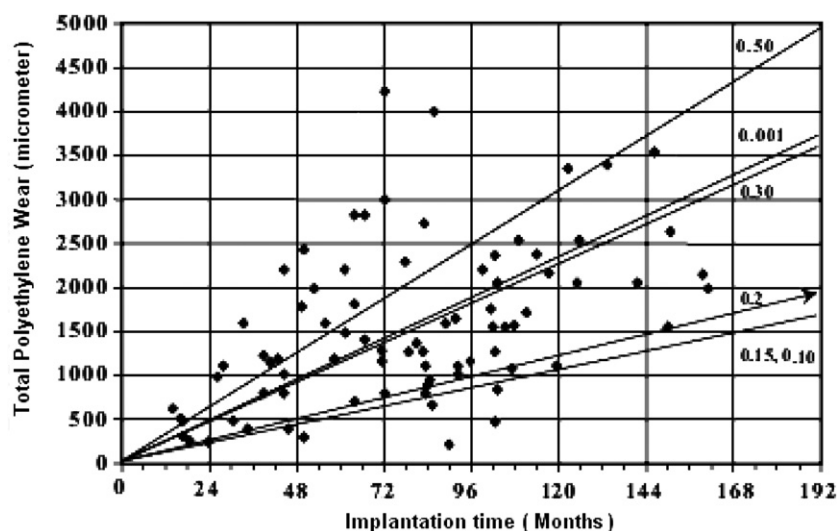


Figure 4. The effect of clearance on the linear wear rate of polyethylene versus implantation time in months [9].

**Table 1.** The effect of clearance on the wear rate of a 32 mm femoral head diameter. The volumetric wear rate is higher for the clearance near zero and  $>0.5 \mu\text{m}$ . The linear wear rate is observed to be less sensitive with increase in clearance [9].

| Clearance | Linear wear rate ( $\text{mm yr}^{-1}$ ) | Volumetric wear rate ( $\text{mm}^3 \text{yr}^{-1}$ ) |
|-----------|--|---|
| 0.001     | 0.23                                     | 122.27  |
| 0.050     | 0.11                                     | 56.69   |
| 0.100     | 0.10                                     | 53.68   |
| 0.150     | 0.10                                     | 56.33   |
| 0.200     | 0.12                                     | 56.89   |
| 0.300     | 0.22                                     | 63.10   |
| 0.500     | 0.31                                     | 114.72  |

**Table 2.** The effect of coefficient of friction on the wear rate of a 32 mm femoral head diameter. The volumetric wear rate increases with an increase in the friction coefficient [9].

| Coefficient of friction | Linear wear rate ( $\text{mm yr}^{-1}$ ) | Volumetric wear rate ( $\text{mm}^3 \text{yr}^{-1}$ ) |
|-------------------------|--|---|
| 0.00                    | 0.121                                    | 56.89   |
| 0.05                    | 0.121                                    | 59.11   |
| 0.10                    | 0.121                                    | 59.81   |
| 0.15                    | 0.120                                    | 61.32   |
| 0.20                    | 0.121                                    | 62.52   |
| 0.25                    | 0.122                                    | 63.10   |
| 0.30                    | 0.120                                    | 63.72   |

**2.1.4. Coefficient of friction.** The wear rate is found to be sensitive to the coefficient of friction. The friction coefficient between the femoral head and the acetabular cup is assumed to be zero initially and it keeps increasing as the wear behavior commences. The volumetric wear rate increases constantly with an increase in the coefficient of friction, while the linear wear rate remains stable [9].

Table 2 summarizes the results achieved for 32 mm femoral head with the clearance of 0.2 mm. The friction coefficient increases from 0.0 to 3.0 and shows the effects on the linear and the volumetric wear rate. An increase of  $0.12 \pm 1$  mm was observed in linear wear rate for an increase up to 0.3 in the coefficient of friction [9]. The total increase of 12% was observed in the volumetric wear rate, which indicates that the wear rate is less sensitive to the friction coefficient [9].

**2.1.5. Sliding distance.** The sliding distance affects the wear behavior of the hip prosthesis [10]. Bennett *et al* [10] proved that the direction of the individual contact points on the femoral head is a predominant problem in causing wear of the UHMWPE acetabular cup. The shape and the length of the wear paths on the femoral head were also found to be influencing the wear rate of the acetabular cup liners [10].

## 2.2. Articulating surfaces

Cho *et al* [8] discussed the interactions and wear conditions between the femoral head and acetabular cup. The interactions between surfaces significantly affect the life span of an artificial hip in THR. Metals and ceramics have been successfully used as the femoral heads in THR applications. Alumina and zirconia are the only ceramic heads used for an artificial hip joint because of their excellent performances during testing. Published articles [6, 8, 14, 15] show a better wear performance of ceramic heads (alumina, zirconia) than metal heads (CoCr) with UHMWPE acetabular component. Because of high toughness and strength, zirconia is widely used as a femoral head.

**2.2.1. Ceramic-on-UHMWPE versus metal-on-UHMWPE.** Wang and Essner [14] compared the wear behavior of metal and ceramic femoral heads. The third-body wear rate was higher than the wear rate without PMMA particles in serum [14]. The metallic femoral heads are more susceptible to scratches, and therefore allow more PMMA particles to adhere to the head surfaces. On the other hand, the ceramic femoral heads are less susceptible to scratches, so do not allow PMMA particles to adhere to the surfaces [14]. Figure 1 shows the CoCr and alumina femoral heads after *in vitro* study [14]. The



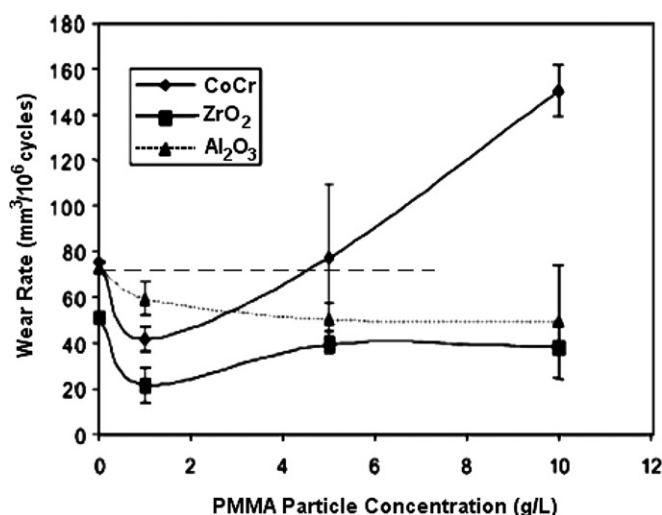


**Figure 5.** The wear rate increase in CoCr, alumina and zirconia with increase in PMMA particle concentration in serum from 0 to 10 g l<sup>-1</sup> [14].

CoCr head had more discrete patches and damage than found on the alumina head. These formed scratches and damage are due to the higher wear rate in the metal–polyethylene combination. The ceramics produce lower wear rate when articulating with UHMWPE because of their lower coefficient of friction [12]. Major disadvantages which limit the long-term performance of ceramic heads are their brittleness and the limited tensile and yield strengths. A clinical study by Hwang *et al* [12] reported that the ceramic–polyethylene combination showed two to four times lower wear rates than the metal–polyethylene combination.

The initial surface roughnesses of CoCr, alumina and zirconia were approximately 0.01, 0.012 and 0.008  $\mu\text{m}$ , respectively. The same study was also performed with the presence of PMMA particles in serum for CoCr, alumina and zirconia femoral heads with UHMWPE combination. Figure 5 shows the wear rates obtained for all three femoral heads for PMMA concentrations from 0 to 10 g l<sup>-1</sup>. In the absence of the PMMA particles in serum, UHMWPE showed 30% lower wear rates with zirconia than with alumina and CoCr ( $P < 0.05$ ) [14].

As the PMMA concentration increased to 1 g l<sup>-1</sup>, the alumina heads showed 30% higher wear rates than CoCr with UHMWPE. Zirconia showed the lowest average wear rates. For the increased concentration from 1 to 5 g l<sup>-1</sup> of PMMA particles, alumina had a constant drop in the average wear rate. The increase in wear rate was observed in both CoCr and zirconia, with zirconia showing the lowest average wear rate. With an increase in the concentration of PMMA particles from 5 to 10 g l<sup>-1</sup>, CoCr showed a 100% increase in wear rate with UHMWPE while stable average wear rates were observed for both the alumina and the zirconia heads articulated with UHMWPE cups [14].

With increase in the surface roughness of femoral head components, the wear rate was found to increase. The wear rate dependency was revealed in the hip simulator study, which showed the wear rate of the UHMWPE cups proportional to

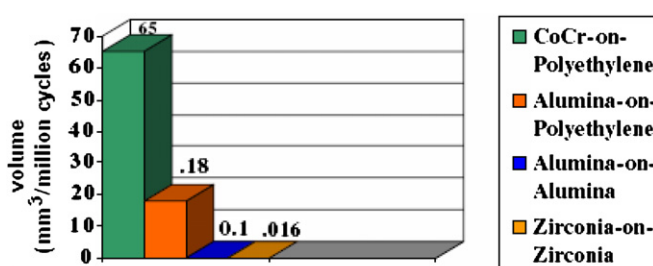


**Figure 6.** The volumetric wear rate (mm<sup>3</sup>/million cycles) for different articulating combinations [6].

(This figure is in colour only in the electronic version)

**Table 3.** The wear factor for metal-on-UHMWPE, ceramic-on-ceramic and metal-on-metal combinations. Ceramic-on-ceramic bearing couple has the lowest wear factor [15].

| Material           | Wear factor, $K \times 10^{-7}$ (mm <sup>3</sup> N <sup>-1</sup> m <sup>-1</sup> ) |
|--------------------|--|
| Metal-on-UHMWPE    | 2.00 $\pm$ 0.5   |
| Ceramic-on-ceramic | 0.20 $\pm$ 0.06  |
| Metal-on-metal     | 12.00 $\pm$ 1.0  |

the square root of surface roughness (Ra). The incapability of the PMMA particles to adhere on the ceramic head surfaces helped achieve excellent wear resistance with UHMWPE over the metal-on-UHMWPE [14].

**2.2.2. Ceramic-on-ceramic versus other combinations.** UHMWPE is extensively used with ceramic femoral heads in THR applications due to its higher wear resistance, better wear performance and ease of availability [16]. In long-term articulations, the polyethylene produces higher wear debris of micrometer and sub-micrometer sizes as proposed in an *in vitro* study by Howling *et al* [15]. The study reported that debris particles are less biodegradable which leads to loosening and osteolysis in the long-term use of polyethylene. Due to higher toughness and strength of the ceramic materials, ceramic-on-ceramic combinations have been focused on as weight bearing couples. The ceramic-on-ceramic combination has the lowest wear factor compared to the other combinations (table 3).

The advantages of ceramic articulating surfaces over polyethylene and metal were discussed by Slonaker and Goswami [6]. The study reported that the ceramic-on-ceramic combination shows a 4000 times lower wear rate compared to the metal-on-polyethylene combination (figure 6). The CoCr-on-polyethylene combination showed the highest wear rate of 65 mm<sup>3</sup>/million cycles amongst all the other bearing conditions. The slight difference of 0.084 mm<sup>3</sup>/million cycles was found between alumina-on-alumina and zirconia-on-zirconia combinations. As expected, zirconia-on-zirconia showed the expected lowest wear rate of 0.016 mm<sup>3</sup>/million cycles.

### 2.3. Improvements in wear rates of UHMWPE

**2.3.1. Conventional UHMWPE.** The ceramic-on-ceramic coupling has been a successful coupling in THR applications

**Table 4.** The wear rate behavior with an increase in the irradiation dose level from 25 to 300 kGy. The ultimate tensile strength reduces with an increase in the cross-link density. However, cross-link density has less effect on the yield strength [17].

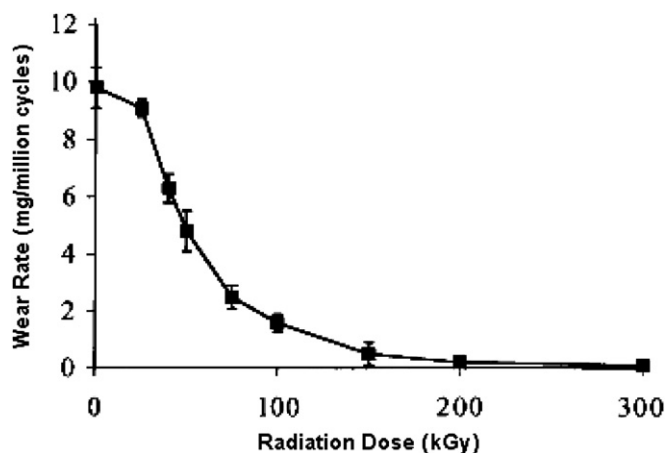
| Sample ID       | Absorbed radiation dose level, $D$ (kGy) | Ultimate tensile strength, UTS (MPa) | Yield strength, YS (MPa) | Cross-link density, $d_c$ ( $\times 10^{-4}$ mol dl $^{-1}$ ) | POD wear rate, WR (g MC $^{-1}$ ) |
|-----------------|--|--------------------------------------|--------------------------|---|-----------------------------------|
| Control         | 0  | 46 $\pm$ 3.0                         | 22.0 $\pm$ 0.4           | –   | 9.8 $\pm$ 0.7                     |
| CISM-25         | 25                                       | 37 $\pm$ 0.6                         | 19.6 $\pm$ 0.5           | 105.1   | 9.1 $\pm$ 0.3                     |
| CISM-40 (gamma) | 40                                       | 38 $\pm$ 1.9                         | 18.8 $\pm$ 0.6           | 130.7   | 6.3 $\pm$ 0.5                     |
| CISM-50         | 50                                       | 37 $\pm$ 4.9                         | 19.6 $\pm$ 0.5           | 158.7   | 4.8 $\pm$ 0.7                     |
| CISM-75         | 75                                       | 37 $\pm$ 4.0                         | 19.9 $\pm$ 0.1           | 180.8   | 2.5 $\pm$ 0.4                     |
| CISM-100        | 100                                      | 35 $\pm$ 5.1                         | 20.2 $\pm$ 0.1           | 197.6   | 1.6 $\pm$ 0.3                     |
| CISM-150        | 150                                      | 28 $\pm$ 2.0                         | 19.6 $\pm$ 0.2           | 208.9   | 0.5 $\pm$ 0.4                     |
| CISM-200        | 200                                      | 29 $\pm$ 1.6                         | 19.6 $\pm$ 0.4           | 218.9   | 0.2 $\pm$ 0.1                     |
| CISM-300        | 300                                      | 27 $\pm$ 2.5                         | 20.0 $\pm$ 0.1           | –   | 0.1 $\pm$ 0.1                     |

due to the lower coefficient of friction of ceramic material [12]. The lower coefficient of friction helps the implant produce less wear debris during articulation and higher wear resistance of the hip prosthesis. On the other hand, the stiffness of the ceramic–ceramic coupling increases the risk of hip implant failure. The mechanical properties of ceramics including brittleness and the limited yield and tensile strength confine the success of ceramic-on-ceramic coupling. Hwang *et al* [12] reported insertion of the UHMWPE liner in between ceramic–ceramic combination. The ceramic-on-UHMWPE combination plays a vital role in improving the wear resistance and decelerating the production of wear debris which controls wear rate in the artificial THR [12].

In THR applications, UHMWPE is successfully used as a load bearing surface in combination with the ceramic femoral head, ensuring the absorption of the articulating load during the gait cycle. Many advantages such as higher wear resistance, high toughness, remarkable biocompatibility and low friction help UHMWPE stand firmly amongst the other biomaterials in THR applications [16]. A clinical *in vitro* study by Wang and Essner [14] described that the wear rate of UHMWPE was found to be independent of the concentration of PMMA particles present in serum, while coupled with zirconia and alumina femoral heads.

**2.3.2. Highly cross-linked UHMWPE.** Use of the highly cross-linked UHMWPE, as an articulating surface, has revealed excellent results on wear rates in comparison with the conventional UHMWPEs. During an *in vitro* study by Ries [18], highly cross-linked UHMWPE showed 90% reduced wear rates as compared to the conventional UHMWPE. The cross-linking process improves the wear resistance while sacrificing the mechanical properties, such as tensile and yield strength, hardness, toughness, modulus and the fatigue crack propagation resistance [17, 18]. The reduced mechanical properties may act as a major limiting factor in the highly stressed contact application, for instance total knee arthroplasty.

Muratoglu *et al* [17] reported wear behavior of three basic types of UHMWPE: (i) radiation-cross-linked ram extruded GUR 4150 UHMWPE, (ii) peroxide-cross-linked GUR 1050 resin and (iii) peroxide-cross-linked Himont 1900 resin. All three biomaterial types showed nearly the same behavior for

**Figure 7.** Bi-directional POD wear rate (mg/million cycles) versus radiation dose (kGy) for CISM-UHMWPE. The wear rate was undetectable [17].

ultimate tensile and yield strength as well as pin-on-disc (POD) wear rate when tested on a bi-directional pin-on-disc machine. Amongst all three biomaterials, the results achieved from the radiation-cross-linked GUR 4150 resin are included in the present study.

An *in vivo* study by Wannomae *et al* [21] examined that melting is more effective than annealing in reducing the free radicals during cross-linking, which helps to reduce the oxidation of UHMWPE liners in long-term use. The final processed specimen is referred as the cold irradiated, subsequently melt-annealed (CISM). Table 4 describes the wear rate behavior of the radiation-cross-linked UHMWPE (CISM) along with its ultimate tensile strength, yield strength, and crosslink density as a function of the increasing radiation dose level [17]. The increase in the dose level from 0 to 300 kGy in a total of eight subsequent passes shows an obvious decrease in the ultimate tensile strength from 46 to 27 MPa as well as a slight decrease in yield strength from 22 MPa to 20 MPa. Yield strength is found to be less sensitive to the increase in the dose level compared to the ultimate strength. The crosslink density increases with an increase in the dose level while a significant decrease in POD wear rate is observed from 9.8 g MC $^{-1}$  to 0.1 g MC $^{-1}$  with an increase in the dose level from 0 to 300 kGy. Figure 7 illustrates a decrease in

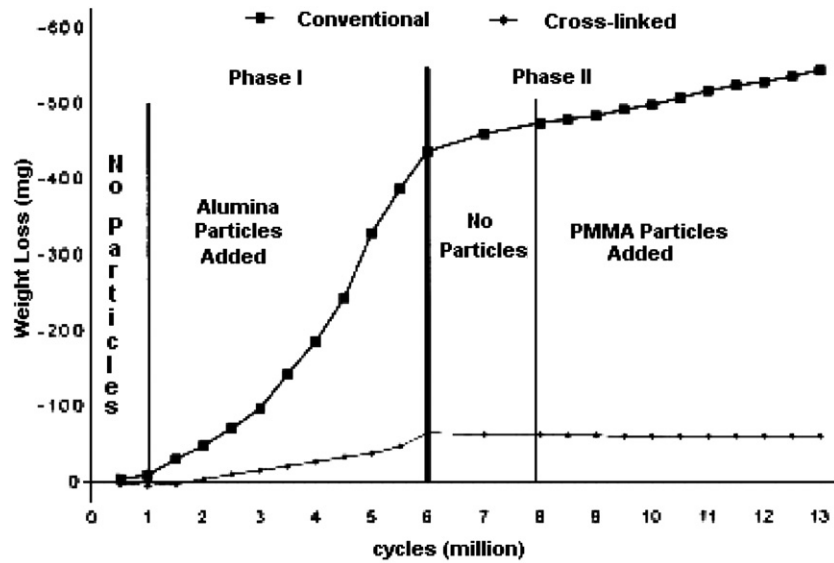


**Figure 8.** The comparison of the weight loss of highly cross-linked UHMWPE and conventional UHMWPE over 13 million cycles in the presence of Al<sub>2</sub>O<sub>3</sub> and PMMA particles in the serum [13].

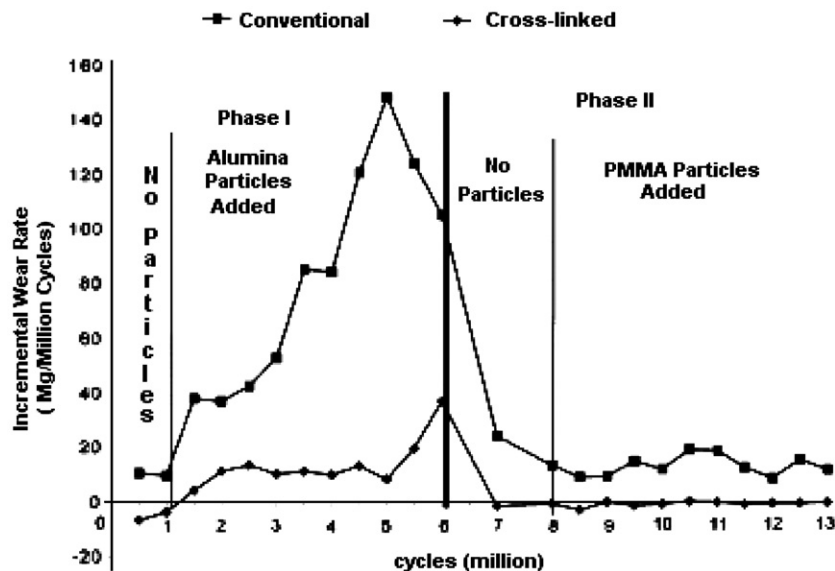


**Figure 9.** The incremental wear rate of conventional and highly cross-linked UHMWPE with the presence of Al<sub>2</sub>O<sub>3</sub> and PMMA particles in the serum [13].

the bi-directional POD wear rate of the radiation-crosslinked UHMWPE (CISM) up to an undetectable level for an increase in the dose level from 25 to 300 kGy [17].

An *in vitro* study of the third-body wear behavior of highly cross-linked polyethylene, reported by Bragdon *et al* [13], shows higher wear resistance compared to the conventional UHMWPE under a peak load of 750 lb (3336 N) with  $\pm 23^\circ$  of flexion–extension,  $\pm 10^\circ$  of external–internal rotation, and  $\pm 8.5^\circ$  of abduction–adduction. The test lasted for a total of 13 million cycles. Of these 13 million cycles, 5 million cycles are for Al<sub>2</sub>O<sub>3</sub>, 5 million cycles for PMMA particles in serum, and 3 million cycles without third-body particles in serum. Figure 8 shows the results in weight loss (mg) examined at every million cycles; whereas figure 9 shows an incremental wear rate per million cycles over the entire

test of 13 million cycles. The test results showed an average incremental wear rate of  $37 \pm 38$  mg/million cycles for the highly cross-linked UHMWPE, which is 86% less than the  $149 \pm 116$  mg/million cycles for the conventional UHMWPE in the presence of aluminum oxide particles in the serum ( $P < 0.01$ ). Similarly, the highly cross-linked UHMWPE showed an average incremental wear rate of  $0.5 \pm 0.7$  mg/million cycles, which is 97% less than the  $19 \pm 5$  mg/million cycles for the conventional UHMWPE in the presence of PMMA particles in serum [13].

Although the cross-linking process reduces the mechanical properties of the virgin polymer, it provides an outstanding wear resistance to the UHMWPE. Use of the ionizing radiation during the cross-linking process lowers the oxidation resistance of UHMWPE, which may limit the



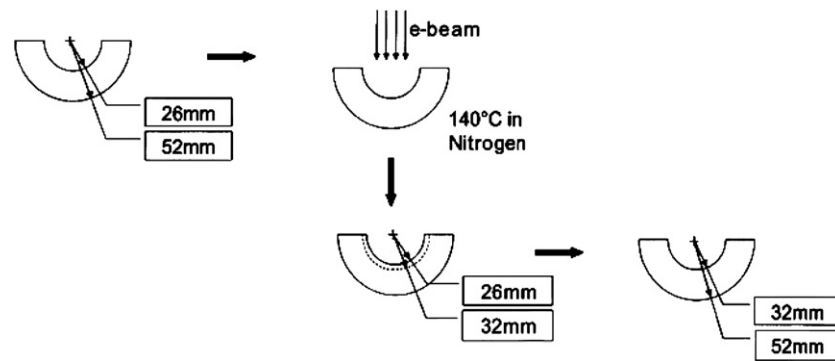


**Figure 10.** The gradient cross-linking process used to produce a 26 mm UHMWPE acetabular component without an oxidative superficial layer. UHMWPE is melted at 140 °C under nitrogen and then partially irradiated using a 2 MeV electron beam which causes a limited penetration through the acetabular liners. The machining process reduces the inner diameter of the cup from 32 mm to 26 mm [24].

success of UHMWPE in THR applications. This drawback encourages the enhancement of the cross-linking process to achieve a better performance for long lasting use of UHMWPE in THR applications. The new phenomenon known as *gradient cross-linking* is used nowadays to overcome the stated problem [20, 22, 24, 25].

**2.3.3. The gradient cross-linked UHMWPE.** In order to maintain the mechanical properties of the cross-linked UHMWPE, the limited penetration of an electron beam is applied across the acetabular component. This partial irradiation process is known as *the gradient cross-linking of UHMWPE* [24]. Use of gradient cross-linking of UHMWPE for the acetabular component results in a higher cross-link density at the superficial layer of the articulating surface which improves the wear resistance of the UHMWPE liner. At the same time, a lower cross-link density is achieved at the external surface of the acetabular component, which helps retain the mechanical properties and reduce the generation of wear debris in the virgin polymer [24].

In the process of gradient cross-linking (shown in figure 10), UHMWPE is melted at 140 °C under nitrogen and then partially irradiated using a 2 MeV electron beam, which causes a limited penetration through the acetabular liners. The irradiation process induces the oxidation of the UHMWPE liners at its superficial layer, which is machined to remove the oxidized layer. The machining process reduces the inner diameter of the cup from 32 mm to 26 mm inner diameter. The process of gradient cross-linking comes to an end with the cross-link density of  $0.15 \pm 0.01 \text{ mol dm}^{-3}$  at the articulating surface, and  $0.12 \pm 0.01 \text{ mol dm}^{-3}$  at the outer surface of the acetabular cup [24]. Figure 11 shows the weight loss comparison between the gradient cross-linked and the conventional UHMWPE observed *in vitro* at the applied load of 750 lb. The conventional UHMWPE liners showed an average weight loss of  $115 \pm 25 \text{ mg}$  in 4.5 million cycles, while the gradient cross-linked UHMWPE liners showed an average weight gain of  $15 \pm 9 \text{ mg}$  in 4.5 million cycles. Another study also looked at weight gain in the gradient cross-linked polyethylene caused by the unbalanced increase in the fluid uptake of the articulating surfaces. The constant articulations

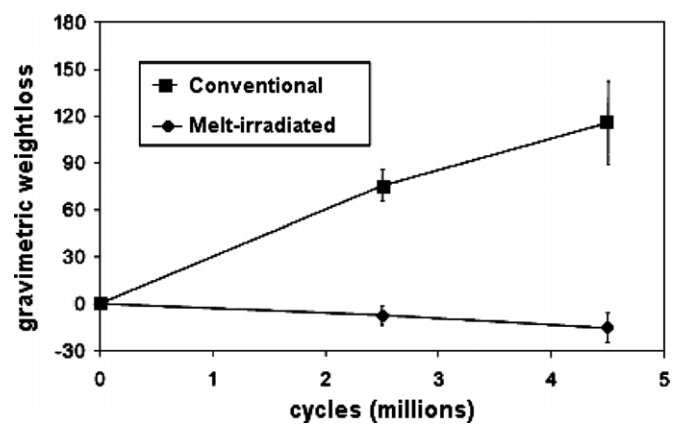


**Figure 11.** The weight loss comparison of gradient cross-linked UHMWPE and conventional UHMWPE over 4.5 million cycles [24].

make the articulating surfaces susceptible to the absorption of the lubricant, resulting in the weight gain.

### 3. Closing remarks

This paper reviews the third-body wear in THR. Principal mechanisms were: (1) serum particles gather on the superficial layer of the acetabular cup that would reduce the contact between the femoral and acetabular component surfaces; (2) PMMA particles may stick onto the femoral head surface, which can plough the interior of the acetabular cup, thus increasing the wear rate; and (3) PMMA particles can roll in between the articulating surfaces instead of sticking to the ball or the cup surfaces.

The factors affecting wear rate were: surface roughness, coefficient of friction (of the articulating surfaces), clearance (between the acetabular cup and the femoral head), and sliding distance. Zirconia showed the lowest wear rate amongst all the different tested materials *in vitro*. The critical value of surface roughness was reported to be  $0.10 \mu\text{m}$ . Clearance near zero or above 0.5 mm shows the highest wear rate and between 0.15 mm and 0.5 mm clearance was found to be an ideal range *in vitro*. The study on wear rate against the friction coefficient reported the linear wear rate to be less dependent on the friction

coefficient. The volumetric wear rate increased 12% or more for the clearance increasing from 0 to 0.5 mm. The sliding distance was established to be an affecting parameter for the wear rate behavior of a hip prosthesis.

Ceramic-on-UHMWPE produced lower wear rates than metal-on-UHMWPE because it has a lower coefficient of friction; also, ceramic femoral heads are found to be less susceptible to scratches. The ceramic-on-UHMWPE combination provides better performance under third-body wear phenomenon. A stable average wear rate was observed for the ceramic heads with an increase in PMMA concentration from 1 to 10 g l<sup>-1</sup> in serum, while 100% increase in average wear rate was detected in the metal heads. Ceramic-on-ceramic is favored over other combinations of weight bearing couples because of their lowest wear factor. The ceramic-on-ceramic combination showed 4000 times lower wear rate than the other combinations.

The ceramic-on-UHMWPE showed a significant reduction in weight loss by inserting an UHMWPE liner in between the ceramic-on-ceramic combination. Improved mechanical properties of UHMWPE such as wear resistance, toughness, biocompatibility and friction coefficient were obtained. A clinical *in vitro* study showed 90% reduction in the wear rates for the cross-linked UHMWPE. The wear resistances of the cross-linked UHMWPE and conventional UHMWPE were investigated. As compared to conventional UHMWPE, the cross-linked UHMWPE showed 86% and 97% less incremental wear rate with the presence of alumina and PMMA particles, respectively.

A significant decrease in the linear wear rate was observed with the increase in the dose level for cross-linked UHMWPE. The cross-linking process improves the wear resistance while sacrificing the mechanical properties, such as tensile and yield strength, hardness, toughness, and the fatigue crack propagation resistance. The reduction in mechanical properties was retained by using the gradient cross-linking.

## References

- [1] Gomez P and Morcuende J 2005 A historical and economic perspective on Sir John Charnley, Chas F. Thackray Limited, and the early arthroplasty industry *Iowa Orthop. J.* **25** 30–7
- [2] Buford A and Goswami T 2004 Review of wear mechanisms in hip implants: paper I—general *Mater. Des.* **25** 385–93
- [3] St John K R, Zardiackas L D and Poggie R A 2004 Wear evaluation of cobalt-chromium alloy for use in a metal-on-metal hip prosthesis *J. Biomed. Mater. Res. B* **68B** 1–14
- [4] Kurtz S, Hozack W, Marcolongo M, Turner J, R Clare and Edidin A 2003 Degradation of mechanical properties of UHMWPE acetabular liners following long-term implantation *J. Arthroplasty* **18** (Suppl. 1) 68–78
- [5] Sambasivan S, Fischer D A, Shen M C and Hsu S M 2004 Molecular orientation of ultrahigh molecular weight polyethylene induced by various sliding motions *J. Biomed. Mater. Res. B* **70B** 278–85
- [6] Slonaker M and Goswami T 2004 Review of wear mechanisms in hip implants: paper II—ceramics IG004712 *Mater. Des.* **25** 395–405
- [7] Goswami T and Alhassan S 2008 Wear rate model for UHMWPE in total hip and knee arthroplasty *Mater. Des.* **29** 289–96
- [8] Cho H J, Wei W J, Kao H C and Cheng C K 2004 Wear behavior of UHMWPE sliding on artificial hip arthroplasty materials *Mater. Chem. Phys.* **88** 9–16
- [9] Teoh S H, Chan W H and Thampuran R 2002 An elasto-plastic finite element model for polyethylene wear in total hip arthroplasty *J. Biomech.* **35** 323–30
- [10] Bennett D, Orr J and Baker R 2000 Movement loci of selected points on the femoral head of individual total hip arthroplasty patients using three-dimensional computer simulation *J. Arthroplasty* **15** 909–15
- [11] Turell M, Friedlaender G, Wang A, Thornhill T and Bellare A 2005 The effect of counterface roughness on the wear of UHMWPE for rectangular wear paths *Wear* **259** 984–91
- [12] Hwang D S, Kim Y M and Lee C H 2007 Alumina femoral head fracture in uncemented total hip arthroplasty with a ceramic sandwich cup *J. Arthroplasty* **22** 468–71
- [13] Bragdon C, Jasty M, Muratoglu O, O'Connor D and Harris W 2003 Third-body wear of highly cross-linked polyethylene in a hip simulator *J. Arthroplasty* **18** 553–61
- [14] Wang A and Essner A 2001 Three-body wear of UHMWPE acetabular cups by PMMA particles against CoCr, alumina and zirconia heads in a hip joint simulator *Wear* **250** 212–6
- [15] Howling G I, Sakoda H, Antonarulajah A, Marrs H, Stewart T D, Appleyard S, Rand B, Fisher J and Ingham E 2003 Biological response to wear debris generated in carbon based composites as potential bearing surfaces for artificial hip joints *J. Biomed. Mater. Res. B* **67B** 758–64
- [16] Park K D, Kim J, Yang S J, Yao A and Park J B 2003 Preliminary study of interfacial shear strength between PMMA precoated UHMWPE acetabular cup and PMMA bone cement *J. Biomed. Mater. Res. B* **65B** 272–9
- [17] Muratoglu O, Bragdon C, O'Connor D, Jasty M, Harris W, Gul R and McGrady F 1999 Unified wear model for highly crosslinked ultra-high molecular weight polyethylenes (UHMWPE) *Biomaterials* **20** 1463–70
- [18] Ries M 2005 Highly cross-linked polyethylene: the debate is over—in opposition *J. Arthroplasty* **20** (Suppl. 2) 59–62
- [19] Kurtz S, Mazzucuo D, Rimnac C and Schroeder D 2006 Anisotropy and oxidative resistance of highly crosslinked UHMWPE after deformation processing by solid-state ram extrusion *Biomaterials* **27** 24–34
- [20] Rieker C, Konrad R, Schon R, Schneider W and Abt N 2003 *In vivo* and *in vitro* surface changes in a highly cross-linked polyethylene *J. Arthroplasty* **18** (Suppl. 1) 48–54
- [21] Wannomae K, Bhattacharyya S, Freiberg A, Estok D, Harris W and Muratoglu O 2006 *In vivo* oxidation of retrieved cross-linked ultra-high-molecular weight polyethylene acetabular component with residual free radicals *J. Arthroplasty* **21** 1005–11
- [22] Oral E, Rowell S and Muratoglu O 2006 The effect of  $\alpha$ -tocopherol on the oxidation and free radical decay in irradiated UHMWPE *Biomaterials* **27** 5580–7
- [23] Oral E, Christensen S, Malhi A, Wannomae K and Muratoglu O 2006 Wear resistance and mechanical properties of highly cross-linked, ultrahigh-molecular weight polyethylene doped with vitamin E *J. Arthroplasty* **21** 580–91
- [24] Muratoglu O, O'Connor D, Bragdon C, Delaney J, Jasty M, Harris W, Merrill E and Venugalan 2002 Gradient crosslinking of UHMWPE using irradiation in molten state for total joint arthroplasty *Biomaterials* **23** 717–24
- [25] Muratoglu O, Bragdon C, O'Connor D, Jasty M and Harris W 2001 A novel method of cross-linking ultra-high-molecular-weight polyethylene to improve wear, reduce oxidation, and retain mechanical properties *J. Arthroplasty* **16** 149–60